ABSTRACT

Title of Dissertation:	SPATIAL AND TEMPORAL DYNAMICS OF THE CHESAPEAKE BAY SEA NETTLE
	Suzan Shahrestani, Doctor of Philosophy, 2018
Dissertation directed by:	Associate Professor, Dr. Hongsheng Bi, Marine Estuarine Environmental Sciences

The jellyfish *Chrysaora chesapeakei* forms large summer blooms in Chesapeake Bay, and has substantial ecological and economic impacts on local ecosystems. Limited information on this species is mostly due to difficulties collecting spatial information on jellyfish in dynamic coastal ecosystems. Spatial gaps of *C. chesapeakei* were addressed by applying a multi-scale approach across life stages and within a source-sink context, reflected by the ecology and habitat utilization of *C. chesapeakei*. An Adaptive Resolution Imaging System (ARIS, SoundMetrics, Inc.) was used to collect high-resolution data on medusae in 2016 and 2017, within a Patuxent River waterscape. Polyp settlement plates were deployed at eight sites to understand the distributional range of the sessile benthic stage in Chesapeake Bay, but polyps successfully overwintered at only one of the sites, indicating that settlement alone was insufficient to explain *C. chesapeakei* dispersal to new habitat. Using high-resolution sonar data, a multi-scale spatial analysis was conducted to understand

medusae dispersion and abundance. Medusae were three times more abundant in 2017 than in 2016. However, differences in water-column concentration were not apparent at the fine-scale (<5m) where medusae were randomly dispersed in both years. At the mesoscale (10km), spatial dependency was observed in both years, with more transport of jellyfish to dispersal habitat in the high-abundance year (2017). Overall, polyp settlement and overwintering survival in potential habitat seem to control the spatial distribution of *C. chesapeakei* at the Bay-wide scale while medusae appear responsible for mesoscale dispersal to new habitat, demonstrating high dispersal to sink habitat in a high-density year and low dispersal in a low-density year.

SPATIAL AND TEMPORAL DYNAMICS OF THE CHESAPEAKE BAY SEA NETTLE

by

Suzan Shahrestani

Dissertation submitted to the Faculty of the Graduate School of the
University of Maryland, College Park, in partial fulfillment
of the requirements for the degree of
Doctor of Philosophy
2018

Advisory Committee:
Dr. Hongsheng Bi, Chair
Dr. Denise Breitburg
Dr. Raleigh Hood
Dr. Edward Houde
Dr. Dong Liang

Acknowledgements

I would like to thank the Drach and Mellody families for contributing to the award that funded the research on jellyfish polyps in Chapter 3 of this dissertation. The Chesapeake Biological Lab, in Solomons, MD and the Graduate Education Committee provided additional support. I also thank the facilities and managers of the state of Maryland that hosted polyp settlement towers, including: the United States Naval Academy (Annapolis), the Environmental Education Center (Baltimore), Horn Point Laboratory (Cambridge), the Patuxent River Environmental Research Lab (St. Leonard), the Karen Noonan Center (Crocheron) and the Environmental Education Center (Baltimore). We thank the Oyster Recovery Partnership and True Chesapeake Oyster Co. for loaning me hundreds of oyster shells I would also like to thank Ocean Marine Industries, Inc. for their support in lending us the sonar equipment used in this Chapter 2. Finally I thank Morgan State Univiersity and the Patuxent Environmental Research Lab, including Dr. Chunlei Fan, and William Yates for making all of our sonar field work possible (Chapter 4).

This work could not have been possible without the unwavering support of the many people in my life. Firstly, I'd like to thank my wonderful major advisor Dr. Hongsheng Bi. I won't say that it was easy working with him, because it wasn't. He challenged me along every step of the way and made me into the curious and bold scientist I am today. All the while providing me with a safety net of kindness, compassion, support and input from his brilliant brain! I will look back on my years as his student with love and pride. He is stuck with me for life!

Secondly, I’d like to thank my committee members, Dr. Denise Breitburg, Dr. Raleigh Hood, Dr. Edward Houde and Dr. Dong Liang for belief in me and my work. It didn’t take long for me to realize that they were all on my side and wanted me to succeed. Partcularly Dr. Denise Breitburg whose expertise on jellyfish, guidance, and mentorship through my doctoral research has been invaluable. I'd also like to give special aknowledgement to Dr. Chunlei Fan, a Morgan State University collaborator and honorary committee member, not only was Chunlei the best boat captain I could ask for, but he also introduced me to his wonderful undergraduate intern Nikelene Mclean whose assitence in the field made the hours feel shorter and the mid-summer heat less hot. In my own lab, I’ve had the honor of working with and befriending two brilliant young women, Cara Simpson and Katie Lankowicz. I can't wait to see who they become and what they will accomplish. I’ve also had the privilege of working with and learning from a number of visiting scholars specifially, Libin Zhang, Junting Song and Linlin Wang and want to thank them for a brilliant scientific and cultural exchange.

As part of my research I walked the CBL research pier over 250 times. Every year I watched the juville needlefish grow, the cownose swim in with their pups, the ospreys trying to nest, and this past year, I watched the sea-grass come in. It’s been a beautiful experience conducting research in my own backyard, and it wouldn’t have been possible without the CBL community. I’d like to give a special thank you to the good friends I have made over the years, including Andrea Sylvia, Jessica Wingfield, Erin Crandall and Kevin Kahover. I’d also like to thank members of the CBL staff for dealing with my scatter-brain, especially Jeannette Duran for always getting me

where I needed to go, and Elaine Proctor who always helped me find what I was looking for.

My family and friends have never doubted me, not for one second, and that gave me the courage to not doubt myself. I'd like to aknowledge my mother, Fawziyeh Malhas, for her warmth and generosity, and for giving me a childhood full of wonder in the NYC zoos, museums and aquariums that would inspire me so deeply. And to my father, Ali Shahrestani, I'd like to thank him for the many late nights he stayed up with me as a kid, teaching me about math, science, politics and the way of the world. My father taught me to be brave, and made me believe I could do anything I could dream, no matter what anyone had to say about it. There is nothing like going through life with a younger and older sister that keep you balanced in the middle. To my beautiful sisters, I'd like to thank them for being my biggest supporters and always cheering me on. To my best friends, Anita Rishi, Eileen Garcia and Latha Jayakumar, I thank you for being open, loving and honest friends who always have my back.

Finally, I'd like to thank my husband Zane Campbell. I could easily replace all the words in these chapters with ways in which he has helped me. From field work, to zip-tying, to cutting PVC, drilling oysters, welding, cutting steel, machineing, bolting and frankly picking me up off the floor when I'd had enough, I could not have done this without him. He was there through my long wrestling match with R, he was there through my late-night caffinated hours, and he was there when I made my greatest research findings. We will be side-by-side throuh my next journey because, there's no point in making it with out him.

Table of Contents

List of Tables

List of Figures

Chapter 1: Introduction

Although simple in body plan, jellyfish or gelatinous zooplankton represent a diverse array of species that span phyla (e.g., Ctenophora vs. Cnidaria). Jellyfish adaptability, rapid reproductive response time, and stinging capabilities have large and seasonally predictable impacts on recreational and commercial enterprises (Purcell et al. 2007, Graham et al. 2014). A greater understanding of the spatial patterns and ecological processes that drive the abundance and dispersion of impactful gelatinous species, was the major undertaking of this study because in-depth research and historical research are limited. Disregarding jellyfish bloom impact on ecosystem structure and production is a concern, considering the voracious appetites of jellyfish and their consumption of zooplankton (competition) and ichthyoplankton (predation) that can have detrimental effects on fish populations (Cowan et al. 1992, Purcell et al. 1994a, Suchman & Sullivan 2000, Purcell & Arai 2001, Sommer et al. 2002, Brodeur et al. 2008). Furthermore, jellyfish can have notable ecological impact in coastal regions. They may limit the potential of energy transfer in foodwebs by displacing carbon to a microbial respiratotry sink (Condon et al. 2011).

It has been suggested that the adaptability of jellyfish to environmental stressors may lead to increases in their abundance in regions with degrading marine ecosystems (Mills 2001, Purcell et al. 2007, Richardson et al. 2009, Brotz et al. 2012, Purcell 2012, Graham et al. 2014). Although they can adapt, scyphozoan species are susceptible to hypoxia, variation in temperature and salinity, and habitat loss (Breitburg et al. 2003, Wiegner et al. 2003, Breitburg & Fulford 2006, Lucas et al.

2012a), making predictions of abundance difficult in dynamic estuarine environments.

Researchers lack a strong understanding of jellyfish population dynamics because historical and current data are insufficient to draw conclusions (Condon et al. 2012, Condon et al. 2013). The uncertainty is, in part, due to a lack of long-term monitoring data and limited sampling across different life stages (Gibbons & Richardson 2013, Brodeur et al. 2016).

The Jellyfish Life-History

Many scyphozoan species have a complex life history (Arai 2012) that contrasts with the simplicity of their morphological structure, i.e., metagenic species that exhibit alternation of generations. Dioecious male and female medusae of many scyphozoans (Fig. 1.1A) produce planula larvae (Fig. 1.1B) by way of proximity spawning (external fertilization). Planula larvae are then cued to settle on available hard substrate in optimal coastal, shallow habitat. Once planula larvae settle they transform into polyps which form colonies through asexual reproduction (Fig. 1.1C-F). Benthic polyps show a preference for substrate type and many species readily proliferate on unnatural hard substrate, with implications for higher rates of planula settlement and polyp abundance with increasing human influence on marine habitats (Brewer 1984, Pitt 2000, Holst & Jarms 2007, Hoover & Purcell 2009, Duarte et al. 2013). Increases in habitat via man-made structure and losses of natural habitat (i.e. oyster reefs) potentially can lead to shifts in the abundance and biogeographic distribution of jellyfish species whose polyp stage may be closely integrated into and

dependent on the local ecosystem, i.e., adapted to optimal habitat (Breitburg & Fulford 2006, Breitburg et al. 2010, Hubot et al. 2017).

After the settlement of planula larvae and subsequent growth of polyps, asexual reproduction (budding) of newly formed polyp colonies ramps up before the colonies go dormant to survive harsh winter conditions in an encysted (quiescent) stage (Fig. 1.1D). Polyp survival through this encysted stage leads to inoculation of ephyrae into their local habitat in the spring months via strobilation (transverse fission, Fig. 1.1E), which is stimulated by environmental cues (Arai 1997). Multiple strobilation events lead to release of juvenile jellyfish (ephyrae) into local source habitats from a single polyp or strobilae that usually occurs multiple times in a season (Lucas et al. 2012b).

The Chesapeake Bay Jellyfish

On the Atlantic seaboard, there are two distinct species of the sea nettle (*Chrysaora quinnquecirrha and C. chesapeakei*). *C. chesapeakei* (henceforth referred to as *Chrysaora*) is predominantly found in the Chesapeake Bay, USA during summer months (Bayha et al. 2017), and was the target species of my research. *Chrysaora* contributes substantially to controlling populations of zooplankton (Purcell 1992) as a top predator in the many sub-estuaries that make up the USA's largest estuary (Clifford & Cargo 1978, Feigenbaum & Kelly 1984, Baird & Ulanowicz 1989, Sullivan & Kremer 2011). Recently, genetic testing resulted in a phylogenic analysis that distinguished the *Chrysaora chesapeakei* neotype, based on genetic differences and morphological structure. Distinguishing structures included lappet number, tentacle number, oral arm length and the dimensions of nematocysts.

The newly defined range of the Bay species indicates the Atlantic sea nettles found in the Gulf of Mexico and US Atlantic estuaries as Atlantic Bay nettles (*C. quinqecirrha*) or *C. chesapeakei* (Bayha et al. 2017).

Existing studies on the interannual variation of pelagic adults or medusae of *C. chesapeakei* (Dawson et al. 2001, Purcell 2005, Zhang et al. 2012) have focused mainly on delineating explanatory factors (salinity, temperature, advection, trophic, etc.) that contribute to the spatial and temporal bloom dynamics, including *Chrysaora* medusae in Chesapeake Bay (Brown et al. 2002, Decker et al. 2007). However, these studies primarily examined medusae in the Chesapeake Bay mainstem, which may act as a sink for the populations and do not describe polyp distribution in source creeks. There are a number of studies on *Chrysaora* early life stages such as ephyrae and polyps, but research has been mostly limited to laboratory experiments with few *in-situ* observations (Table 1.1).

Visual counts or shore-based surveys of *Chrysaora* made from a pier at the Chesapeake Biological Laboratory *(*Patuxent River, Solomon's, Maryland) date back to 1960 and are one of the few known historical datasets documenting temporal patterns of jellyfish abundance worldwide. The data were collected by multiple observers walking the length of the CBL research pier and performing visual counts. The data are mostly complete from 1960 to 1990 when they were predominantly collected by David Cargo who led the study (Table 1.2). In general, these pier counts data reveal greater *Chrysaora* abundance from 1960-1986 and show a considerable decline after 1990 (Purcell 2005, Breitburg & Fulford 2006, Breitburg & Shahrestani *Unpublished Data*).

Total daily streamflow was used to explain the interannual variation of *Chrysaora* in the Patuxent River (Cargo and King 1990), whereby decreased flow led to higher salinities optimal for sessile polyp survival and proliferation. However, Cargo and King did not account for seasonality of peak abundance in describing the variation in abundance between years. To ensure that peak magnitudes of abundance were not excluded, e.g., *Chrysaora* peaking in July vs August, Breitburg and Fulford (2006) considered the four-week peak mean of jellyfish abundance, and found that a decline in *Chrysaora* abundance circa 1990 co-occurred with drastic declines in oyster abundance. The authors suggested this decrease may be explained by a decline in oyster shell availability for settlement of *Chrysaora* polyps to below a critical threshold (Breitburg and Fulford 2006).

Although Breitburg and Fulford's (2006) study provided no information on spatial structure and documented a single point of observation through time, i.e. 4-week peak mean from 1960-present, another shore-based study on *Chrysaora* in Chesapeake Bay did examine the spatial structure of patch dynamics (Tay & Hood 2017). In that study, visual pier counts on the Choptank River revealed that jellyfish patches occurred at the kilometer scale and that patch size scaled with abundance or density within the patch (Tay & Hood 2017). However, the existing shore-based data sets on *Chrysaora* in the Patuxent and Choptank rivers were collected within the river channel i.e., dispersal habitat outside of the species' primary source areas. This makes the dock side visual insufficient in evaluating the magnitude of *Chrysaora* abundance, especially considering the Patuxent River and Choptank River waterscape

and the dispersion patterns of *Chrysaora* as it plays out its life history within a source-sink context, i.e. full bloom magnitude realized in source habitat.

Dynamics of Dispersion and Abundance

Understanding the spatial patterns and the related ecological processes are fundamental problems in ecology and studies of population dynamics (Turner et al. 1989, Wiens 1989, Levin 1992, Rahbek 2005). To quantify patterns of abundance at different spatial scales, it is essential to sample the proper spatial extent, i.e., study area with an adequate resolution, which is often determined by the life history and dispersion patterns of the target species. Similar to the dispersal of mangrove seedlings to shallow coastal habitat via tidal and coastal processes (Duke et al. 1998), medusae need to be dispersed within range of optimal habitat for their planula larvae to settle successfully (Brewer 1991, Lucas 1996, 2001, Sponaugle et al. 2002, Arai 2009). Considering the life-span (four days) and limited swimming capability of a planula larva gives clues to the spatial scale at which physical (substrate, flow field, salinity, temperature), and biological (reproduction, medusae aggregations) processes may be affecting successful settlement within a local habitat (Cargo 1979, Brewer 1984, Brewer & Feingold 1991, Pitt 2000, Lucas 2001, Hamner & Dawson 2009, Holst & Jarms 2010, Lucas et al. 2012b, Aglieri et al. 2014, Pitt et al. 2014, Dong et al. 2015).

When observing the processes of a sub-estuary at the mesoscale extent (<10 km, Fig. 4.1) settlement and growth of polyp colonies may occur within localized areas that reflect source-sink dynamics, whereby the successful dispersal of ephyrae and medusae to optimal habitat (i.e. available substrate, environmental conditions) is

facilitated by downstream flow from the sluggish headwaters of creeks and coves (Cargo & Schultz 1966, Purcell & Grover 1990, Purcell 1992, Olesen et al. 1994, Breitburg & Burrell 2014, Shahrestani & Bi 2018a). In the Patuxent River, there is a strong, non-linear relationship between flow and residence time (Hagy et al. 2000), which may affect the downstream transport of *Chrysaora*. Wind dynamics (lagged direction and speed) were found to have a significant effect on the distribution and abundance of *Chrysaora* in the Neuse River Estuary of North Carolina, where southerly winds increased abundances downstream (Kaneshiro-Pineiro & Kimmel 2015). However, the particular mechanisms that control dispersion patterns (aggregation or dispersal) from a local source habitat to adjacent dispersal and sink habitat are unclear.

At the fine scale (<5m) the production of planula larvae is the result of sexual reproduction between male and female scyphozoan medusae, i.e. proximity spawning (Arai 1997, Graham et al. 2001, Hamner & Dawson 2009, Aglieri et al. 2014). For species like *Chrysaora* fertilization occurs when sperm from nearby male medusae recruit to and fertilize the eggs stored in brood pouches on the oral arms of female medusae (Arai 1997). In the lab, optimal breeding of *Chrysaora* occurs when male gonads are directly injected into oral cavities of females (Cargo 1975), which suggests the importance of spatial proximity between mates with respect to reproductive success. Though spatial information at multiple scales plays a crucial role in understanding the population dynamics of *Chrysaora*, traditional sampling methods limit the spatial extent and resolution of research, ultimately producing

estimates of abundance and dispersion that are out of context or at a scale that is either too broad or too narrow.

Challenges of Jellyfish Sampling

Undersampling in shallow estuaries occurs Most traditional sampling methods integrate a volume of water that is sampled and eliminate possibilities of detecting spatial patterns within that sampled volume. Difficulties in gear deployment are due in part to limited access to sites with research vessels, as well as gear avoidance and the patchy spatial patterns of target organisms that are difficult to observe (Rozas & Minello 1997, Bayley & Herendeen 2000, Breitburg & Burrell 2014). When sampling bell-shaped medusae, traditional net sampling approaches only provide low-resolution data (Haddock 2004) and can be difficult due to the fragile nature of gelatinous species.

Considering habitat usage by pelagic fishes in developing sampling plans and accounting for gear selection have increased accuracy in estimating fish abundance (Rozas & Minello 1997). With regard to jellyfish species, surveying for patches of medusae often excludes sampling within the extent of optimal jellyfish habitat. In many cases, jellyfish sampling is added on to sampling surveys targeting fish or plankton (Boero et al. 2008, Duarte et al. 2013, Gibbons & Richardson 2013, Brodeur et al. 2016). Partially sampling jellyfish habitat at a coarse resolution limits the understanding of the spatial dynamics of gelatinous species, potentially resulting in an underestimation of their impact on ecosystem function and structure.

High-Resolution Sampling

Developments in sonar imaging provide an efficient way to obtain near image quality of free-swimming species in hard to reach areas, e.g., permanent structures like docks and piers, and hard to see environments, e.g., highly turbid waters. The ARIS3000 (Fig. 2.1, Fig. 3.3), is an advanced sonar-based imaging system that, processes reflected acoustic signals into near-photographic images allowing for fine-scale imaging even in turbid waters (Boswell & Wilson 2008).

The ARIS can be towed along a transect or set in place for single-point deployment, with processing procedures remaining similar across deployment type and species investigation. Data from a sonar camera deployed from a single point, reveals size and density, behavior, swim direction and swim speed. Recordings have been designed to capture behaviors among fish size within an estuary during tidal (Becker et al. 2011a) and diel cycles(Becker et al. 2011b), as well as a transit between the ocean and estuarine systems (Becker et al. 2016). Single point recordings, by the ARIS sonar camera, of organism transit through water control structures in salt marshes have shown patterns of fish behavior that contrast with fish size (Kimball et al. 2010). Sonar cameras are not limited to single point deployment and are configurable for mobile application. The Dual-frequency IDentication SONar or DIDSON (the model that precedes the ARIS) has been used to observe fish size and behavior under the dark unshaded waters of a pier continuum, within a heavily urbanized part of New York City (Able 2005b).

With regard to jellyfish, sonar imaging technologies are particularly useful because jellyfish are often patchily distributed and are easily damaged by nets.

Furthermore, in very turbid waters typical of high production areas, such as the shallows of Chesapeake Bay, it is difficult to deploy optical imaging systems that utilize photons. The sonar recordings of syphozoans like *Aurelia aurita* made with the DIDSON, represented more accurate observations than conventional net tows, deeming it a robust method to survey population densities (Makabe et al. 2012). Other studies evaluated jellyfish abundance within the water column and found estimates to be much more accurate than net tows (Han & Uye 2009a).

This type of data is unprecedented until recently and is very useful to research by the marine science community, because it allows for sampling of millions of cubic meters in a few hours. While nets require far more effort in the field and compress multiple data points (jellyfish location in the water column) into a single spatial point, the sonar camera provides sufficient resolution to identify individual organisms in the water column at fine scales, e.gl, down to $1/10^{th}$ of a meter. Although there is a high processing demand for the large quantities of data collected by sonar cameras, the robust results on the spatial structure of target species are well worth the challenge and effort.

Objectives and Hypotheses

The major challenge of my research was to overcome sampling limitations to incorporate and investigate the spatial structure of *Chrysaora* in Chesapeake Bay and its tributaries. Spatial information is a crucial component needed to link *Chrysaora* abundance and dispersion across life-stages and habitats in Chesapeake Bay. Specifically, my goal was to understand how *Chrysaora* life stages are adapted to a dynamic estuary. To do so I needed to (1) investigate how different life stages play a role in defining *Chrysaora* population dynamics, (2) capture and explore the spatial dynamics (scale, extent) that constrained and defined those life-stages, and (3) identify important factors that controlled *Chrysaora* population dispersion and abundance across life-stages.

Through the use of historical datasets, advanced technologies, innovative sampling, mathematical models and spatially explicit analyses I have prepared this dissertation that describes research that explores the spatial range and dispersion dynamics of *Chrysaora* polyps and medusae in Chesapeake Bay. This dissertation incorporates material from three papers by the author (Shahrestani et al. 2017); (Shahrestani & Bi 2018b, Shahrestani et al. *Submitted*). Chapter 2 includes data and information from Shahrestani et al. (2017), coauthored with Hongsheng Bi, Viacheslav Lyubchicha, and Kevin M. Boswell. Chapter 3 is based on Shahrestani and Bi (*accepted*). Information from each of these papers has also been incorporated into this introductory Chapter.

I investigated the source life stage, the benthic polyp, and explored its distribution throughout Chesapeake Bay (large-scale) and polyp seasonal dynamics between sites

(mesoscale). I also collected high-resolution data on *Chrysaora* medusae to bolster the understanding of the relationships between life stages and their shared habitat. Finally, image analysis procedures were formulated to overcome the challenges of processing 2 million frames (ARIS data). The ARIS data were used to conduct analyses on *Chrysaora* spatial structure and density at both the meso and fine scale in the Patuxent River subestuary, Chesapeake Bay. My chapter-specific objectives, hypotheses, and a summary of my results are provided below.

Chapter 2

Objective: Overcome sampling limitations of jellyfish (extent and scale) to collect high-resolution data on the spatial structure of *Chrysaora* medusae and mitigate the challenges of large data output via automated image analysis procedures.

Research Goals:

A) Calibrate towed deployment of the ARIS sonar camera in a Patuxent River waterscape to allow for the detection of *Chrysaora* in the water column.

B) Develop image analysis procedures that can be used to extract necessary information from recorded data including sea-floor depth, field-of-view and volume sampled.

C) Explore jellyfish identification and classification through the use of machine learning and an image training library to count jellyfish.

Chapter 3

Objective: Explore the role of polyps in controlling the success or failure of *Chrysaora* dispersal to new source habitat i.e. spatial range, and the implications for a local population of medusae.

Hypotheses:

A) The Chesapeake Bay-wide distribution (presence or absence) of *Chrysaora* polyps is largely determined by the advective forces of potential habitat.

B) For *Chrysaora* polyps, settlement in a new habitat is not realized until the newly formed polyp colonies survive the harsh winter (in an encysted state) to subsequently source pelagic *Chrysaora* stages to new habitat in the following year.

C) Protected, enclosed and sluggish creeks of mid-Bay tributaries provide source habitat for *Chrysaora* polyp settlement and survival through winter.

Chapter 4

Objective: Capture and analyze the multi-scale spatial dynamics of *Chrysaora* medusae as they unfold in a Chesapeake Bay waterscape, from source to dispersal habitat in two years with varying (3-fold) abundance.

Hypotheses:

A) Differences in medusa spatial dynamics constitute a multi-scale response to the interannual variation in abundance of *Chrysaora* noted between the 2016 and 2017 summer season.

B) High-resolution data of depth- and geo-referenced *Chrysaora* medusae show strong patterns of spatial and temporal correlation at the mesoscale (<10km) across both years of sampling, because jellyfish dispersion is responsive to a density gradient of individuals advected from source to dispersal habitat.

C) Between years, fine-scale (<5m) locations of medusae in the water column will reflect clustering or dispersal as potential adaptations for reproductive success and resource allocation.

Summary of Results

Innovative application of sonar technology proved useful in characterizing the fine-scale detection of *Chrysaora* medusae and providing quantitative metrics needed to calibrate the sampling procedures. In exploring the spatial patterns of *Chrysaora* polyps and medusae, my results corroborate previous reports that both life-stages are more prevalent in sluggish creeks than in the mainstem Bay and major tributaries. However, the characteristics that make creeks optimal habitat has been less understood. My results show that residence time is an important factor implicating potential settlement habitat for *Chrysaora* polyps in Chesapeake Bay at the large-scale. At the mesoscale, a protected coastline, an enclosed site, and a stable water column may allow for successful settlement and survival, which are ultimately essential processes that define a *Chrysaora* polyp source population.

In identifying a local waterscape that exemplifies optimal source habitat for *Chrysaora* polyps, I described the spatial structure of the medusae population over the course of two years in which there was major variability in abundance. Although I

hypothesized contrasting responses of fine-scale (<5m) clustering or dispersion, my results indicated that medusae were randomly dispersed in the water column in both low and high-density years. However, these results were scale-variant and changed drastically as I increased the spatial extent and scale to observe patterns of spatial dependency across sites and between years (<10km). At that scale spatial patterns were non-random and demonstrated variability in dispersion between years.

Results of this study exemplify the importance of studying marine organisms, particularly plankton species, in both a species-specific and spatially-explicit context. By exploring the spatial structure and factors that control the multi-scale dispersal of *Chrysaora* at two key life-stages we can begin to understand how gelatinous organisms adapt and survive in dynamic environments.

References

Able KW (2005) A re-examination of fish estuarine dependence: evidence for connectivity between estuarine and ocean habitats. Estuarine

Aglieri G, Papetti C, Zane L, Milisenda G, Boero F, Piraino S (2014) First Evidence of Inbreeding, Relatedness and Chaotic Genetic Patchiness in the Holoplanktonic Jellyfish Pelagia noctiluca (Scyphozoa, Cnidaria). PLOS ONE 9:e99647

Arai M (1997) A Functional Biology of Scyphozoa, Vol. Springer Science & Business Media

Arai MN (2009) The potential importance of podocysts to the formation of scyphozoan blooms: a review. Hydrobiologia 616:241-246

Arai MN (2012) A functional biology of Scyphozoa, Vol. Springer Science & Business Media

Baird D, Ulanowicz RE (1989) The Seasonal Dynamics of The Chesapeake Bay Ecosystem. Ecological Monographs 59:329-364

Bayha KM, Collins AG, Gaffney PM (2017) Multigene phylogeny of the scyphozoan jellyfish family Pelagiidae reveals that the common U.S. Atlantic sea nettle comprises two distinct species (*Chrysaora quinquecirrha and C. chesapeakei*). PeerJ 5:e3863

Bayley PB, Herendeen RA (2000) The efficiency of a seine net. Trans Am Fish Soc 129:901-923

Becker A, Cowley PD, Whitfield AK, Järnegren J, Næsje TF (2011a) Diel fish movements in the littoral zone of a temporarily closed South African estuary. Journal of Experimental Marine Biology and Ecology 406:63-70

Becker A, Whitfield AK, Cowley PD, Järnegren J, Næsje TF (2011b) An assessment of the size structure, distribution and behaviour of fish populations within a temporarily closed estuary using dual frequency identification sonar (DIDSON). Journal of Fish Biology 79:761-775

Becker A, Holland M, Smith JA, Suthers IM (2016) Fish Movement Through an Estuary Mouth Is Related to Tidal Flow. Estuaries and Coasts 39:1199-1207

Boero F, Bouillon J, Gravili C, Miglietta MP, Parsons T, Piraino S (2008) Gelatinous plankton: irregularities rule the world (sometimes). Marine Ecology Progress Series 356:299-310

Boswell KM, Wilson MP (2008) A semiautomated approach to estimating fish size, abundance, and behavior from dual-frequency identification sonar (DIDSON) data. North American Journal of …

Breitburg D, Burrell R (2014) Predator-mediated landscape structure: seasonal patterns of spatial expansion and prey control by *Chrysaora* quinquecirrha and Mnemiopsis leidyi. Marine Ecology Progress Series 510:183-200

Breitburg D, Shahrestani S (*Unpublished Data*)

Breitburg DL, Adamack A, Rose KA, Kolesar SE and others (2003) The pattern and influence of low dissolved oxygen in the Patuxent River, a seasonally hypoxic estuary. Estuaries 26:280-297

Breitburg DL, Fulford RS (2006) Oyster-sea nettle interdependence and altered control within the Chesapeake Bay ecosystem. Estuaries and Coasts 29:776-784

Breitburg DL, Crump BC, Dabiri JO, Gallegos CL (2010) Ecosystem engineers in the pelagic realm: alteration of habitat by species ranging from microbes to jellyfish. Integrative and Comparative Biology 50:188-200

Brewer RH (1984) the influence of the orientation, roughness, and wettability of solid-surfaces on the behavior and attachment of planulae of cyanea (cnidaria, scyphozoa). Biological Bulletin 166:11-21

Brewer RH (1991) Morphological Differences Between, And Reproductive Isolation Of, 2 Populations Of The Jellyfish Cyanea In Long-Island-Sound, USA. Hydrobiologia 216:471-477

Brewer RH, Feingold JS (1991) The effect of temperature on the benthic stages of Cyanea (Cnidaria: Scyphozoa), and their seasonal distribution in the Niantic River estuary, Connecticut. Journal of Experimental Marine Biology and Ecology 152:49-60

Brodeur RD, Suchman CL, Reese DC, Miller TW, Daly EA (2008) Spatial overlap and trophic interactions between pelagic fish and large jellyfish in the northern California Current. Marine Biology 154:649-659

Brodeur RD, Link JS, Smith BE, Ford M, Kobayashi D, Jones TT (2016) Ecological and economic consequences of ignoring jellyfish: a plea for increased monitoring of ecosystems. Fisheries 41:630-637

Brotz L, Cheung WWL, Kleisner K, Pakhomov E, Pauly D (2012) Increasing jellyfish populations: trends in Large Marine Ecosystems. Hydrobiologia 690:3-20

Brown CW, Hood RR, Li Z, Decker MB, Gross TF, Purcell JE, Wang HV (2002) Forecasting system predicts presence of sea nettles in Chesapeake Bay. Eos, Transactions American Geophysical Union 83:321-326

Cargo DG, Schultz LP (1966) Notes on the biology of the sea nettle, *Chrysaora quinquecirrha*, in Chesapeake Bay. Chesapeake Science 7:95-100

Cargo DG (1975) Comments on the Laboratory Culture of Scyphozoa. In: Smith WL, Chanley MH (eds) Culture of Marine Invertebrate Animals: Proceedings — 1st Conference on Culture of Marine Invertebrate Animals Greenport. Springer US, Boston, MA, p 145-154

Cargo DG (1979) Observations on the settling behavior of planular larvae of *Chrysaora* quinquecirrha. International Journal of Invertebrate Reproduction 1:279-287

Clifford HC, Cargo DG (1978) Feeding rates of the sea nettle, *Chrysaora* quinquecirrha, under laboratory conditions. Estuaries 1:58-61

Condon RH, Steinberg DK, Del Giorgio PA, Bouvier TC, Bronk DA, Graham WM, Ducklow HW (2011) Jellyfish blooms result in a major microbial respiratory sink of carbon in marine systems. Proceedings of the National Academy of Sciences:201015782

Condon RH, Graham WM, Duarte CM, Pitt KA and others (2012) Questioning the Rise of Gelatinous Zooplankton in the World's Oceans. BioScience 62:160-169

Condon RH, Duarte CM, Pitt KA, Robinson KL and others (2013) Recurrent jellyfish blooms are a consequence of global oscillations. Proceedings of the National Academy of Sciences 110:1000-1005

Cowan JH, Birdsong RS, Houde Ed, Priest Js, Sharp Wc, Mateja Gb (1992) Enclosure Experiments On Survival And Growth Of Black Drum Eggs And Larvae In Lower Chesapeake Bay. Estuaries 15:392-402

Dawson MN, Martin LE, Penland LK (2001) Jellyfish swarms, tourists, and the Christ-child. In: Jellyfish Blooms: Ecological and Societal Importance. Springer, p 131-144

Decker MB, Brown CW, Hood RR, Purcell JE and others (2007) Predicting the distribution of the scyphomedusa *Chrysaora quinquecirrha* in Chesapeake Bay. Marine Ecology Progress Series 329:99-113

Dong J, Sun M, Purcell JE, Chai Y, Zhao Y, Wang A (2015) Effect of salinity and light intensity on somatic growth and podocyst production in polyps of the giant jellyfish Nemopilema nomurai (Scyphozoa: Rhizostomeae). Hydrobiologia 754:75-83

Duarte CM, Pitt KA, Lucas CH, Purcell JE and others (2013) Is global ocean sprawl a cause of jellyfish blooms? Frontiers in Ecology and the Environment 11:91-97

Duke NC, Ball MC, Ellison JC (1998) Factors influencing biodiversity and distributional gradients in mangroves. Glob Ecol Biogeogr Lett 7:27-47

Feigenbaum D, Kelly M (1984) Changes in the lower Chesapeake Bay food chain in presence of the sea nettle *Chrysaora quinquecirrha* (Scyphomedusa). Marine Ecology Progress Series 19:39-47

Gibbons MJ, Richardson AJ (2013) Beyond the jellyfish joyride and global oscillations: advancing jellyfish research. Journal of Plankton Research 35:929-938

Graham WM, Pages F, Hamner WM (2001) A physical context for gelatinous zooplankton aggregations: a review. Hydrobiologia 451:199-212

Graham WM, Gelcich S, Robinson KL, Duarte CM and others (2014) Linking human well-being and jellyfish: ecosystem services, impacts, and societal responses. Frontiers in Ecology and the Environment 12:515-523

Haddock SHD (2004) A golden age of gelata: past and future research on planktonic ctenophores and cnidarians. In: Fautin DG, Westfall JA, Cartwrigh P, Daly M, Wyttenbach CR (eds) Coelenterate Biology 2003: Trends in Research on Cnidaria and Ctenophora. Springer Netherlands, Dordrecht, p 549-556

Hagy JD, Boynton WR, Sanford LP (2000) Estimation of net physical transport and hydraulic residence times for a coastal plain estuary using box models. Estuaries 23:328-340

Hamner WM, Dawson MN (2009) A review and synthesis on the systematics and evolution of jellyfish blooms: advantageous aggregations and adaptive assemblages. Hydrobiologia 616:161-191

Han CH, Uye SI (2009) Quantification of the abundance and distribution of the common jellyfish Aurelia aurita sl with a Dual-frequency IDentification SONar (DIDSON). Journal of Plankton Research

Holst S, Jarms G (2007) Substrate choice and settlement preferences of planula larvae of five Scyphozoa (Cnidaria) from German Bight, North Sea. Mar Biol 151:863-871

Holst S, Jarms G (2010) Effects of low salinity on settlement and strobilation of scyphozoa (Cnidaria): Is the lion's mane Cyanea capillata (L.) able to reproduce in the brackish Baltic Sea? Hydrobiologia 645:53-68

Hoover RA, Purcell JE (2009) Substrate preferences of scyphozoan Aurelia labiata polyps among common dock-building materials. Hydrobiologia 616:259-267

Hubot N, Lucas CH, Piraino S (2017) Environmental control of asexual reproduction and somatic growth of Aurelia spp. (Cnidaria, Scyphozoa) polyps from the Adriatic Sea. PLoS One 12:16

Kaneshiro-Pineiro MY, Kimmel DG (2015) Local Wind Dynamics Influence the Distribution and Abundance of *Chrysaora quinquecirrha* in North Carolina, USA. Estuaries and Coasts 38:1965-1975

Kimball ME, Rozas LP, Boswell KM, Cowan Jr JH (2010) Evaluating the effect of slot size and environmental variables on the passage of estuarine nekton through a water control structure. Journal of Experimental Marine Biology and Ecology 395:181-190

Levin SA (1992) The problem of pattern and scale in ecology: the Robert H. MacArthur award lecture. Ecology 73:1943-1967

Lucas CH (1996) Population dynamics of *Aurelia aurita* (Scyphozoa) from an isolated brackish lake, with particular reference to sexual reproduction. Journal of Plankton Research 18:987-1007

Lucas CH (2001) Reproduction and life history strategies of the common jellyfish, Aurelia aurita, in relation to its ambient environment. Hydrobiologia 451:229-246

Lucas CH, Graham WM, Widmer C (2012a) Jellyfish Life Histories: Role Of Polyps In Forming And Maintaining Scyphomedusa POPULATIONS. In: Lesser M (ed) Advances in Marine Biology, Vol 63, Vol 63. Elsevier Academic Press Inc, San Diego, p 133-196

Lucas CH, Graham WM, Widmer C (2012b) Jellyfish Life Histories: Role of Polyps in Forming and Maintaining Scyphomedusa Populations. Advances in marine biology 63:133

Lucas CH, Jones DOB, Hollyhead CJ, Condon RH and others (2014) Gelatinous zooplankton biomass in the global oceans: geographic variation and environmental drivers. Global Ecology and Biogeography 23:701-714

Makabe R, Kurihara T, Uye S-I (2012) Spatio-temporal distribution and seasonal population dynamics of the jellyfish *Aurelia aurita* s.l. studied with Dual-frequency IDentification SONar (DIDSON). Journal of Plankton Research 34:936-950

Mills CE (2001) Jellyfish blooms: are populations increasing globally in response to changing ocean conditions? Hydrobiologia 451:55-68

Olesen NJ, Frandsen K, Riisgard HU (1994) Population-Dynamics, Growth And Energetics Of Jellyfish *Aurelia-Aurita* In A Shallow Fjord. Marine Ecology Progress Series 105:9-18

Pitt KA (2000) Life history and settlement preferences of the edible jellyfish Catostylus mosaicus (Scyphozoa : Rhizostomeae). Marine Biology 136:269-279

Pitt KA, Budarf AC, Browne JG, Condon RH (2014) Bloom and Bust: Why Do Blooms of Jellyfish Collapse? In: Pitt KA, Lucas CH (eds) Jellyfish Blooms. Springer Netherlands, Dordrecht, p 79-103

Purcell JE, Grover JJ (1990) Predation And Food Limitation As Causes Of Mortality In Larval Herring At A Spawning Ground In British-Columbia. Marine Ecology Progress Series 59:55-61

Purcell JE (1992) Effects of predation by the scyphomedusan *Chrysaora quinquecirrha* on zooplankton populations in Chesapeake Bay, USA. Marine Ecology Progress Series 87:65-76

Purcell JE, Nemazie DA, Dorsey SE, Houde ED, Gamble JC (1994) Predation mortality of bay anchovy Anchoa mitchilli eggs and larvae due to scyphomedusae and ctenophores in Chesapeake Bay. Marine Ecology Progress Series 114:47-58

Purcell JE, Arai MN (2001) Interactions of pelagic cnidarians and ctenophores with fish: a review. Hydrobiologia 451:27-44

Purcell JE (2005) Climate effects on formation of jellyfish and ctenophore blooms: a review. J Mar Biol Assoc UK 85:461-476

Purcell JE, Uye S-i, Lo W-T (2007) Anthropogenic causes of jellyfish blooms and their direct consequences for humans : a review. Marine Ecology Progress Series 350:153-174

Purcell JE (2012) Jellyfish and Ctenophore Blooms Coincide with Human Proliferations and Environmental Perturbations. In: Carlson CA, Giovannoni SJ (eds) Annual Review of Marine Science, Vol 4, Vol 4. Annual Reviews, Palo Alto, p 209-235

Rahbek C (2005) The role of spatial scale and the perception of large-scale species-richness patterns. Ecology letters 8:224-239

Richardson AJ, Bakun A, Hays GC, Gibbons MJ (2009) The jellyfish joyride: causes, consequences and management responses to a more gelatinous future. Trends in Ecology & Evolution 24:312-322

Rozas LP, Minello TJ (1997) Estimating densities of small fishes and decapod crustaceans in shallow estuarine habitats: a review of sampling design with focus on gear selection. Estuaries 20:199-213

Shahrestani S, Bi H, Lyubchich V, Boswell KM (2017) Detecting a nearshore fish parade using the adaptive resolution imaging sonar (ARIS): An automated procedure for data analysis. Fisheries Research 191:190-199

Shahrestani S, Bi H (2018a) Settlement and survival of *Chrysaora* chesapeakei polyps: implications for adult abundance. Marine Ecology Progress Series in press

Shahrestani S, Bi H (2018b) Settlement and survival of *Chrysaora* chesapeakei polyps: implications for adult abundance. Marine Ecological Progress Accepted

Shahrestani S, Bi H, Lankowicz K, Fan C, McLean N, Zhang L (*Submitted*) Spatial structure of *Chrysaora chesapeakei* medusae within a shallow coastal waterscape. Limnology and Oceanography

Sommer U, Stibor H, Katechakis A, Sommer F, Hansen T (2002) Pelagic food web configurations at different levels of nutrient richness and their implications for the ratio fish production: primary production. Hydrobiologia 484:11-20

Sponaugle S, Cowen RK, Shanks A, Morgan SG and others (2002) Predicting self-recruitment in marine populations: Biophysical correlates and mechanisms. Bull Mar Sci 70:341-375

Suchman CL, Sullivan BK (2000) Effect of prey size on vulnerability of copepods to predation by the scyphomedusae Aurelia aurita and Cyanea sp. Journal of Plankton Research 22:2289-2306

Sullivan LJ, Kremer P (2011) Gelatinous Zooplankton and Their Trophic Roles, Vol. Elsevier Academic Press Inc, San Diego

Turner MG, Dale VH, Gardner RH (1989) Predicting across scales: theory development and testing. Landscape ecology 3:245-252

Wiegner TN, Seitzinger SP, Breitburg DL, Sanders JG (2003) The effects of multiple stressors on the balance between autotrophic and heterotrophic processes in an estuarine system. Estuaries 26:352-364

Wiens JA (1989) Spatial scaling in ecology. Functional ecology 3:385-397

Zhang F, Sun S, Jin X, Li C (2012) Associations of large jellyfish distributions with temperature and salinity in the Yellow Sea and East China Sea. Hydrobiologia 690:81-96

Figures and Tables

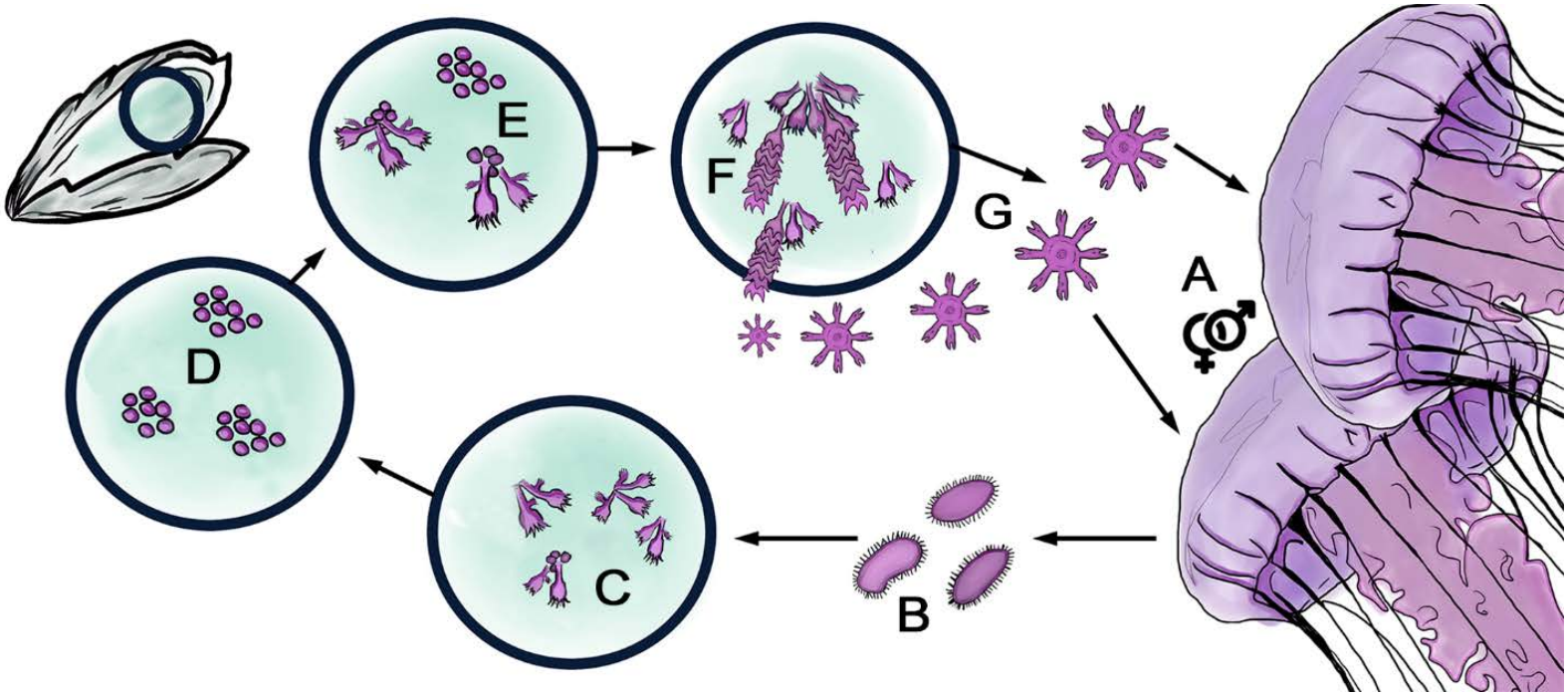

Figure 1. 1 The depiction of the scyphozoan life cycle adapted from descriptions and figures in Arai (2012). Lifecycle was amended to include seasonality of *Chrysaora chesapeakei* polyps in Chesapeake Bay. Dioecious male and female medusae **(A)** reproduce via proximity spawning from summer-early fall, whereby planula larvae **(B)** are released. Planula larvae are cued to settle on hard

substrate (i.e., oyster shell) and propagate via budding **(C)** to increase densities before encystment in the late fall **(D)**. If encysted polyps survive the winter, they excyst in the spring and begin to propagate via budding **(E)**. With rising temperatures in the spring, excysted and newly budded polyps strobilate **(F)** and release juvenile ephyrae into the water column **(G)**

Table 1.1 Observers for the visual counts of *Chrysaora* chesapeakei at the Chesapeake Biological Laboratory (Solomons, Maryland) research pier.

Years	Observer
1960-1991 (1989 missing)	D. Cargo, M. Wiley, H. Millsaps
1992-1993	M. Wiley
1994-1998	H. Millsaps
2001-2002	E. Setzler-Hamilton
2005-2008	R. Burrell
2013-present time	S. Shahrestani, H. Bi

Table 1.2 Variables contributing to the survival and distribution of *Chrysaora* polyps in Chesapeake Bay.

Variable	Source	Conclusions
Substrate	(Cargo & Schultz 1966, Duarte et al. 2012)	Sheltered oyster shell and rock are preferred substrates for settlement.
Nutrition	Littleford 1939	Low food availability decreases polyp size without encystment.
Predation	(Cargo & Schultz 1967)	Nudibranchs eat polyps but not podocysts.
DO	Condon et al. 2012	No encystment in low DO.
pH	Winans and Purcell 2010	No data for *Chrysaora quinquecirrha*. *Aurelia labiata* polyps tolerant of pH (7.9, 7.5, 7.2)
Salinity	(Cargo & King 1990b)	Optimal is 10-25 ppt Encystment occurs at salinities <7.
Temp	Cargo and Shultz 1967, Loeb 1972, Calder 1972, Purcell et al. 1999	Cooling towards 2-5 C causes encystment; Warming to 15-18 C causes excystment. Prolonged cooling and then warming to 20-21 C induces strobilation.

Chapter 2: Detecting nearshore pelagic organisms using the adaptive resolution imaging sonar (ARIS): An automated procedure for data analysis[1]

Abstract

Recent developments in sonar imaging provide an efficient way of obtaining near video quality of free-swimming fish in hard to reach areas, e.g., permanent structures like docks and piers, and hard to see environments, e.g., highly turbid waters. However, processing large volumes of data output by sonar imaging systems remains a major challenge. In the present study, we developed an automated image processing procedure to process footage recorded for 59 consecutive hours using an Adaptive Resolution Imaging Sonar, ARIS Explorer 3000 (Sound Metrics INC) deployed at a fixed location. Our approach successfully counted large free-swimming fish at a precision rate >94% and estimated sample volume with manual and automatic calculations being highly correlated (r = 0.96). An auto-regressive time series model (of the sixth or higher order) with a zero-inflated Poisson distribution was used to estimate local abundance. Fish counts were low to zero during the first 31 h of sampling, and a major influx of fish occurred in the last 28 h. The observed pattern was co-incidental with local weather patterns: intermittent thunderstorms in the first 32 h and relatively calm weather in the last 24 h. Though thunderstorms limited our conclusions on fish-pier usage with tidal and diurnal cycles, it is apparent that weather conditions play a role in pier usage by large fish. Overall, the ARIS3000

[1]Shahrestani, Suzan, et al. "Detecting a nearshore fish parade using the adaptive resolution imaging sonar (ARIS): An automated procedure for data analysis." *Fisheries research* 191 (2017): 190-199.

deployment, automated data processing and statistical analyses used in this study proved successful in studying fish affiliations with piers in shallow habitats.

Introduction

Sonar cameras like the DIDSON and ARIS (SoundMetrics Inc.) are valuable tools used to sample marine species abundance, size and behavior within hard-to-observe, structurally complex, turbid and dark environments. The adaptive resolution imaging system (ARIS) has solved many limitations regarding marine and freshwater sampling, with ground-truthed observations of fish populations and other species (Boswell et al. 2007, Becker et al. 2011a, Crossman et al. 2011, Able et al. 2014). However, the advancements in technology come at a cost, e.g., processing large quantities of information is required to maintain the resolution of the data.

If deployments are short, and data output is small, manual counting is a viable option. However, for longer or repeated deployments, with longer durations of sonar data, manual processing becomes very taxing and arduous. Furthermore, subsampling and reducing the number of images to be manually processed causes a loss in resolution. Semi-automated post-processing of sonar data can be accomplished using available software (Echoview, Software Pty Ltd) which reduces processing effort and maintains high-resolution data. Acoustic signals from the sonar data are processed to reveal fish size, abundance, speed, and direction of travel (Boswell et al. 2008). However, acoustic-based procedures are quite complex, and the required software can be very expensive. In contrast, post-processing of data using image analysis is a low-cost and simple method that has proven successful in many scientific applications. Furthermore, semi-automated processing requires some measure of human input to

complete the processing procedure while automating the procedure requires no interaction outside of initialization. Semi-automating a procedure allows for more flexibility, i.e. (generalized commercial software), though full automation has the benefit of not requiring a human operator. Several semi-automated image processing procedures have been used to count zooplankton images successfully with a suite of tools available in Matlab and R, i.e. ZOOSCAN (Grosjean et al. 2004) and ZOOVIS (Bi et al. 2015). The process involves breaking down sonar data into individual frames and then using algorithms to detect, segment, and measure target objects (fish and other species) through a semi-automated iterative process.

The principal objective of this chapter was to use image analysis as a tool to ameliorate manual processing of long lengths of sonar data collected from the Patuxent River, in the Chesapeake Bay. To do so, I: (1) recorded fish over the course of three days to capture tidal and diurnal cycles using an ARIS sonar camera, (2) developed and implemented an automated image processing procedure to process 59 hours of sonar data, (3) analyzed data within an appropriate statistical time-series framework.

It should be noted that fish were used as model organisms in this chapter because we did not record jellyfish in our 2015 deployment. However, most of the methods described in this chapter detail the processing procedures applied to all sonar data collected and processed in this dissertation to calibrate sampling with a sonar camera. While jellyfish classification requires more robust techniques like Deep Neural Networking (DPP) when compared to fish classification, I was able to filter out more than half of the 2,000,000 images that contained no data (fish or jellyfish),

which greatly cut down on processing time for both automated (fish) and manual (jellyfish) counting procedures. Furthermore, I used automated image analysis techniques to process the sample volume of the data (frame by frame) to standardize counts between frames. All methodology required for deployment of the sonar camera and processing of the data for Chapters 3-4 are detailed in this chapter.

Materials and Methods

Study Area and ARIS Deployment

The Chesapeake Biological Laboratory (CBL) research pier (222 m in length) is located in the lower mesohaline portion of the Patuxent River (a subestuary of Chesapeake Bay), approximately 2.5 km away from the river mouth (Fig. 2.1). The research pier is approximately 350 m away from an NOAA monitoring station (StationID 8577330), which was the source of tidal data. All tidal heights used in this study are relative to the Mean Lower Low Water (MLLW) and are available on the NOAA website (Fig. 2.2, http://tidesandcurrents.noaa.gov). Other environmental data (pressure), were obtained from the Patuxent River Naval Air Station located in St. Mary's, Maryland.

To observe fish presence near the CBL research pier an ARIS3000 was deployed and captured high-resolution sonar data for 59 h. For this study, the ARIS was configured to operate at 3.0 MHz, providing a high-resolution acoustic image, with a maximum sampling range of 5 m. The range end can be manually adjusted to vary sample volume and was fixed to ensure the sea floor was consistently visible, particularly during high tide. The ARIS was integrated into a 2-axis rotator (AR2) which allows for manual or automated control of the sonar heading (azimuth) and

pitch. The AR2 was attached to a mounting pole affixed to a floating dock at the end of the research pier (Fig. 2.1). The transducer was submerged just below the water's surface and was aimed downward (vertical) towards the seafloor (Fig. 2.3A). The whole system moved freely with the floating pier during tidal oscillation. The horizontal deployment was first considered to maximize sample volume whereby the range is not limited by the sea floor, and to improve the resolution of the data with subsequently more accurate fish metrics. However, due to the shallow nature of the study site, horizontal deployment caused sonar beams to be lost once above the water's surface resulting in noisy data unfit for image analysis.

The ARIS deployment occurred during the day and night, over the course of four days from 7/14/2014 through 7/17/2014, capturing data over the course of 5 high tides and 5 low tides. The sampling was continuous with one large gap of approximately 9 h. During the 9 h of no recording, the deployment of the instrument needed to be reconfigured to account for an oncoming storm.

Calculating Sample Volume

To calculate the sampling volume, an equation to calculate the volume of a truncated pyramid with a rectangular base was utilized. This shape best matched the detectable sample space of an ARIS3000 deployed with a downward orientation (Fig. 2.3). The equation calculates the volume, by cutting away a portion of a pyramid on a plane 1m from the top of the pyramid, parallel to its base. Truncation of the first meter of the pyramid accounts for undetected space (i.e. near-field dead-zone). The volume of a truncated pyramid is calculated using Equations (1, 2 & 3).

$$Volume = \frac{h}{6}\left(A_1 + A_2 + \sqrt{A_1 + A_2}\right) \quad (1)$$

$$A_{1=} \text{ (0.5*h) x (0.25*h)} \quad (2)$$

$$A_{2=} \text{ (0.5*1m) x (0.25*1m)} \quad (3)$$

Whereby, *h* is the height of the truncated pyramid (the sample range – 1-meter undetectable space), A_1 is the area of the base of the pyramid, and A_2 is the area of the plane (Fig. 2.3B). To calculate the area of the rectangular base and plane, methods were used similar to those described by Han and Uye (2009b) whereby the height of the pyramid is multiplied by 0.25 to calculate the width, and 0.5 to calculate the length of the rectangular pyramid base. Sample ranges were extracted from the raw ARIS data output and matched with data using assigned time-stamps.

Image Processing

The sonar data comprised ~59 h of recorded video, resulting in approximately 637,200 static acoustic images (frames) recorded at a rate of 3 fps (frames per second). The signals were converted to video files (MP4 format) using ARISfish (version 2.5, Soundmetrics). Before video conversion, the background (i.e., substrate and other static objects <3cm) was removed following an adaptive algorithm available in ARISfish. The size threshold for background subtraction was set to avoid removal of small forage fish ranging in size from 3 – 10cm. To analyze the large volume of images, image processing techniques similar to Bi et al. (2015), were developed in Matlab 8.3 using the Computer Vision Toolbox, Image Processing Toolbox and Statistical Toolbox (MathWorks Inc., Natick, MA, 2014). In Matlab,

developed algorithms broke down the MP4 videos into individual TIFF images that were 568 by 468 pixels in size.

The TIFF images extracted from the MP4 videos were subsampled every 5 seconds (15 frames) for a total of 42,480 frames. Each static frame was processed with a series of algorithms to calculate sample volume and detect fish within each frame. Fish observations and sample volume were averaged over five-minute intervals, to account for the temporal autocorrelation inherent in such fine-scale data (Section 2.4). The major process to extract fish and volume data from the frames includes three modules: (1) calculating pixels per meter, (2) identifying and segmenting target objects and (3) classifying and counting fish among a pool of target objects.

To assign real-world units to metrics of fish measurements I needed to convert pixel width to metric units, using values of PPM. The PPM of each frame differs with variations in sampling range, so PPM calculations were carried out for each processed frame. To calculate PPM the centroids of the 1m and 2m range markers were used. Range markers correspond to the viewing distance from the instrument (Fig. 2.4A); the highest value marker representing the range end (not visible in Fig. 2.4A). The 1-meter pixel distance between the 1m and 2m range markers is thus the difference between the y-axis pixel coordinates of their range marker centroids. To identify the pixel coordinates of the range markers, image analysis techniques, coupled with machine learning classification were developed. The average pixel area of the range markers in the frames was (5*9 pixels), so objects in a frame with areas larger than 10*10 pixels were removed. With only smaller objects remaining (range markers,

small fish, and noise) the algorithms segmented each Region of Interest (ROI) and used an SVM (Support Vector Machine) classifier to identify each ROI as either a "1", "2", or "other."

The SVM procedure was utilized to classify and locate the y-axis of segmented range markers. SVM classification is a binary process that compares segmented ROIs to a library of known objects. Often referred to as "one-versus-all", the classifier categorizes all ROIs into two groups. With the "one" and "all", being an unidentified ROI versus a library of known ROIs respectively. For example, after segmenting the range markers in a frame, one segmented ROI with an unknown meter denotation (1, 2, 3, etc.) is compared to a library of 100 synthetic '2' images available in the Computer Vision Toolbox. If the unknown range marker is indeed a '2', the SVM classifier will label it with a 1 (positive prediction), while if the unknown range marker is not a '2', but a small fish, the classifier will label it with a 0 (negative prediction). In this way, the process could identify, label and locate all the segmented ROIs fed through the SVM classifier. The SVM classifier then compares each given ROI to the objects in the synthetic digit library. The comparisons are made using Histograms of Oriented Gradients (HOGs) descriptors. HOG descriptors describe the spatial pattern of an object by gridding the object into cells and then creating a histogram of gradient directions within each cell. For details, see Bi et al. (2015). In the present study, a sensitivity analysis was performed to identify the most appropriate cell size for the HOG descriptors (4*4). The chosen cell size is unique to the range markers in the study, and best described the typography. Once the range markers were identified and labeled, the coordinates of their centroids were used to

calculate the vertical pixel width, between a “1” and “2” range marker, revealing the number of pixels that make up the width of one meter. This information was used to calculate the PPM unique to each frame, allowing me to convert from metric units to pixels.

All images were enhanced to optimize the identification and segmentation of fish ROIs. The process was started by applying a watershed transformation. This operation considers watershed regions with light areas as “high elevation” and dark areas as “low elevation” and produces “catchment basins”. Watershed transformations take advantage of the high graphical resolution of the ARIS data because it accounts for shading within RGB images (Fig. 2.4D). Continuing enhancement, images are converted to grayscale, and edge detection is applied to separate individual ROIs. Edge detection in this study was performed using multi-edge detection (Fig. 2.4E) that utilizes a wavelet analysis (Li 2003). Simply put, an edge detector performs like a high-pass filter that perceives edges, or contours of an image where brightness changes suddenly. The edge detection identified target objects such as fish and the sea floor. Once the edges of an object were detected, they were filled in (Fig. 2.4F) and segmented by cropping the ROI from the original image with a bounding box, which is the smallest possible rectangle that can contain the object (Fig. 2.4A).

Each cropped ROI (Fig. 2.4A) was described using HOGs and fed through an SVM classifier trained with a library of fish, seafloor objects, and “other” objects such as noise. The library of fish was compiled using 10 fish images in lateral, posterior and anterior views. The positive identifications of fish-ROIs in each frame

were enumerated and represented the large fish count for each image. Small fish were difficult to enumerate due to the overlap of individual fish within their swimming school (Fig. 2.4B). The small fish data in this study were manually counted, and analysis of the area, size, and height of 200 subsampled small fish-ROIs and 300 large fish-ROIs was used to set limits for small and large size classifications of positively identified fish in each frame. The function 'regionprops', included in the Image Processing Toolbox of Matlab, reports area as well as major and minor axis lengths of an ellipse fit to a fish-ROI, which corresponds to length and width of the fish-ROI respectively. Size classifications of counted fish were determined by examining the distribution of fish-ROI surface area, length, and height which represent rough approximations of fish size (Fig. 2.5).

Validation and Error

In validating the accurate estimation of the distance between range markers, 500 frames were randomly sub-sampled in R (version 3.2.2), and distances between the 1 m and 2 m range marker were manually measured within each frame using the ruler tool in Photoshop (version CS6). In validating PPM, Pearson's correlation test and a paired t-test were used to test for significant differences between manually and automated PPM values.

A second validation procedure was performed to assess the accuracy of counting large fish. Empty frames were excluded from the validation procedure, due to the overwhelming number of zeros that skewed the data. Large fish were manually counted in 3,447 frames where large fish were detected and used to calculate the true

positive rate (percentage) of correctly counted fish. True positive matches were considered for values with less than a 1.5 difference in mean values of fish across 5-minute intervals. Here, true positive rates closer to 1 (100%) is considered optimal. Finally, descriptive statistics and a paired t-test were used to compare automated and manually counted fish. Much of the differences between computer counts of fish ROIs and observer counts were due to demersal fish oriented at the bottom that could not be automatically parsed from the sea floor. The main cause of this error is due to the compression of a 3D sample space (X*Y*Z), to a 2D (X*Y) image. Objects in the 3D sample space occupying the same X, Y position and differing in their Z coordinate (i.e. sea floor and demersal fish) overlap and are counted as one object.

Forecasting Fish Counts

Fish densities were calculated for each frame using the fish count and sample volume of each frame and then averaged over 5-minute intervals. The data were split into training (70% or 430 observations) and test set (the last 30% or 183 observations, Fig. 2.6). The training set was used to specify and estimate the models, whereas the testing set was employed only to assess the models' performance (see more on data splitting in Chapter 8.5.4 by (Chatfield 2000) and references therein). Fast decays in empirical autocorrelation functions (ACF) and results of the augmented Dickey-Fuller test (Said & Dickey 1984) were used to confirm stationarity of the time series. For the large fish count data with potential temporal autocorrelation, an autoregressive–moving-average (ARMA) models (Equation (4)) with zero-inflated Poisson (ZIP) or negative binomial distributions (NBI) were developed. These

models can be considered a simplified version of generalized autoregressive moving average models (GARMA, (Benjamin et al. 2003, Rigby & Stasinopoulos 2005, Stasinopoulos & Rigby 2007))):

$$\ln(\mu_t) = \beta_0 + \sum_{j=1}^{p} \varphi_j \{\ln(y^*_{t-j}) - \beta_0\} + \sum_{j=1}^{q} \theta_j \{\ln(y^*_{t-j}) - \ln(\mu_{t-j})\} \quad (4)$$

where μ_t is a conditional mean, β_0 is intercept; φ_j and θ_j are autoregressive and moving average coefficients, and p and q are respective orders; $y^*_{t-j} = \max(y_{t-j}, c)$ and $0 < c < 1$ to replace any 0 values of y_{t-j} before applying the ln function. To check for the presence of autoregressive conditional heteroscedasticity (ARCH), ACF were examined (not shown here, available from the authors upon request) of squared residuals from the models. Four models were tested on the fish data: AR(3) and AR(6) models with ZIP and NBI distributions.

For comparative assessment of time series models, the testing set and the following criteria: mean absolute error (MAE) of 1-step ahead forecasts and observed coverage of the 95% prediction intervals (parametric and bootstrap) were utilized. Parametric intervals are obtained using the Wald method (Normal approximation, see (Shilane et al. 2010) for more details) when dealing with model residuals (i.e., for large fish counts). bootstrap intervals (Efron 1992) by resampling the model residuals with replacement were also obtained.

Results

Validation of Automated Procedures

The image processing procedure in this study allowed me to subset frames with no ROIs of interest and exclude them from the validation procedure. Of the 30,704 frames processed in this study, 3,447 contained ROIs of interest and were manually processed. The true positive rate of large fish counted was 94.6% (Table 2.1). An analysis of 500 randomly subsampled fish-ROIs, manually identified as large or small fish, revealed less than 1% of small fish-ROIs with heights greater than 3 cm, and widths less than 10 cm. Fish with widths less than 10 cm, and heights over 3 cm were large fish with anterior or posterior orientations. Small-fish-ROI area was on average 6 cm^2 (Fig. 2.5B), while large fish-ROIs had an average area of 89 cm^2 (Fig. 2.5A). Fish-ROIs with widths (approximated total length) less than 10 cm were classified as small fish.

Fish Pier-Usage

For the first 30 h of sampling, fish were counted in very low numbers. The peak of large-fish density occurred after sunset on July 16th, 2014 (Fig. 2.6). Small-fish peaks were observed in the early mornings between 05:00 and 08:00 of the third and fourth day (July 16th - 17th, 2014). The fish counts were not correlated with diurnal or tidal cycles. On the first and second nights of this study, there were severe thunderstorms that may have regulated fish occupancy of the shallows. Though the temporal resolution is high, the study duration only allowed us to capture one storm

event, and thus limits the conclusions on correlations with environmental conditions that operate at larger temporal scales.

Forecasting Fish Counts with Time Series Modeling

Fast decays in autocorrelation functions and results of augmented Dickey-Fuller test (Said & Dickey 1984) confirmed stationarity of the time series. Following examination of ACF analysis, large fish counts exhibited serial dependence, which is expressed as an autoregressive process of the sixth (AR(6)) or higher order. Bayesian information criteria (BIC) concurred with visual inspection of ACF plots in selecting the AR(6) model for large fish counts, but Akaike information criterion (AIC) suggested the selection of an AR(3) model contrary to visual analysis. The residual diagnostics of the AR(3) and AR(6) models with ZIP and NIB distributions showed satisfactory results and are further summarized in Table 2.2.

The best model used to forecast the large fish counts is the AR(6) model paired with ZIP distribution (Table 2.2). It had the lowest MAE and the highest interval coverage among all tested models, though bootstrap confidence intervals revealing point estimate variations were the same for both the AR(3)+ZIP and AR(6)+ZIP models. Note that bootstrapping performed better when normality of residuals did not hold (AR(3)+ZIP and AR(6)+ZIP). In the cases when Shapiro–Wilk normality test p-values were >0.05, and the hypothesis of normality could not be rejected (AR(3)+NBI and AR(6)+NBI), parametric approximations were no worse than bootstrap. I opted to use bootstrap to calculate the intervals since it allowed relaxation of distributional assumptions for the slightly heavy-tailed residuals. One-step-ahead forecasts of the AR(6)+ZIP model can be seen in (Fig.2.7).

Discussion

Fish-pier affiliations with man-made structures manifest with complex spatiotemporal complexities that affect trophodynamics in shallow estuarine environments (Able 2005a). These affiliations are often understudied, due to the logistical demands of sampling. This study demonstrates methods of unobtrusive sonar sampling that can be continuously deployed for long durations of time in hard-to-sample areas. The high temporal resolution at both larger and smaller scales is coupled with high-quality images that can reveal fish behavior, size, species, and abundance. In deploying the instrument, I recorded fish presence at a research pier for a small window of time. However, based on the results, continuous monitoring of fish from a fixed location with automated processing appears to be highly feasible. The low effort required for the image processing procedure counteracts laborious manual processing that often limits longer durations of sampling. The high spatial and temporal resolution and accurate counting algorithms could greatly enhance research efforts toward estimation of fish abundance and habitat utilization. Furthermore, the methods and potential applications of this study are versatile and could be utilized to answer questions on fish interactions with other structures, i.e. artificial reefs (Bollinger & Kline 2015), fish attraction devices (FADs) as well as the developed, modified and natural shoreline.

The Automated Procedure

The low cost, effort and time required for automated processing when compared to manual processing is perhaps the greatest advantage of this procedure.

Rich datasets are much more efficiently processed, subsequently improving the access to high-resolution data. Continuous monitoring efforts usually bogged down by high data output, can be matched with automated processing to reveal patterns across a range of temporal scales. The automated process is also customizable, which could increase accuracy if the statistical properties of target fish are incorporated into the algorithms to fine-tune identification procedures. Furthermore, because sample space is accounted for, the procedure can also be used to process data captured with mobile deployments or in other sampling scenarios.

The automated procedure processed 59 hours of video captured in low clarity water under the CBL research pier. I was able to record data of large fish at a recording rate of 3 fps, and then process the data automatically counting large fish with a precision >94%. The cause for error in the processing procedure for counting large fish was due, in part, to demersal fish that were oriented at the bottom of the seafloor. Here, an overlap of information, due to the projected beam volume, made it difficult to detect the edges and segment the large fish (Fig. 2.4B). These issues have also been described in other studies using imaging sonars (Able et al. 2014). The procedure worked best on large fish oriented at the middle or top of the frame or water column. Edge detection algorithms (Li 2003) operated with optimal results and provided fish shape characteristics that enabled more accurate fish count using statistical properties such as approximated surface area, length, and width. Fish species could not be identified with great certainty, though demersal fish often resembled croaker and white perch common to the area (Jung & Houde 2003). Fish in the upper parts of the water column exhibited features similar to juvenile striped bass,

bluefish, and other major pelagic fish found in Chesapeake Bay (Jung & Houde 2003). Other species that were conclusively identified in the sonar data include the American eel (*Anguilla rostrata*), cownose ray (*Rhinoptera bonasus*) as well as several blue crabs (*Callinectes sapidus*). At first inanimate objects were mislabeled as fish (branches and rocks), which led us to perform a visual analysis on ROIs incorrectly identified as fish and incorporate them into the classifier library as ‘other'. Here the HOGs descriptors guiding the classifier worked well in distinguishing large fish from inanimate objects such as rocks and branches and reduced the error of the procedure.

Conversion from the ARIS files to MP4 files consumed the most time, as the video files are converted in real-time so that 59 hours of video would take ~59 hours to convert to MP4 videos. Future developments of open-source software (i.e. ARISreader, https://github.com/nilsolav/ARISreader) will eliminate video conversion, allowing for image extraction directly from ARIS files. After breaking down the 59 hours of data and subsampling every 5 seconds, I was able to process ~40,000 frames in under 24 hours. Gauging the time required to process data requires consideration of the classifier library (controlling error rate) and the number of frames containing fish ROIs. The complexity of these factors is inherent in the actual data acquired and may vary from deployment to deployment. It is for these reasons that I was unable to quantify the overall computational demand and speed for this procedure. However, increasing the temporal scale i.e. from seconds to minutes, proportionally decreases the processing time; decreasing the number of frames to be processed.

The automated procedure was mostly limited by the frame rate (3 fps) of the data collected in this study. In future studies, data quality, resolution and image processing would improve with maximized frame rates of 10 or more fps. With mobile deployment, a foreseeable difficulty may be optimizing tow speed for best camera performance to avoid movement noise. The process was also limited to certain species because others were excluded. The fish exclusion was attributed to the nature of sonar data collection and image output that prevented the algorithm from parsing demersal fish species from the sea floor.

The small schooling fish recorded in this study, could not be distinguished by species but more than likely comprised the three-dominant species of forage fish found in Chesapeake Bay; bay anchovies, silversides, or juvenile Menhaden (Jung & Houde 2003). Troubleshooting of issues attributed to small fish errors are in development, and future deployments at faster recording rates will aid in reducing the small fish counting error. Other concerns refer to the subjectivity often required in manual processing that automated processing does not address. In many instances, it was difficult to distinguish fish from inanimate objects. Only by going back to the data was one able to discern whether the object was indeed a fish by its swimming behavior. The automated procedure relies instead, on the HOG descriptors and SVM classifier to make the appropriate decisions in distinguishing fish from inanimate objects that may be less accurate though consistent.

Time-Series Forecasting

The data output of the fixed deployment methods was representative of time-series observations made over 59 hours. Sampling (recording) at a rate of 3 fps meant that the same fish were processed more than once in consecutive frames. Fish could potentially be tracked moving across the field of view on consecutive frames, but the track-line would cease once the fish exited the sample space. It would be impossible to differentiate between a new fish entering the sample space, and a previous visitor. The autocorrelation inherent in such datasets must be accounted for, so as not to inflate the type I error of statistical methods that assume normality and independence when testing for trends. In a similar deployment scheme (fixed-location), Hughes and Hightower (2015) modeled manually processed sonar counts by applying a Bayesian framework to estimate the expected number of anadromous fish migrants through a square meter of fish passage (sonar sampling space) per hour. The framework allowed them to calculate the daily passage rate using a Poisson generalized linear regression model which was a function of both 'Day' (time of acoustic camera deployment) and 'Stratum' (location of acoustic camera deployment). To account for the autocorrelation in their dataset, they modeled Day as their random autoregressive effect. I applied an alternative method of modeling count data by applying time-series forecasting techniques which are useful in detecting trends in datasets with autocorrelative structure. I averaged count data over 5-minute increments and used the best fit model which considered the count data (Poisson distribution), autoregressive trends and zero-inflation. Overall, I found the results of the model to be satisfactory. The performance of the model can further be substantiated by

considering the great differences observed between the training and test sets, whereby the training set had many zeros with most of the counts being observed in the test set (Fig. 2.6).

Conclusion

I outlined a procedure to process massive amounts of data from the ARIS3000 and show a successful method of image analysis to ameliorate the data-processing demand inherent in high-resolution data. The automated processing algorithms performed well, and I was able to provide a statistical framework using time-series models to estimate local abundance of fish at a fine temporal scale. Though I was unable to make any conclusive statements about fish-pier usage, the variability and extent of pier usage by fish was observed in great detail. The ability to capture accurate estimates of fish abundance continuously using a fixed location deployment will greatly aid the understanding of how fish interact with their habitats both natural and man-made. Furthermore, the techniques applied in this study were unique to the deployment and location but can easily be adapted to other deployments and further technological advancements to imaging systems. Though I was not able to apply automated methods to detect and classify jellyfish, the procedures detailed in this chapter are essential to generate sample volume and seafloor structure for all sonar data used in my research.

References

Able KW (2005) A re-examination of fish estuarine dependence: evidence for connectivity between estuarine and ocean habitats. Estuarine, Coastal and Shelf Science 64:5-17

Able KW, Grothues TM, Rackovan JL, Buderman FE (2014) Application of Mobile Dual-frequency Identification Sonar (DIDSON) to Fish in Estuarine Habitats. Northeastern Naturalist 21:192-209

Becker A, Cowley PD, Whitfield AK, Järnegren J, Næsje TF (2011) Diel fish movements in the littoral zone of a temporarily closed South African estuary. Journal of Experimental Marine Biology and Ecology 406:63-70

Benjamin MA, Rigby RA, Stasinopoulos DM (2003) Generalized Autoregressive Moving Average Models. Journal of the American Statistical Association 98:214-223

Bi H, Guo Z, Benfield MC, Fan C, Ford M, Shahrestani S, Sieracki JM (2015) A semi-automated image analysis procedure for in situ plankton imaging systems. PLoS One 10:e0127121

Bollinger M, Kline R (2015) Validating side scan sonar as a fish survey tool over artificial reefs in the Gulf of Mexico. The Journal of the Acoustical Society of America 137:2334-2334

Boswell KM, Wilson MP, Wilson CA (2007) Hydroacoustics as a tool for assessing fish biomass and size distribution associated with discrete shallow water estuarine habitats in Louisiana. Estuaries and Coasts 30:607-617

Boswell KM, Wilson MP, Cowan JH (2008) A Semiautomated Approach to Estimating Fish Size, Abundance, and Behavior from Dual-Frequency Identification Sonar (DIDSON) Data. North American Journal of Fisheries Management 28:799-807

Chatfield C (2000) Time-series forecasting, Vol. Chapman and Hall/CRC

Crossman JA, Martel G, Johnson PN, Bray K (2011) The use of Dual-frequency IDentification SONar (DIDSON) to document white sturgeon activity in the Columbia River, Canada. Journal of Applied Ichthyology 27:53-57

Efron B (1992) Bootstrap Methods: Another Look at the Jackknife. In: Kotz S, Johnson NL (eds) Breakthroughs in Statistics: Methodology and Distribution. Springer New York, New York, NY, p 569-593

Grosjean P, Picheral M, Warembourg C, Gorsky G (2004) Enumeration, measurement, and identification of net zooplankton samples using the ZOOSCAN digital imaging system. ICES Journal of Marine Science 61:17

Han CH, Uye SI (2009) Quantification of the abundance and distribution of the common jellyfish Aurelia aurita s.l. with a Dual-frequency IDentification SONar (DIDSON). Journal of Plankton Research 31:805-814

Hughes JB, Hightower JE (2015) Combining Split-Beam and Dual-Frequency Identification Sonars to Estimate Abundance of Anadromous Fishes in the Roanoke River, North Carolina. North American Journal of Fisheries Management 35:229-240

Jung S, Houde ED (2003) Spatial and temporal variabilities of pelagic fish community structure and distribution in Chesapeake Bay, USA. Estuarine, Coastal and Shelf Science 58:335-351

Li J (2003) A wavelet approach to edge detection. Sam Houston State University

Rigby RA, Stasinopoulos DM (2005) Generalized additive models for location, scale, and shape (with discussion). Journal of the Royal Statistical Society: Series C (Applied Statistics) 54:507-554

Said SE, Dickey DA (1984) Testing for unit roots in autoregressive-moving average models of unknown order. Biometrika 71:599-607

Shilane D, Evans SN, Hubbard AE (2010) Confidence intervals for negative binomial random variables of high dispersion. Int J Biostat 6: Article 10

Stasinopoulos DM, Rigby RA (2007) Generalized additive models for location scale and shape (GAMLSS) in R. Journal of Statistical Software VV

Figures and Tables

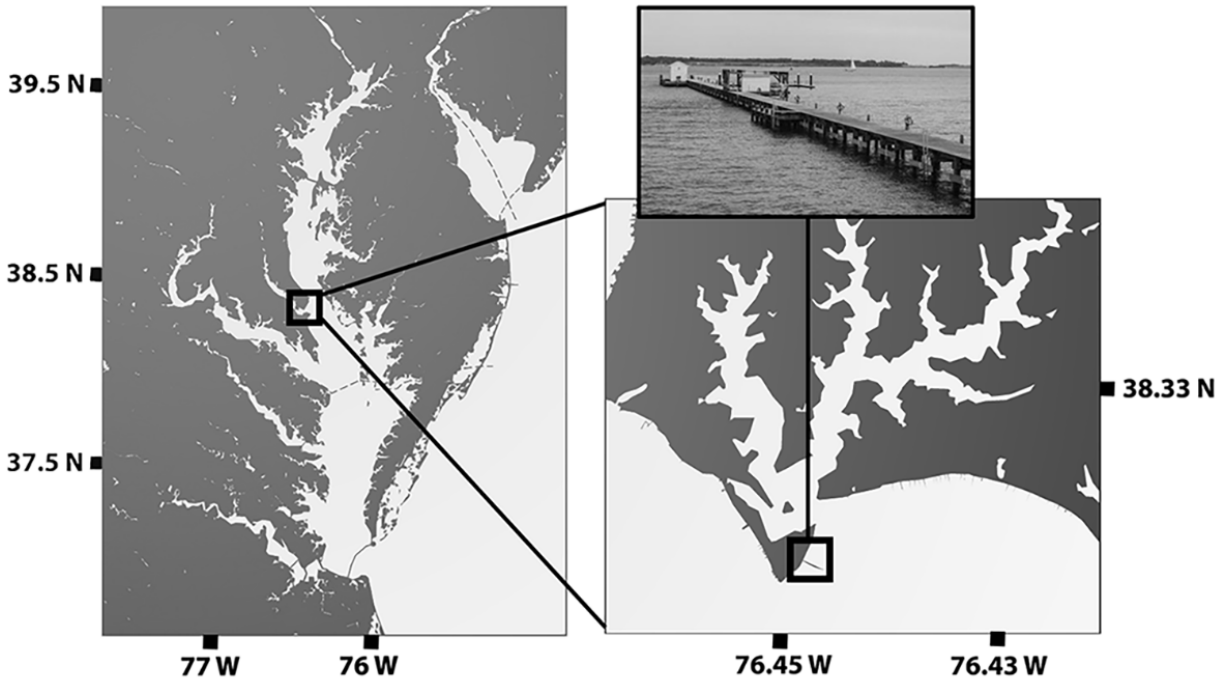

Figure 2.1 The location of the CBL research pier, at the mouth of the Patuxent River in Chesapeake Bay. The ARIS3000 was attached to the floating docks at the far end of the research pier.

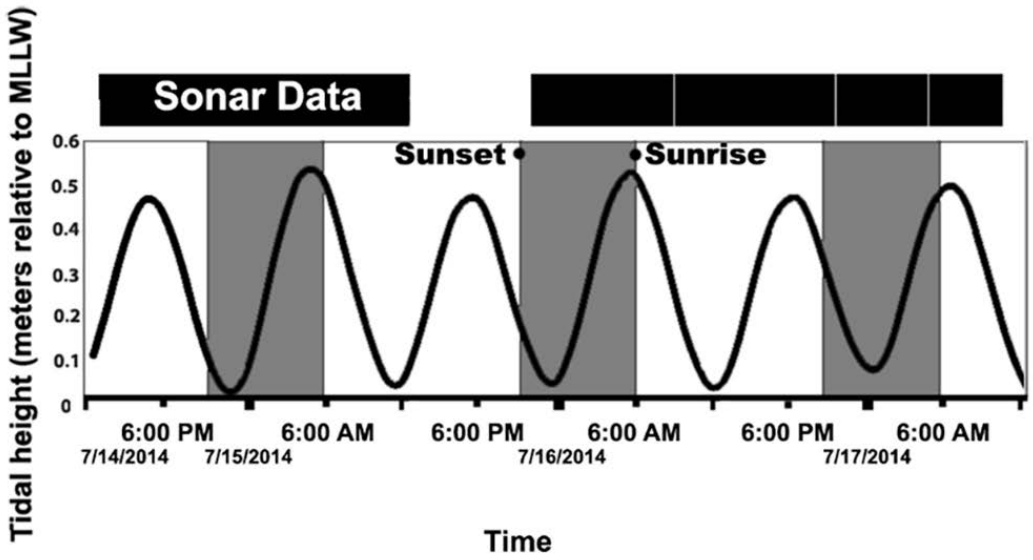

Figure 2.2 Duration of sonar data recorded from July 14, 2014 – July 17, 2014. Horizontal black bands represent individual video fragments. Alternating white and gray vertical bands represent the transition from day to night respectively. The black line indicates the daily tidal cycle at the time of recording.

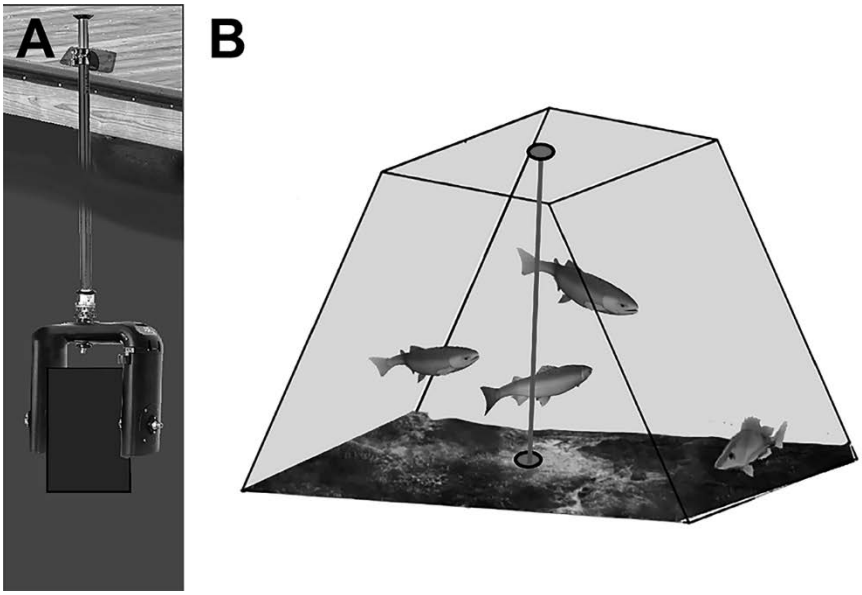

Figure 2.3 (A) Schematic representation of ARIS3000 deployment, with AR2 rotator and mounting pole. Note the downward orientation towards the sea-floor. (B) The depiction of the sample field recorded with the ARIS3000 deployment at a fixed location. The shape represents a truncated pyramid with a rectangular base. Gray vertical line denotes the sample range of the instrument used to calculate the sample volume.

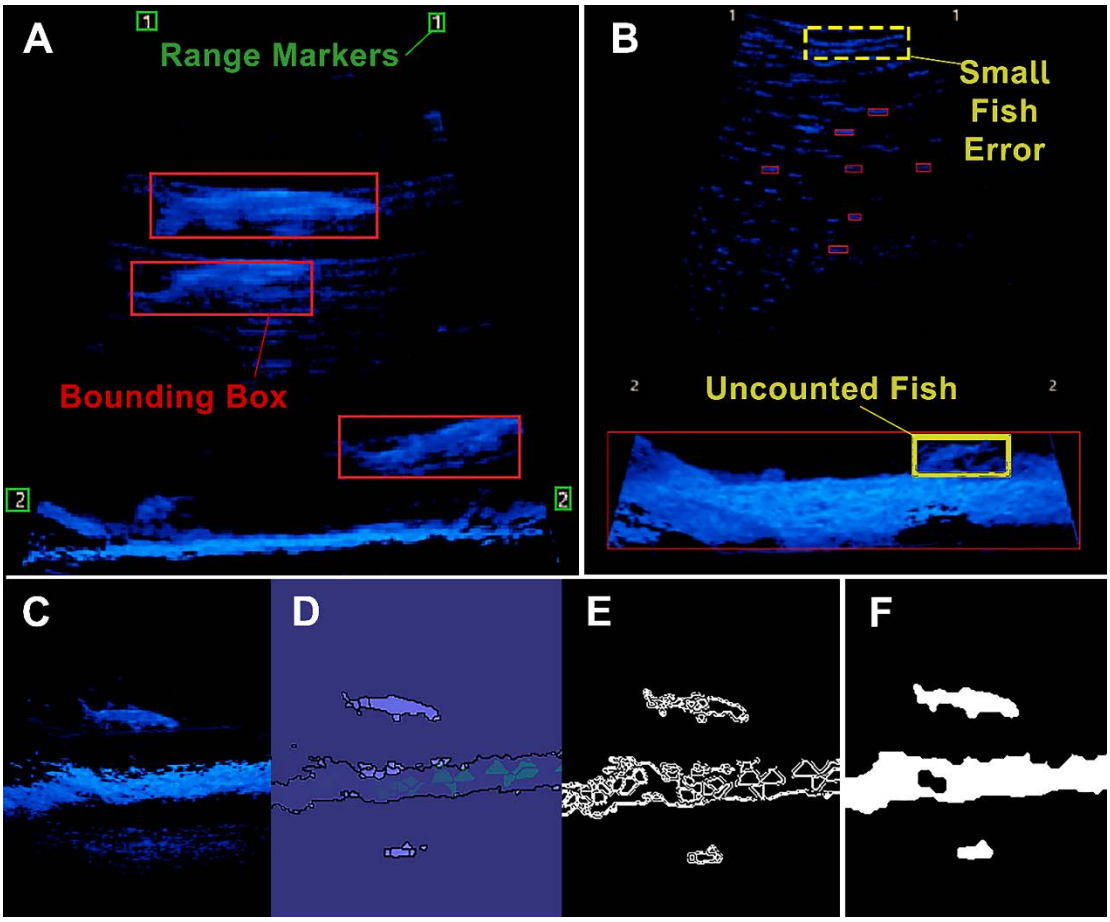

Figure 2.4 Example sample frames undergoing processes from different modules in the automated image processing procedure. Red boxes represent bounding boxes which parse objects from the background and noise. Green boxes locate range markers that were used to create the spatial calibration factor needed to convert from pixels to meters. Yellow solid box in panel B indicates typical uncounted fish because it could not be parsed from the sea-floor. Yellow dashed box shows small fish error due to movement noise. Panels (C-F), show image enhancement procedures: (C) original frame, (D) watershed transformation highlighting separations between high and low contrast areas, (E) Edge detection using a wavelet analysis (Li 2003), (F) Filling in objects to calculate the area of the object bound by detected edges.

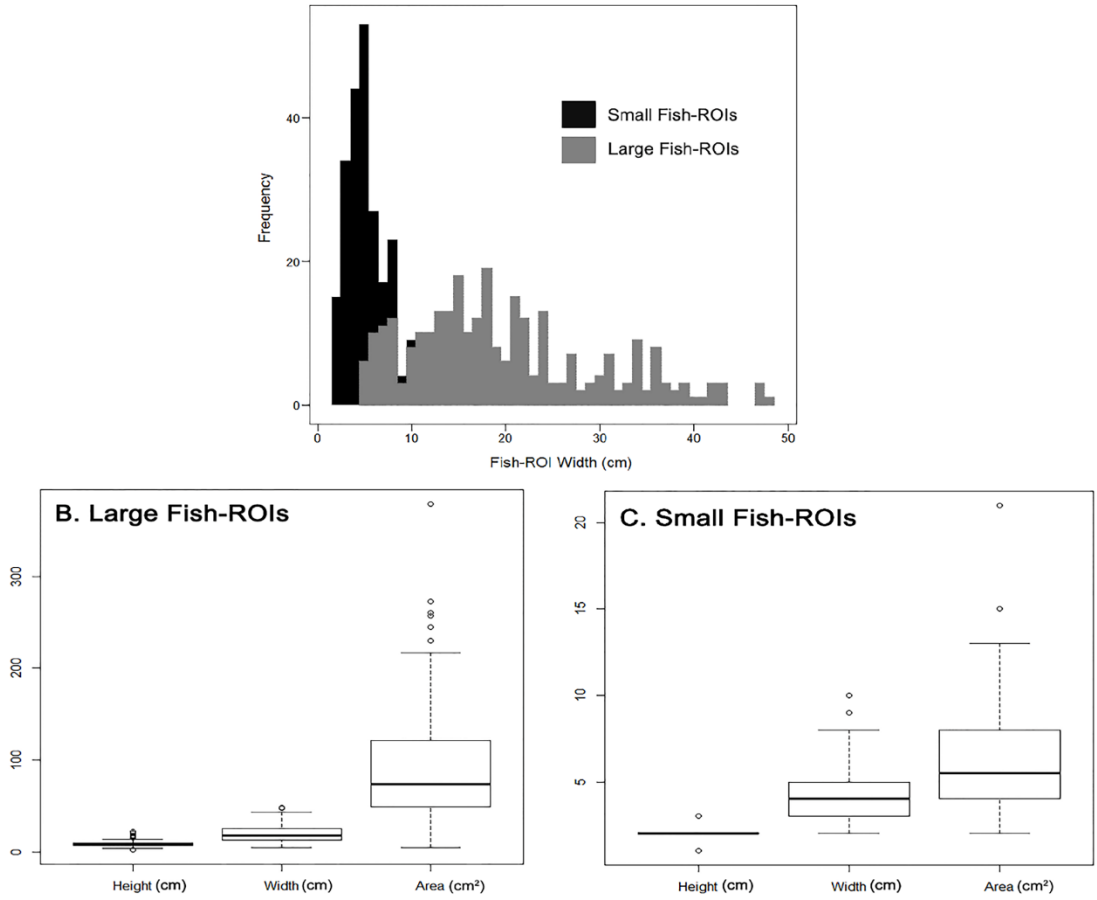

Figure 2.5 Size information on 300 subsampled large fish, and 300 subsampled small fish. (A) Bi-modal distribution of fish-ROI (Regions of Interest) widths (cm), with small fish in black and large fish in gray. (B) Box-and-whisker plot of Large fish-ROI height (mean= 8.86 cm, SD= 3.2 cm), width (mean= 19.79 cm, SD= 9.98 cm) and area (mean= 88.95 cm, SD= 55.62 cm). (C) Small fish-ROI plot summary of height (mean= 1.86 cm, SD= 0.47 cm), width (mean=4.51, SD=1.61) and area (mean= 6.17, SD=2.96).

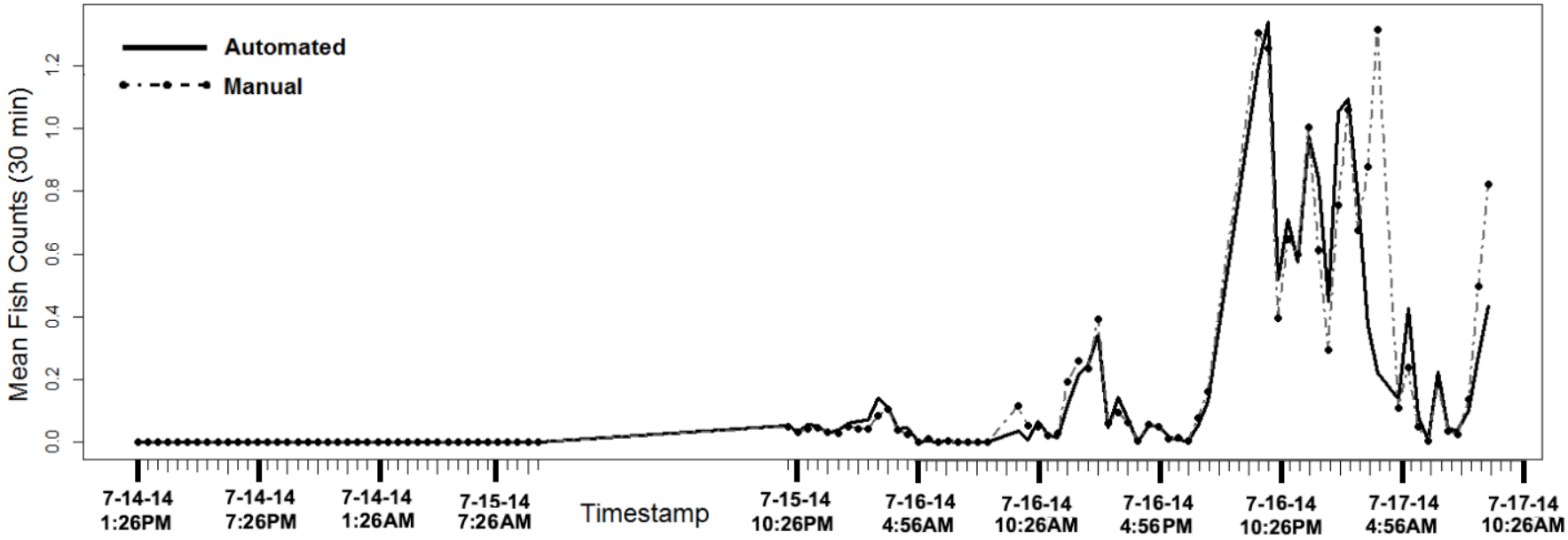

Figure 2.6 Time series of manually visualized observations (solid line) and automated large fish counts (dashed line with points) using Matlab (Mathworks Inc. 2015), averaged over 5-minute intervals.

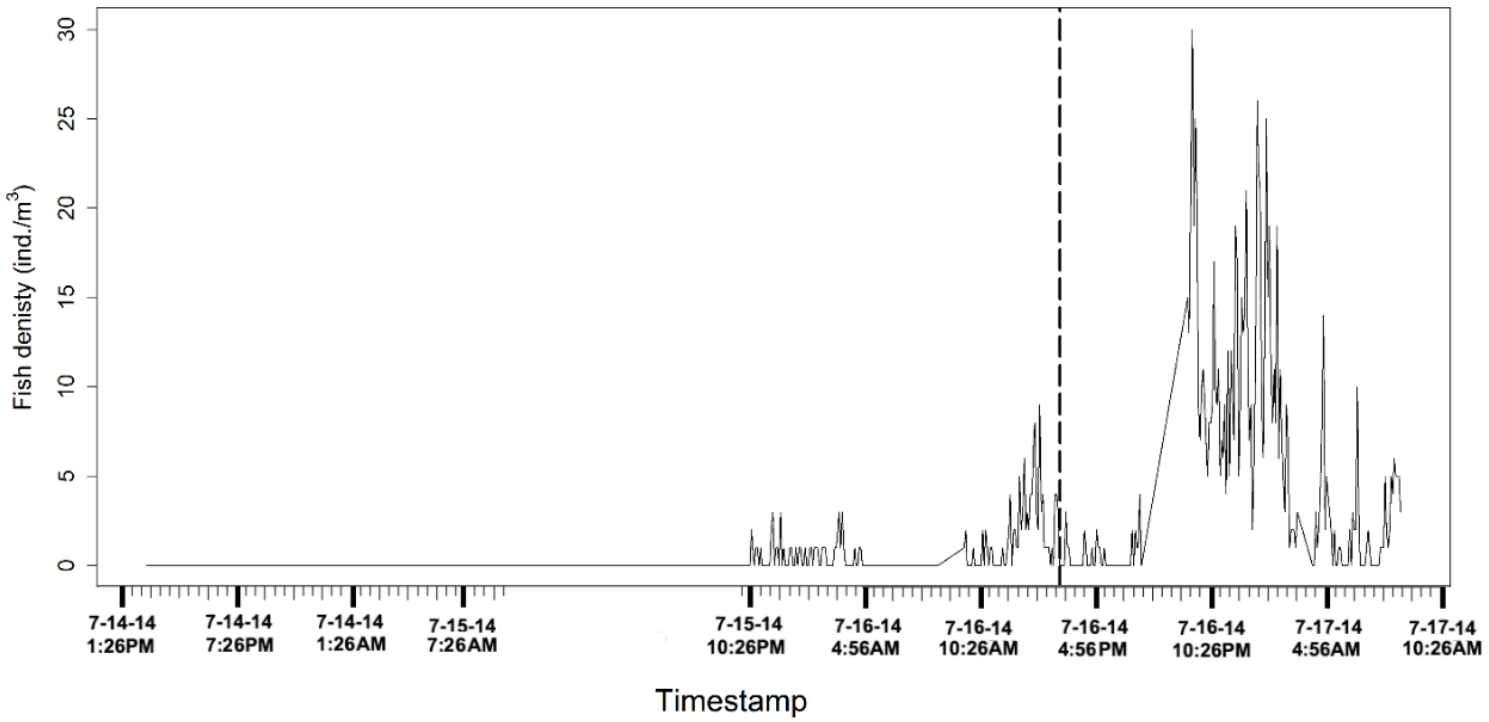

Figure 2.7 Counts of large fish recorded at the CBL pier from 7-14-2014 13:26 to 7-17-2014 09:11 and normalized by water volume over 5-minute intervals. Vertical dashed lines separate training and testing sets.

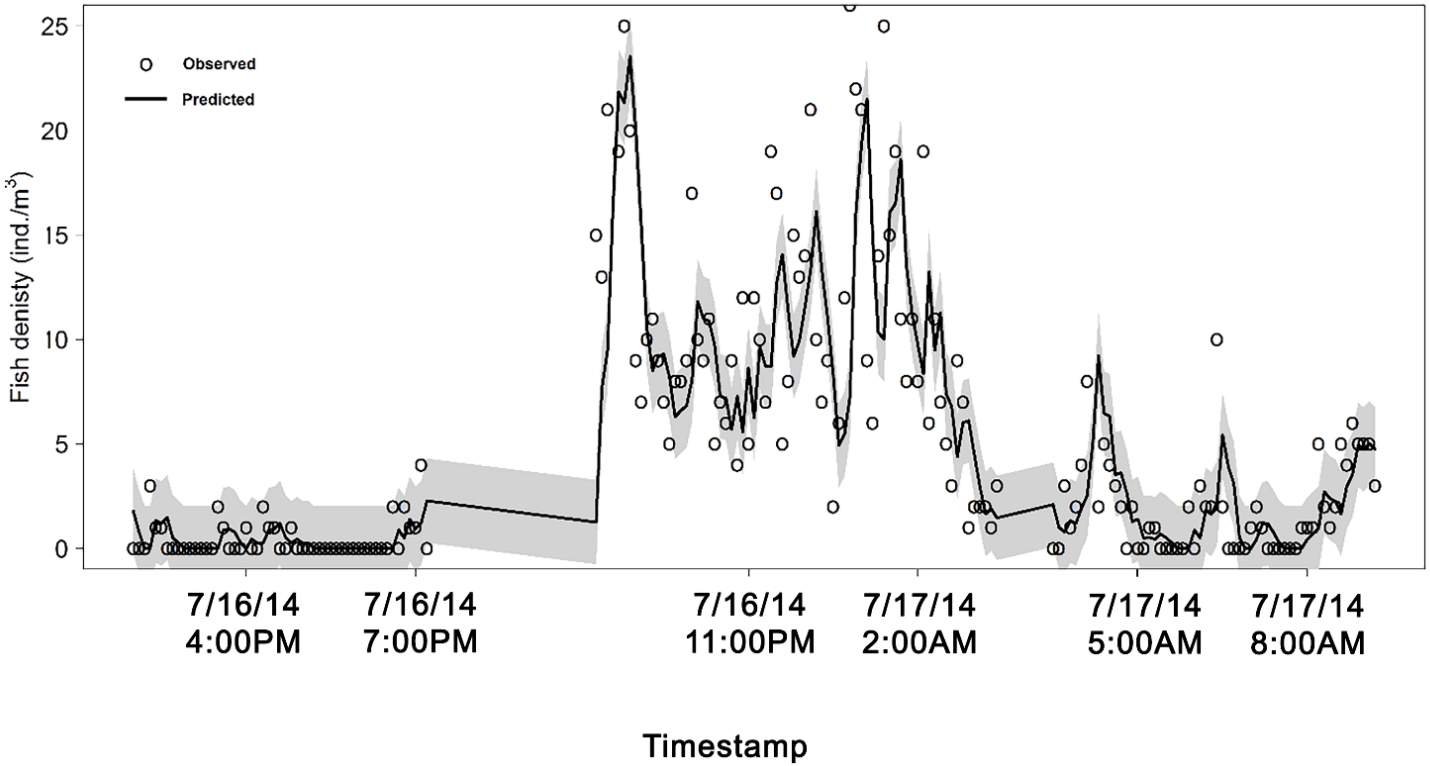

Figure 2.8 Time series forecast showing testing set data (open circles) with predictions (solid line) and 95% bootstrap interval (shaded area). The intervals cover 20.2% and 68.9% of the observed small and large fish counts, respectively.

Table 2.1 Descriptive statistics of manual fish counts performed by a single observer (S. Shahrestani) compared to automatic large fish counts performed with ARIS processing algorithms developed in Matlab (Mathworks Inc. 2015). The true positive rate (TP) and *p*-values for a paired t-test are also shown.

	Count	Mean	SD	TP, %	p
Manual	5103	1.48	1.07	94.6	0.72
Automatic	4594	1.33	1.19		

Table 2.2 Comparative assessment of time series models using the testing data set. The best performance within each model criteria is highlighted in bold. Zero-inflated Poisson distributions (ZIP) and Negative Binomial (NBI) distributions were used for large fish. The autoregressive structure is modeled with AR(3) and AR(6) processes.

	AR(3)+ZIP	AR(3)+NBI	AR(6)+ZIP	AR(6)+NBI
Mean absolute error (MAE), ind. /m^3	2.50	2.58	**2.49**	2.56
Parametric interval coverage, %	60.11	58.47	**61.20**	57.92
Bootstrap interval coverage, %	**62.84**	59.56	**62.84**	57.37

Chapter 3: Settlement and survival of *Chrysaora chesapeakei* polyps: implications for adult abundance[2]

Abstract

Understanding the dynamics of many pelagic scyphozoan blooms requires detailed knowledge of their source stages or sessile polyps. Results from a two-year *in situ* polyp settlement study coupled with historical data and environmental conditions (temperature, salinity and residence time) were analyzed to investigate the formation and distribution of polyp colonies at multiple spatial scales in Chesapeake Bay, USA. A spatially-explicit generalized linear model suggested the importance of flushing rates in describing patterns of the spatial distribution of *Chrysaora* Bay-wide. At smaller scales, seasonal variability of the pelagic stages of *Chrysaora* may be due to the survivability of *Chrysaora* polyps through harsh winter conditions within and between optimal habitat in sub-estuaries. Findings of this study reveal significant species- and stage-specific spatial and temporal patterns of *Chrysaora* within a local shallow habitat and affirm the importance of studying jellyfish species within a species-specific context.

[2] Shahrestani, Suzan, and Hongsheng Bi. "Settlement and survival of *Chrysaora* chesapeakei polyps: implications for adult abundance." *Marine Ecology Progress Series* 601 (2018): 139-151.

Introduction

This chapter aims to describe and analyze abundance patterns of *Chrysaora* polyps in the Chesapeake Bay to understand how components of the hydrodynamic environment such as the stability of the water column and residence time contribute to *Chrysaora* polyp settlement and survival. The hydrodynamic environment of a jellyfish is important in supporting success and dispersal to new habitat because of its role in food acquisition by polyps at a small (< millimeter) scale (Gili & Coma 1998), as well as transport and dispersal of pelagic stages, including planula larvae, ephyrae, and medusae at a larger (kilometer) scale (Cargo & King 1990).

Regarding polyp settlement, research should account for spatial variability in hydrodynamics and residence time in Chesapeake Bay to understand the roles of production and flushing of jellyfish themselves as well as potential resources. For example, nutrient concentrations and plankton biomass positively correlate with residence time, suggesting less food availability in waterscapes with high flushing rates (Bum & Pick 1996). The productivity of areas with long residence time is further corroborated by multiple observations of *Chrysaora* in Chesapeake Bay, whereby both polyps and medusae are found in higher abundances in the sluggish headwaters, with higher residence times (Cargo & King 1990a, Purcell 1992, Purcell et al. 1994b, Breitburg & Burrell 2014).

This chapter explores the spatial-temporal variability of residence time as a factor in explaining patterns of recruitment success and overwintering survival in Chesapeake Bay. I also analyzed portions of the *Chrysaora* life cycle through field studies and spatially explicit modeling, integrating *in situ* planula recruitment

observations, as well as historical datasets to explore *Chrysaora* dispersion dynamics in Chesapeake Bay. Evidence gained from investigations of *Chrysaora* polyp populations in shallow habitat, suggests late summer/early fall planula recruitment is essential as a first step in the successful colonization of new source habitat. However, I hypothesized that it is the overwintering survival of *Chrysaora* polyps within a shallow habitat that contributes to the blooms of medusae the following summer. Understanding the environmental factors that contribute to the perennial success of *Chrysaora* provides insight into the localized adaptations that lead to jellyfish dispersal to new habitat within a temperate estuarine system.

.

Materials and Methods

Study Sites

Chesapeake Bay is the most extensive estuary in the United States with a coastline longer than California's. The complex hydrodynamic state of Chesapeake Bay results from the Bay's geomorphology, discharge, tidal influences and wind at varying scales. Together, these parameters govern water exchange between Chesapeake Bay and the coastal Atlantic leading to interannual variation in residence times ranging from 110 to 264 days and showcasing spatial trends through the seasons (Du & Shen 2016). The eight study sites (Fig. 3.1) of the polyp monitoring study spanned the mid and upper portions of the Chesapeake Bay on both the eastern and western shores. Selected sites were within salinity ranges consistent with polyp presence reported previously in Chesapeake Bay (Cargo & Schultz 1966). Salinity

and temperature at the sites were monitored using Eyes on the Bay data available through the Maryland Department of Natural Resources website (Table 3.1, buoy locations marked on Fig. 3.1, http://eyesonthebay.dnr.maryland.gov/).

Field Methods

Site-specific recruitment and overwinter success of *Chrysaora* polyps were estimated using polyp settlement towers (Fig. 3.2). Sections of half-inch PCV pipe were joined together with marine safe silicone glue to create settlement towers with three tiers (Fig. 3.2A). Each individual tier supported a plate created to simulate oyster boxes for planula settlement. One side of a plate was assembled by zip tying cleaned and drilled oyster shells to PVC grate (Fig. 3.2A). The oyster-box plates were designed to allow for maximum flow-through of water and to decrease predation. To ensure complete immersion of the towers, they were affixed to docks and piers, with each tower attached to a beam or post with steel cable and suspended 10-15 inches from the sea floor. The site locations were all approximately 3-5 meters in depth and towers were suspended in the water column, with no signs of contact with the sea floor or exposure during low tide. Each site (eight) contained five replicate towers, for a total of 40 towers placed throughout Chesapeake Bay (Fig. 3.1, Fig. 3.2B-3C).

Sampling events (Table 3.3) for the polyp towers occurred three times: in August, and September of 2015, and in March 2016. Each tower contained randomly generated immersion durations of one month, two months and overwinter, October 2015 through March 2016. The tier sampling (immersion duration) was randomly

generated at the start of the experiment to account for small-scale differences in depth between tiers (20-40 cm). Replacement of sample tiers (new plates) occurred in August 2015 and was sampled in September 2015, along with plates assigned two-month immersion durations. In 2016, five towers were deployed at Morgan State University's Patuxent River Environmental Research Lab (PRL), Mackall Cove (Fig. 3.2B), for continued monitoring of polyp populations. Immersion durations were reduced to one to two weeks and increased sampling frequency to five events. During a sampling event, plates were removed from towers and placed in aerated seawater for transport to the laboratory and then replaced with new plates. Oyster shells were processed immediately by identifying and counting polyps under a dissecting microscope in the lab. Oyster shell surface area was calculated using ImageJ software to analyze photographs of all oyster shells from each sampled tier/plate. Dividing polyp count by the surface area of the exposed underside of oyster shells attached to the upper plate of an oyster box calculated polyp density. The density data were standardized to polyp count per 100 cm^2 oyster shell to account for the variability in oyster size.

To estimate *Chrysaora* medusa abundance, a sonar-based imaging system capable of retrieving high-resolution abundance data on medusae were used. As part of a more extensive survey, Mackall Cove (Patuxent River) was surveyed from 26 May 2015– 11 October 2016 (Fig. 3.2B), providing both spatial and temporal overlap with the 2016 settlement-tower study. The ARIS1800 (Fig. 3.3B, Sound Metrics Inc.) was mounted onto the gunwale of the research vessel and the camera submerged via a polearm (Fig. 3.3A) at a consistent depth (0.7 meters from the surface) with a fixed

field of view (7 meters). A live feed of the sonar data was viewed and recorded with a laptop computer and ARISScope Software (SoundMetrics Inc.). A 120V portable generator powered both the camera and computer. The data were processed with ARISFish Software, (SoundMetrics Inc.) whereby recorded sample footage was played back and each *Chrysaora* medusa (Fig. 3.3C) was manually located and marked (clicked) in the water column. Using the ARISFish software, a list of geolocations and depth of each located medusa was generated. Medusae with a bell diameter size of approximately 30 mm were detectable, although larger medusae were much more distinguishable. Volume estimation and density for recorded data were not variable due to the fixed field of view but changed based on the topography of the seafloor. Image analysis techniques (Shahrestani et al. 2017) were adapted to calculate changes in the topography of the sea floor using Matlab, Mathworks Inc. and used to calculate volume and estimate density and abundance of medusae in Mackall Cove. Medusa was standardized in the 2016 summer season by the estimated volume of Mackall Cove (~59, 300 cubic meters).

Data and Statistical Analyses

A Linear Mixed Effects Model (LMM) was used to investigate site-specific recruitment and overwintering success. Differences in *polyp density* between *sites* HPL and PRL and *sample* events (repeated measures, fixed effects), as well as differences between replicate *towers*, *salinity* and *temperature* (random effects) at each of the sites, were used to explore patterns in recruitment. The LMM is robust in handling longitudinal data often needed to explore dynamic variables, including

missing points as well as non-normality, which fits the *in-situ* planula recruitment data well. R Statistical Software was used to perform all statistical procedures in this study. The LMM was developed using the R package 'nlme'.

Data from field sampling of polyps (planulae recruitment) and medusae (density) as well as polyp density and strobilation density from Calder (1974) were used to compare patterns of seasonality and how they reflect variations across the *Chrysaora* life cycle. Data from Calder (1974) were standardized by the number of counted scyphistomae per sample and strobila densities as strobila per sample. The Calder (1974) dataset is valuable in that it monitors polyp and strobila density, capturing the seasonality of *Chrysaora* polyps from March 1972 – February 1973, with implications for periodicity in asexual reproduction (budding and strobilation). The four datasets were centered and scaled in R Statistical Software using the scale function. Data were first centered at 0 and then scaled by dividing the values in each variable by their standard deviations. Normalized values of abundance or density are not directly comparable between all datasets but observed seasonal patterns of density within the datasets reveal valuable information.

A historical dataset (Cargo and Shultz 1966) and results from the 2015 Chesapeake Bay field study (N=8, study sites) were used to develop a Generalized Linear Model (GLM) that predicted the probability of polyp presence in Chesapeake Bay using residence time reported in Sanz-Martín et al. (2016)Du and Shen (2016). Value of residence time were extracted from rasters provided in Du and Shen (2016) for January and July with references to Cargo and Schultz (1966) study sites. A similar operation was performed on salinity maps provided by the Chesapeake Bay

Program (https://www.chesapeakebay.net/what/maps/keyword/salinity) averaged from 1985 – 2006. Multi-scale Ultra-high Resolution (MUR) average Sea Surface Temperature (SST) from 2007-2017 were derived from NOAA's satellite data (https://coastwatch.chesapeakebay.noaa.gov/time_series_sst_gen.php?region=cd). To validate the extraction procedure of the residence time data, the mean average residence time was calculated using rasterized values in Chesapeake Bay (approximately 175 days) which was consistent with Du and Shen (2016). Latitude and longitude of the Cargo and Shultz (1966) study sites (N=52) were derived from the site-map and site information provided in the study, i.e., Hellen's Creek, Patuxent River, using Google Earth Software. For comparative assessments of the presence/absence models, the effects of salinity, SST, and residence time in January and July were tested with different link functions (Probit, Logit, and clog-log, Table 3.5). Model comparisons were made using the Akaike information criterion (AIC), visual observations of residual diagnostics and k-fold (10) cross-validation. A spatially explicit GLM was then constructed using the chosen model (see Table 3.5 for details) to predict and compare probabilities of *Chrysaora* polyp occurrence throughout the different areas of Chesapeake Bay.

Results

Site-Specific Recruitment and Overwinter Success

Planula recruitment to new shell only occurred at two sites PRL and HPL (Table 3.3), i.e., observed polyps. Highest and lowest densities of newly recruited polyps occurred at HPL in August 2015 and September 2015 respectively, although

results from the LMM revealed overall planula recruitment and asexual propagation were not significantly different between sites ($df = 15$, $p>0.05$). The LMM suggested significant variability in temporal patterns of within-season recruitment between sites, among two of the three sampling events although temperature and salinity were not significant in describing the variance observed in the data. In August, density at HPL was significantly higher ($\beta = 57$, $SE=12$, $p<=0.005$), and in September polyp density was lower at HPL ($\beta = -44$, $SE=12$, $p<=0.005$). There were no significant differences in polyp density between sites for the third sampling event at a 5% alpha level ($\beta = 26$, $SE=12$, $p=0.06$). The standard deviation of residuals among tower replicates (random effect) was estimated at 20 polyps per 100 cm^2 oyster shell.

Newly recruited polyp colonies at PRL showed signs of asexual propagation, meaning the combined density of polyps with 1-month immersion durations were less than the densities of plates with 2-month immersion durations over the same period (Table 3.3). Although planula recruitment at HPL was highest in August 2015, there was a notable decrease in recruitment in September 2015. There were no signs of asexual propagation at HPL whereby the combined densities of newly recruited polyps from August 2015 and September 2015 were less than polyp densities with 2-month immersion durations from August 2015 through September 2015 (Fig. 3.4). Densities of polyps from oyster shell immersed from August 2015 through March 2016 (overwintering) had significantly lower polyp densities than settlement towers immersed from August 2015 through September 2015. Overwintering success at HPL was much lower than that of PRL (Fig. 3.4). Strobilation of polyps did not occur

on the oyster shells with newly recruited polyps, and no polyps were found on the oyster shells with immersion durations from early October 2015 through March 2016.

When medusae began appearing in 2016, polyp towers were deployed for the second season in Mackall Cove, sampling at higher frequencies with shorter immersion durations (Table 3.3, Fig. 3.4). Oyster shell with one-week immersion durations did not recruit polyps or they were not yet observable, which lead us to conclude that an immersion duration of one week was insufficient. Two weeks was a sufficient immersion duration, as polyps were found on the first two of the three sampling events. However, medusa abundance went to zero rather quickly by mid-August of 2016 before the replacement of oyster shell/plates for the final sampling event, i.e., no expectation of polyps for the third sampling event in 2016. Planula recruitment was highly variable, ranging from 0 to 95 polyps per 100 cm^2 oyster shell. Variability of polyp density occurred among sample replicates, although there were no significant differences between sample periods with similar polyp densities for 2-week immersion durations from 27 July – 10 August 2016, and 3 – 24 August 2016 (Fig. 3.4, 29 vs. 35, respectively).

Seasonality of Chrysaora Population Dynamics

Polyp density reported in Calder (1974) collected from 1972-1973, revealed two peaks in density in May and then again in September. Polyps were lowest at the start of spring, which was consistent with the field sampling that suggests high overwintering mortality. Polyp density remained above zero into the fall, although in July polyp densities decreased, with a lull in reproductive activity before an increase

in abundance heading into winter (Fig. 3.5). Strobila density had a single peak from early May through the middle of June before it declined to zero in the late summer and early fall (Fig. 3.5). Strobilation and polyp densities are correlated through spring (Table 3.4, Fig. 3.5). Strobilation declined in July, when polyp densities were at their lowest, although polyp density began to increase due to planula recruitment (spawning medusae) and asexual propagation in late summer to early fall, which was also observed with polyps settled on towers in 2015 (Fig. 3.4).

Small *Chrysaora* medusae (30 mm) did not appear in Mackall cove (or in other parts of the Patuxent River) until late June 2016. Highest abundances of medusae in Mackall Cove were observed on 28 June 2016 (388 medusae) with declining abundances through the season, ultimately reaching zero on 11 August 2016. Observed medusae abundance in Mackall Cove correlated with strobilae, polyp density, and planula recruitment when a 1-month lag was applied to the data (Fig. 3.5) – which suggests periodicity in the seasonal dynamics of *Chrysaora* in Chesapeake Bay that also was observed and noted in Calder (1974).

Bay-Wide Polyp Distribution

Model selection implied that Model IV (*shaded*, Table 3.5) was the best GLM describing the presence/absence of polyps in Chesapeake Bay. Model IV described the interaction between residence time in July and January as significant in explaining polyp presence in Chesapeake Bay. The most suitable link function was determined to be 'Probit.' Model IV + Probit had the lowest AIC value (Bozdogan 1987). Comparisons of the models' (I-IV) predictive performance was carried out using k = 10-fold, cross-validation prediction error (CVE) – a "Leave One Out" process, with

results (Table 3.5) suggesting Model IV was most robust in predicting the probability of *Chrysaora* polyps in Chesapeake Bay. The temperature variable was removed early on from the model, because it was not significant in explaining the patterns of the polyp data. Spatially-explicit salinity and residence times were highly correlated in space and time (Table 3.2), and salinity alone was not significant in explaining polyp presence in Chesapeake Bay. Therefore, a spatial-filter was applied to exclude areas with salinity less than the physiological tolerances of *Chrysaora* polyps in Chesapeake Bay (Cargo & Schultz 1966, Cargo & King 1990a, Purcell et al. 1999).

Regarding the interaction of residence time in January and the residence time in July, Model (IV) + Probit predicted localized areas with the highest residence time, in both summer and winter, with the most significant probabilities of polyp occurrence. Results of the model suggest the mid-Bay may be most suitable for polyp settlement, while the Patuxent and Choptank rivers showed the highest predictions of polyps (Fig. 3.6). Limited areas of the lower Bay tributaries revealed lower predictions of polyps than in the headwaters of the Bay (Fig. 3.6). Sampling in the lower Bay was limited to the mainstem, but the model predicts polyp occurrence in localized areas of both the James and York Rivers; two tributaries in the lower Bay.

Discussion

The range and long-term survival of *Chrysaora* polyp colonies were characterized by both residence time (hydrological flushing) and environmental conditions within the shallow habitat of Chesapeake Bay. Successful recruitment, overwintering success and inoculation of *Chrysaora* into shallow habitat each

summer provides a source of reproductive dispersal vectors (medusae) which spawn and produce newly recruited colonies of polyps. In contrast, tropical medusae and strobilae of the Mastigias spp. are found throughout the year in the jellyfish lakes of Palau (Dawson & Martin 2001), whereby the population dynamics of both *Mastigias* and *Chrysaora* spp. are governed by the physiological responses (i.e. senescence of medusae, strobilation) to the seasonality of their environmental conditions. In my research, I explored residence time as a possible factor with utility for describing *Chrysaora* polyp distribution in Chesapeake Bay, because it encompasses facets such as geomorphology, water exchange, salinity and the overall stability of the shallow habitat of *Chrysaora* as it varies with seasonality (Du & Shen 2016).

The spatial model used in this study identified a significant interaction between July and January residence time in predicting polyp distribution, which suggests the variability in residence time across the seasons plays a significant role in polyp distribution over and above July or January residence times alone. The success of planula larvae recruitment to hard substrate (i.e., a consequence of medusa dispersal and planula dispersal) may be affected by summer residence time, while winter residence time may explain the subsequent asexual propagation/overwintering success of newly recruited polyp colonies.

Although salinity and temperature are known variables in describing the distribution of medusae of many species (Dawson et al. 2001, Purcell 2005, Zhang et al. 2012), including *Chrysaora* medusae in Chesapeake Bay (Brown et al. 2002, Decker et al. 2007), many of these studies examine medusae in dispersal habitat outside the range of optimal polyp habitat which does little to explain polyp

distribution in source creeks. However, when considering sites within the range of optimal habitat (i.e. appropriate salinity, temperature, and oxygen), temperature and salinity between sites varied less than residence time between adjacent sites. For example, in the Patuxent River subestuary the river channel and an adjacent cove are separated by a few kilometers, with indistinguishable differences in salinity and temperature, but notable variability in residence time (Hagy et al. 2000). I suggest the patterns observed in polyp abundance were caused by differences in flushing rates (between adjacent sites) which contrasts with the homogeneity of salinity and temperature observed among adjacent sites during the same period.

The physiological limitations of medusa for species that die-off in the cold winter months of temperate zones, including *Chrysaora chesapeakei*, or *Cotylorhiza tuberculate* in the Mediterranean (Kikinger 1992), are different from the physiological limitations of polyps of the same species, which allows for their longevity in a dynamic habitat. Adaptations to environmental conditions such as temperature, salinity, hypoxia and hydrography, manifest across different life stages of scyphozoan species and affect the appearance and abundance of jellyfish populations worldwide (Keister et al. 2000, Breitburg et al. 2003, Lucas et al. 2012a, Purcell et al. 2013, Kolesar et al. 2017). Changes to the environmental features that characterize shallow estuarine habitats also make them especially vulnerable to the pressures of human activities in the rapidly changing Anthropocene, i.e., sea-level rise, increased temperatures and precipitation (Barbier et al. 2011, Kennedy & Turner 2011). While many species of jellyfish tolerate harsh conditions, there are no physiological defenses against habitat loss due to changes in hydrographic conditions,

making jellyfish populations (especially those found in shallow habitat) more susceptible to climate change than once believed.

Data reported from the Cargo and Shultz (1966) study make it difficult to distinguish between polyp source colonies (found in the spring) or newly recruited colonies (found in late summer/early fall) although distinguishing differences in polyp morphology can be observed (Loeb 1972). Closer evaluation of sample dates from the Calder (1974) study aided in distinguishing source colonies from newly recruited polyp colonies. I assumed samples taken by Cargo and Shultz (1966) during May were from established colonies because medusae had not yet matured or spawned. Based on the corresponding site locations of polyps present in May, I concluded that the Patuxent River facilitated and continues to facilitate planula recruitment as well as overwintering success of *Chrysaora* polyps.

Using the Patuxent River (a tributary of the mid-Bay) as an example when exploring patterns of residence time, it becomes apparent that areas of the tributary and its adjacent creeks experience long residence time through the year with low variability between the summer and winter seasons (comparing July to January residence time). Areas with low variability in residence time throughout seasons may provide optimal habitat required for polyp settlement and survival, i.e. areas with stable laminar flow and less water exchange, in contrast to habitat with faster flushing times and high intraseasonal variability in mean residence time. In Calder's (1974) study, carried out in Sarah Creek (Fig. 3.1), polyps were present in high densities, corroborating predictions of the spatially-explicit GLM although the predicted probability of polyps (30-40%) in Sarah Creek is lower than the Patuxent River (50-

60%). Similarly, polyps reported by Cones and Haven (1969) in the York River settled approximately 10 kilometers from the model's predicted areas of polyp presence. The York River in the lower Bay experiences relatively short residence time in both the summer and winter months, which provided a good validation point for the model.

Small-scale variability of polyp predictions throughout shallow habitats of Chesapeake Bay (i.e., differences between the upper and lower portions of the Patuxent River) may be indicative of the local features of a shallow habitat which include wind, available substrate, depth, salinity, and flow rate among others. Many of these factors have been used to explain the variability of polyp settlement and hold merit in describing localized patterns of abundance. For example, in the Cones and Haven (1969) study researchers found polyps on oyster shell suspended in bags from docks in the York River, Virginia, USA, but not on oyster shell deposits that were dredged kilometers away. Fine-scale variability in polyp presence could be indicative of failed planula recruitment to deeper oyster bars, although the Cones and Haven (1969) study did not reveal differences comparing polyp density over different depths of sampled oyster bars.

In temperate zones, observations of localized differences in habitat may also contribute to overwintering success or surviving dormancy, which became apparent in my study. The model predicts similar recruitment success of planulae at two of the tower study sites (PRL and HPL). However, polyps did not survive the winter at HPL, perhaps due to variability between sites with respect to overwintering refugia. For example, a sheltering riparian buffer present at PRL (Fig. 3.2B) was absent from

HPL (Fig. 3.2C). Furthermore, the sample towers placed in the enclosed creek of the Patuxent River had a longer residence time relative to the HPL polyp colonies that recruited to the towers placed in the Choptank river channel, where shorter residence times may have been experienced (Hagy et al. 2000).

For scyphozoan species that exist in temperate zones and contain a polyp stage, medusae densities should correlate with planula recruitment and subsequent populations of newly recruited polyp colonies. However, these colonies do not contribute to the medusa population of that year. Typical consideration of the scyphozoan life cycle that does not incorporate seasonality ignores differences between source colonies excysted in the spring (in the case of summer dominant species) and newly recruited colonies via planula recruitment in the late summer through fall. However, parsing out differences in behavior across multiple stages of polyps reveals valuable information regarding the within-season abundance of medusae. Not a single strobila observation occurred in the 2015-2016 settlement tower studies, which was not surprising considering polyps from summer settlement of planulae never experienced spring-time warming of water temperatures needed to induce strobilation. The study suggests fall strobilation does not occur (regardless of the appropriate temperature range) because polyps recruited in summer and early fall do not experience the strobilation cue, i.e., water temperature increases only in the spring. In the lab, newly recruited polyps do indeed strobilate when polyps are chilled at 20°C and then exposed to increasing temperatures up to 26°C (Loeb 1972). Strobilation of newly recruited polyps has not been observed *in situ*.

Including newly recruited polyps in population dynamics studies of scyphozoan spp. could bias estimates of within-season potential production of medusae because the recruits do not strobilate. I could not distinguish between source polyps and recruits from the results published in Cargo and Shultz (1966). Accordingly, I made the safest assumption, i.e., that polyp presence was an indication of successful planula recruitment alone and not overwinter survival (spring excystment). With this assumption, the spatial model may overpredict the probability of the spatial occurrence of source colonies if I aimed to consider habitat that facilitates both planula recruitment and overwintering success. For temperate scyphozoan species dominant in the summer, early spring polyp sampling should give an accurate estimate of polyp source colonies and their potential impact on within-season medusa abundance because recruits from summer spawning of medusae have not yet appeared. The opposite should be true for species that are cued to excyst and strobilate with decreasing temperatures in the fall, i.e., *Cyanea capillata* in Chesapeake Bay and *Aurelia* spp. in many locations worldwide (Gröndahl 1988, Omori et al. 1995, Liu et al. 2009, Purcell et al. 2009), whereby early-fall polyp density and asexual reproduction should be considered to predict abundance of medusae that winter.

Conclusion

The complexity of the *Chrysaora chesapeakei* life cycle as it unfolds in Chesapeake Bay exhibits its adaptability. Mechanisms at all life stages contribute to the success of the species within a complex and dynamic estuarine environment.

Investigations of spatiotemporal distribution and abundance of jellyfish species are most revealing when explained within the context of their life histories. With regard to *Chrysaora*, small-scale features of polyp source habitat could explain differences in the success of planula recruitment and overwintering survival, while residence time helps define the overall pattern of presence or absence of polyps within Chesapeake Bay at the sub-estuary scale. Springtime strobilation cues are only experienced by excysted spring polyps (*in situ*) that survive the winter, while planula recruitment and asexual reproduction in the fall ramps up polyp density to buffer against the harsh conditions of winter. The current and future changes to hydrographic conditions and temperature in shallow habitat at both large and small scales, for example faster flushing rates, may lead to large shifts in the spatial and temporal distribution patterns of *Chrysaora* polyps inhabiting those habitats. The success of settlement and polyp dormancy through harsh conditions is not only a necessary step in the life cycle of *Chrysaora* but vital in other metagenic jellyfish species that require inoculation of medusae into the water column every year.

References

Barbier EB, Hacker SD, Kennedy C, Koch EW, Stier AC, Silliman BR (2011) The value of estuarine and coastal ecosystem services. Ecological monographs 81:169-193

Bozdogan H (1987) Model selection and Akaike's information criterion (AIC): The general theory and its analytical extensions. Psychometrika 52:345-370

Breitburg D, Burrell R (2014) Predator-mediated landscape structure: seasonal patterns of spatial expansion and prey control by *Chrysaora* quinquecirrha and Mnemiopsis leidyi. Marine Ecology Progress Series 510:183-200

Breitburg DL, Adamack A, Rose KA, Kolesar SE and others (2003) The pattern and influence of low dissolved oxygen in the Patuxent River, a seasonally hypoxic estuary. Estuaries 26:280-297

Brown CW, Hood RR, Li Z, Decker MB, Gross TF, Purcell JE, Wang HV (2002) Forecasting system predicts presence of sea nettles in Chesapeake Bay. Eos, Transactions American Geophysical Union 83:321-326

Bum BK, Pick FR (1996) Factors regulating phytoplankton and zooplankton biomass in temperate rivers. Limnology and Oceanography 41:1572-1577

Calder DR (1974) Strobilation of the Sea Nettle, *Chrysaora quinquecirrha*, under Field Conditions. Biol Bull 146:326-334

Cargo DG, Schultz LP (1966) Notes on the biology of the sea nettle, *Chrysaora quinquecirrha*, in Chesapeake Bay. Chesapeake Science 7:95-100

Cargo DG, King DR (1990) Forecasting the abundance of the sea nettle,*Chrysaora quinquecirrha*, in the Chesapeake Bay. Estuaries 13:486-491

Cones HN, Haven DS (1969) Distribution of *Chrysaora quinquecirrha* in the York River. Chesapeake Science 10:75-84

Costello J, Sullivan B, Gifford D, Van Keuren D, Sullivan L (2008) Seasonal refugia, shoreward thermal amplification, and metapopulation dynamics of the ctenophore Mnemiopsis leidyi in Narragansett Bay, Rhode Island (vol 51, pg 1819, 2006). LIMNOLOGY AND OCEANOGRAPHY 53:873-873

Dawson MN, Martin LE (2001) Geographic variation and ecological adaptation in *Aurelia* (Scyphozoa, Semaeostomeae): some implications from molecular phylogenetics. Hydrobiologia 451:259-273

Dawson MN, Martin LE, Penland LK (2001) Jellyfish swarms, tourists, and the Christ-child. In: Jellyfish Blooms: Ecological and Societal Importance. Springer, p 131-144

Decker MB, Brown CW, Hood RR, Purcell JE and others (2007) Predicting the distribution of the scyphomedusa *Chrysaora quinquecirrha* in Chesapeake Bay. Marine Ecology Progress Series 329:99-113

Du J, Shen J (2016) Water residence time in Chesapeake Bay for 1980–2012. Journal of Marine Systems 164:101-111

Gili J-M, Coma R (1998) Benthic suspension feeders: their paramount role in littoral marine food webs. Trends in Ecology & Evolution 13:316-321

Gröndahl F (1988) A comparative ecological study on the scyphozoans *Aurelia aurita*, *Cyanea capillata* and *C. lamarckii* in the Gullmar Fjord, western Sweden, 1982 to 1986. Marine Biology 97:541-550

Gröndahl F (1989) Evidence of gregarious settlement of planula larvae of the scyphozoan *Aurelia aurita*: an experimental study. Marine ecology progress series:119-125

Hagy JD, Boynton WR, Sanford LP (2000) Estimation of net physical transport and hydraulic residence times for a coastal plain estuary using box models. Estuaries 23:328-340

Holst S, Jarms G (2007) Substrate choice and settlement preferences of planula larvae of five Scyphozoa (Cnidaria) from German Bight, North Sea. Marine Biology 151:863-871

Holst S, Sötje I, Tiemann H, Jarms G (2007) Life cycle of the rhizostome jellyfish *Rhizostoma octopus* (L.)(Scyphozoa, Rhizostomeae), with studies on cnidocysts and statoliths. Marine Biology 151:1695-1710

Keister JE, Houde ED, Breitburg DL (2000) Effects of bottom-layer hypoxia on abundances and depth distributions of organisms in Patuxent River, Chesapeake Bay. Marine Ecology Progress Series 205:43-59

Kennedy TL, Turner TF (2011) River channelization reduces nutrient flow and macroinvertebrate diversity at the aquatic terrestrial transition zone. Ecosphere 2:1-13

Kikinger R (1992) *Cotylorhiza tuberculata* (Cnidaria: Scyphozoa)-Life history of a stationary population. Marine Ecology 13:333-362

Kolesar SE, Rose KA, Breitburg DL (2017) Hypoxia Effects Within an Intra-guild Predation Food Web of *Mnemiopsis leidyi* Ctenophores, Larval Fish, and Copepods. In: Justic D, Rose KA, Hetland RD, Fennel K (eds) Modeling Coastal Hypoxia: Numerical Simulations of Patterns, Controls and Effects of Dissolved Oxygen Dynamics. Springer International Publishing, Cham, p 279-317

Liu W-C, Lo W-T, Purcell JE, Chang H-H (2009) Effects of temperature and light intensity on asexual reproduction of the scyphozoan, *Aurelia aurita* (L.) in Taiwan. Hydrobiologia 616:247-258

Liu Y, Tay J-H (2002) The essential role of hydrodynamic shear force in the formation of biofilm and granular sludge. Water research 36:1653-1665

Loeb MJ (1972) Strobilation in the Chesapeake Bay sea nettle *Chrysaora quinquecirrha.* I. The effects of environmental temperature changes on strobilation and growth. Journal of Experimental Zoology 180:279-291

Lucas CH, Graham WM, Widmer C (2012) Jellyfish Life Histories: Role of Polyps in Forming and Maintaining Scyphomedusa Populations. Advances in marine biology 63:133

Omori M, Ishii H, Fujinaga A (1995) Life history strategy of *Aurelia aurita* (Cnidaria, Scyphomedusae) and its impact on the zooplankton community of Tokyo Bay. ICES Journal of Marine Science 52:597-603

Purcell JE (1992) Effects of predation by the scyphomedusan *Chrysaora quinquecirrha* on zooplankton populations in Chesapeake Bay, USA. Marine Ecology Progress Series 87:65-76

Purcell JE, White JR, Roman MR (1994) Predation by gelatinous zooplankton and resource limitation as potential controls of Acartia tonsa copepod populations in Chesapeake Bay. Limnology and Oceanography 39:263-278

Purcell JE, White JR, Nemazie DA, Wright DA (1999) Temperature, salinity and food effects on asexual reproduction and abundance of the scyphozoan *Chrysaora quinquecirrha*. Marine Ecology Progress Series 180:187-196

Purcell JE (2005) Climate effects on formation of jellyfish and ctenophore blooms: a review. J Mar Biol Assoc UK 85:461-476

Purcell JE, Hoover RA, Schwarck NT (2009) Interannual variation of strobilation by the scyphozoan *Aurelia labiata* in relation to polyp density, temperature, salinity, and light conditions *in situ*. Marine Ecology Progress Series 375:139-149

Purcell JE, Breitburg DL, Decker MB, Graham WM, Youngbluth MJ, Raskoff KA (2013) Pelagic Cnidarians and Ctenophores in Low Dissolved Oxygen Environments: A Review. In: Coastal Hypoxia: Consequences for Living Resources and Ecosystems. American Geophysical Union, p 77-100

Shahrestani S, Bi H, Lyubchich V, Boswell KM (2017) Detecting a nearshore fish parade using the adaptive resolution imaging sonar (ARIS): An automated procedure for data analysis. Fisheries Research 191:190-199

Stoodley P, Dodds I, Boyle J, Lappin-Scott H (1998) Influence of hydrodynamics and nutrients on biofilm structure. Journal of applied microbiology 85

Zhang F, Sun S, Jin X, Li C (2012) Associations of large jellyfish distributions with temperature and salinity in the Yellow Sea and East China Sea. Hydrobiologia 690:81-96

Figures and Tables

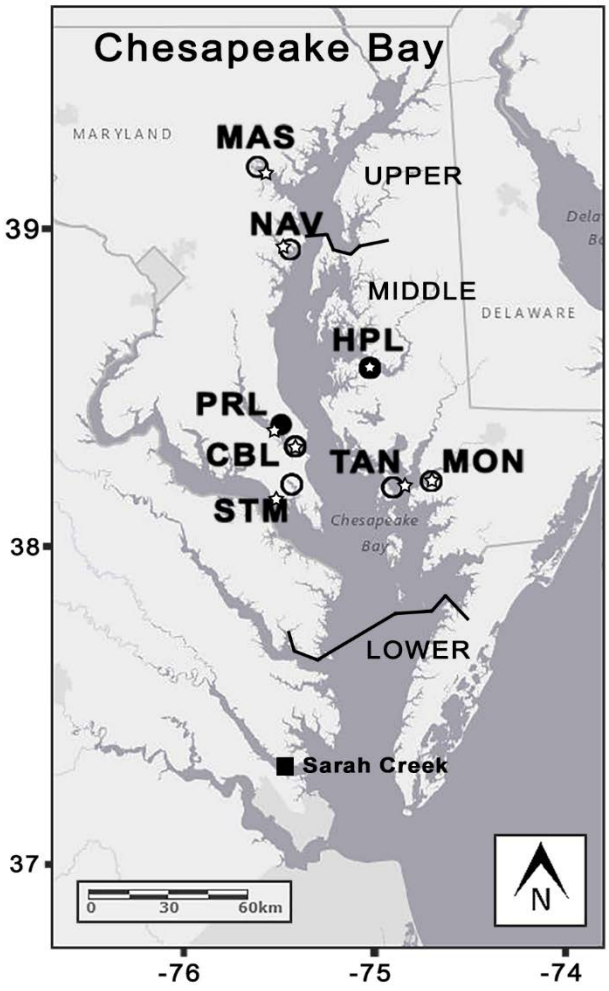

Figure 3.1 Settlement tower study-sties were selected based on salinity (5-35 ppt) and accounted for spatial coverage of Chesapeake Bay with sites on the western and eastern shores. Black circles represent sites with observed polyps, while white circles are study-sites with no noted polyps. White stars indicate water quality monitoring stations (S1). Horizontal black lines divide the three portions of Chesapeake Bay (upper, middle and lower), with no sites selected in the lower portion of the Bay. Eight study sites were selected: (1) Masonville Cove (MAS), an adjacent creek of the Patapsco River, (2) Naval Academy (NAV) located on the Severn river channel (3)

Horn Point Laboratory (HPL) located on the Choptank river channel, (4) Patuxent River Environmental Research Lab (PRL) location in an adjacent creek of the Patuxent River, the (5) Chesapeake Biological Lab (CBL) located at the mouth of the Patuxent River, the (6) Karen Noonan Center (KNC) located on the Tangier Sound, (7) Monie Creek (MON), a tributary of the Tangier Sound and a (8) residential pier on the St. Mary's River channel (STM). The black square is located in Sarah Creek (York River) and is the study site utilized by Calder (1974)

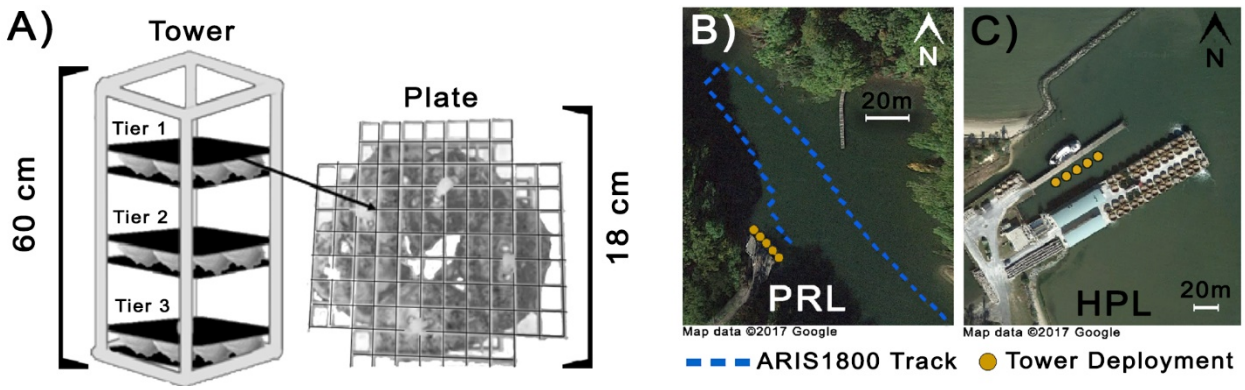

Figure 2.2 (A) Deployment of polyp settlement towers for *Chrysaora chesapeakei* polyps and plates (N=40) occurred at eight selected study sites throughout Chesapeake Bay. Each tower was designed with three tiers to account for varying immersion durations and repeated sampling events. Each tier supported an oyster-box plate, made by sandwiching two sections (18cm x 18cm) of PVC grate, fitted with zip-tied oysters. **(B)** The Patuxent River Environmental Research Lab (PRL) and the **(C)** Horn Point Laboratory (HPL) are two example sites with yellow circles representing five replicate settlement towers and their typical deployment from docks and piers at all other sites. Blue dashed lines **(B)** represent ARIS1800 sonar survey track lines carried out in the summer of 2016 at PRL used to estimate medusa abundance in Mackall Cove

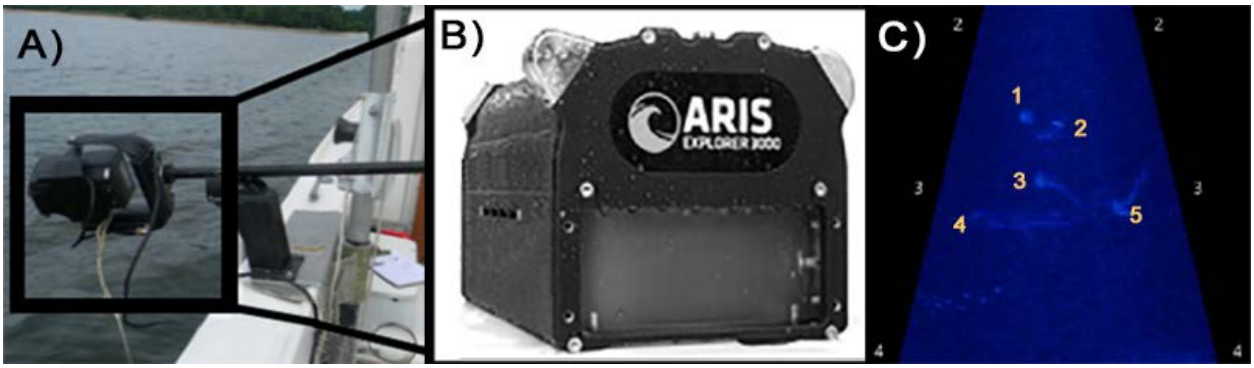

Figure 3.3 (A) Sonar camera deployment using the **(B)** ARIS1800 and example data **(C)** with five observed jellyfish (yellow number markers)

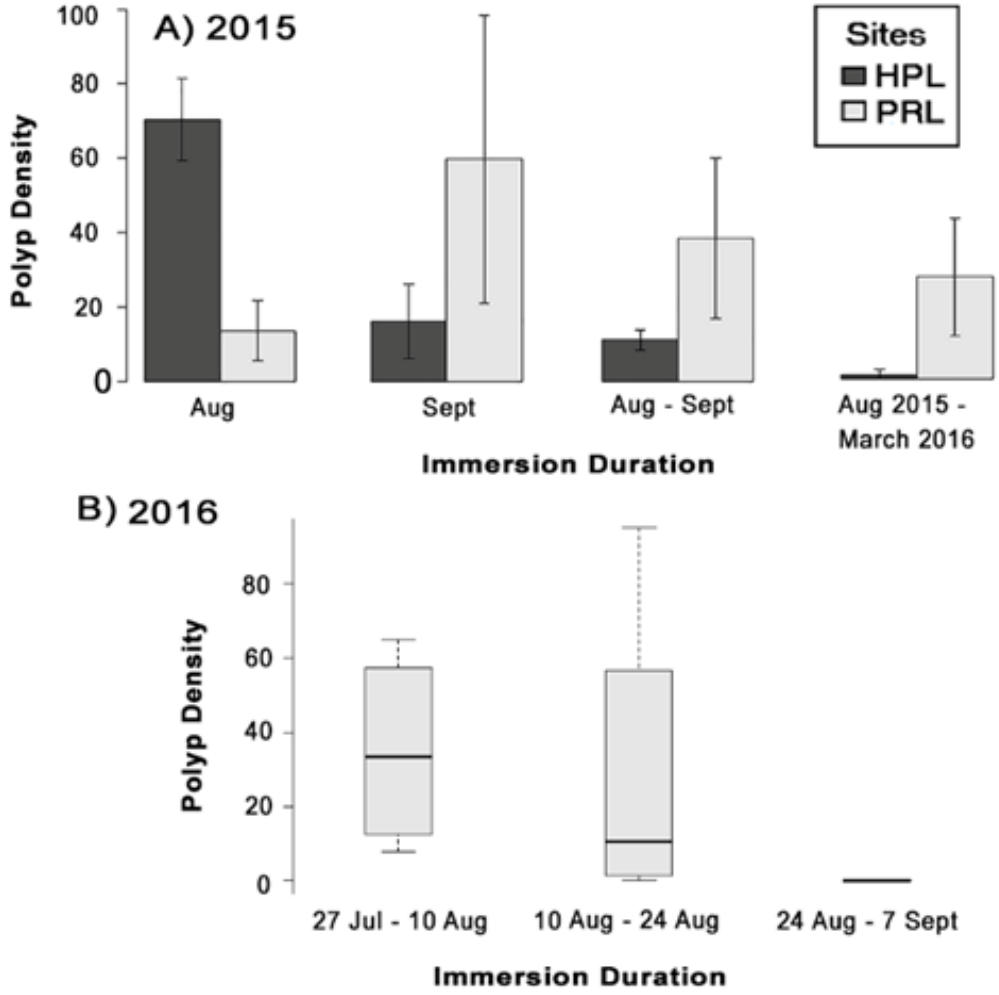

Figure 3.4 Planula recruitment of *Chrysaora* chesapeakei represented by polyp density or newly recruited polyps to 100 cm^2 oyster shell. **(A)** 2015 polyp densities and estimated error bars (SD) for sites with observed polyps, which are limited to sites PRL and HPL. **(B)** Observed densities of polyps on oyster shell with two-week immersion durations from 27 July 2016 – 7 Sept 2016 at PRL. Boxes are median and interquartile range, whiskers are minimum and maximum.

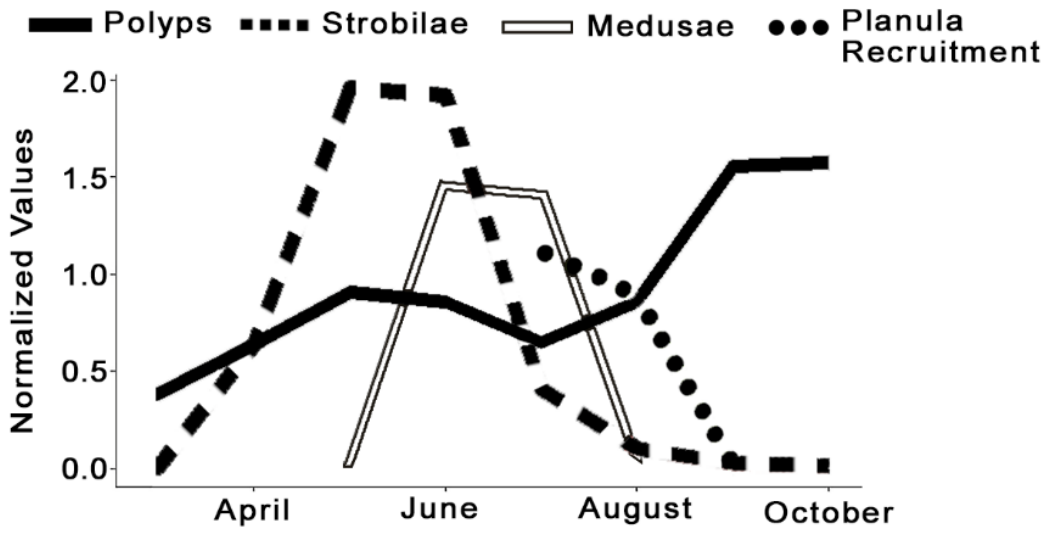

Figure 3.5 Seasonality of *Chrysaora chesapeakei* as described by the normalization of four datasets including information on polyp density (solid black line) and strobilae density (dashed black line) reported in Calder (1974) collected from Sarah Creek, York River. The remaining normalized datasets included medusa abundances (solid gray line) observed in Mackall Cove, Patuxent River in 2016 as well as planulae recruitment in 2016 (dotted black line) collected from polyp settlement towers deployed at the Patuxent River Environmental Research Laboratory (PRL) in 2016.

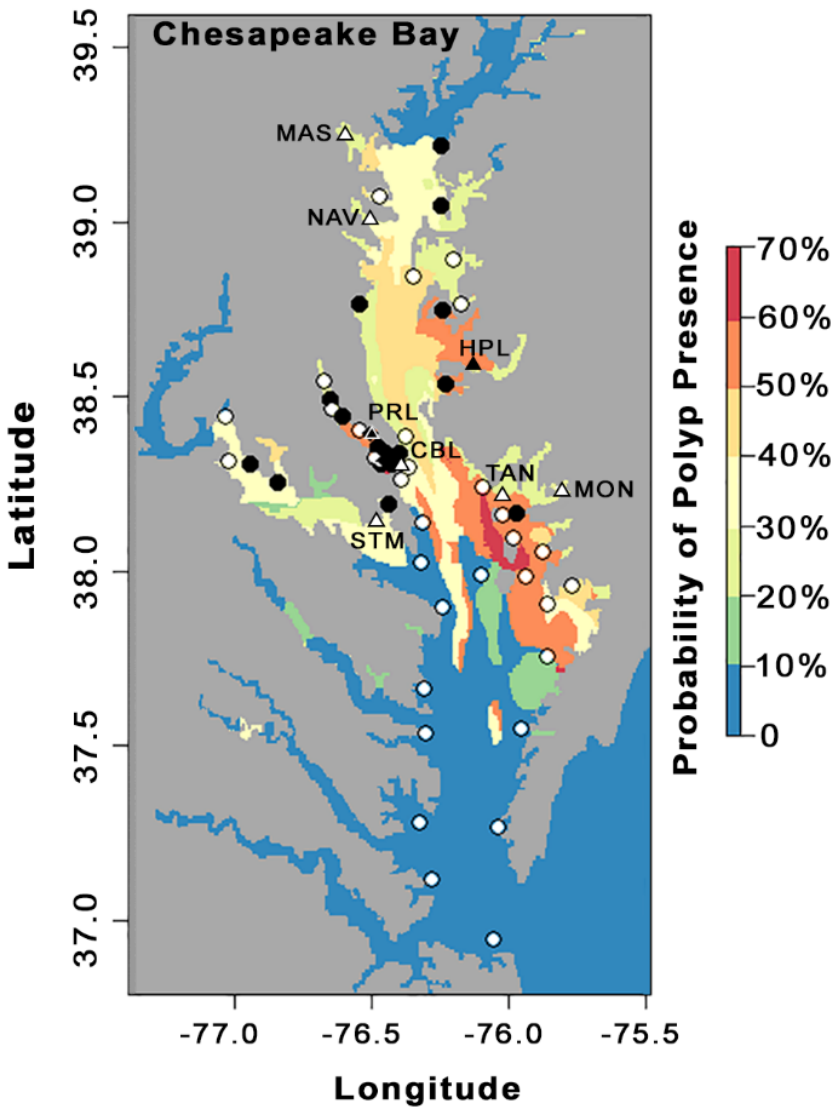

Figure 3.6 Spatially-explicit GLM predictions of *Chrysaora chesapeakei* polyps using a binomial distribution and "probit" link function as well as a salinity filter (<5ppt). The probability of polyp presence is described by a cold (lower probability of polyp occurrence) to warm color (higher probability of polyp presence) gradient. Closed circles represent sites with observed polyp presence from the Cargo and Shultz (1966) study, and open circles represent sites with no polyps from the same study. Black triangles represent sites from the 2015 settlement tower study with

polyps present, while white triangles are sites with no observed polyps from the same study: (1) Masonville Cove (MAS), an (2) Naval Academy (NAV), (3) Horn Point Laboratory (HPL, (4) Patuxent River Environmental Research Lab (PRL), the (5) Chesapeake Biological Lab (CBL), the (6) Karen Noonan Center (KNC), (7) Monie Creek (MON), and a (8) residential pier on the St. Mary's River channel (STM)

Table 3.1 Coordinates and locations for the 2015 *Chrysaora chesapeakei* polyp recruitment field sites. Continuous water quality data for monitoring stations associated with each site are available via Eyes on the Bay website operated by the Maryland Department of Natural Resources (http://eyesonthebay.dnr.maryland.gov/)

Site	Location		Water Body	Monitoring Station
	Latitude	Longitude		
MAS	39°14'40.36"N	76°35'48.96"W	Patapsco River	Masonville Cove Pier (MSC)
NAV	38°59'10.10"N	76°29'6.64"W	Severn River	WT7.1 - Severn River
HPL	38°35'35.56"N	76° 7'44.52"W	Choptank River	ET5.2 - Choptank River
PRL	38°23'38.18"N	76°30'13.40"W	Patuxent River	LE1.2 - St. Leonard
CBL	38°19'1.55"N	76°27'4.05"W	Patuxent River	LE1.4 - Drum Point
STM	38°11'43.65"N	76°27'21.51"W	St. Mary's River	St. Georges Creek (SGC)
MON	38°12'30.02"N	75°48'16.43"W	Wicomico River	Little Monie Creek (LMN)
TAN	38°13'13.64"N	76° 2'18.35"W	Tangier Sound	EE3.1 - N. Tangier Sound

Table 3.2 Pearson correlation coefficients (r) and respective p-values among summer and winter Residence Time (RT) averaged over (1980-2012) and salinity averaged over 1985 – 2006, throughout Chesapeake Bay. Values from all variables were extracted from a 1400 x 875 (row by column) raster of Chesapeake Bay for a total of 348,581 spatially-explicit samples (N) for each variable.

	Salinity	
	r	**p-values**
RT (July)	-0.83	<<0.001
RT (January)	-0.77	<<0.001
RT (Jan * July)	-0.75	<<0.001

Table 3.3 *Chrysaora chesapeakei* settlement-tower sampling design for study sites with observed polyps in 2015 and 2016 at the Horn Point Laboratory (HPL) on the Choptank River and Patuxent River Environmental Research Lab (PRL) in Mackall Cove. Polyp density is calculated as the mean newly recruited polyps to 100 cm^2 oyster shell for five replicate towers placed at each site

Year	Site	Immersion Duration	Time Period	Polyp Density
2015	HPL	1 month	August	70
	HPL	1 month	September	11
	HPL	2 months	August & September	15
	HPL	6 months	October (2015) – March (2016)	0
	HPL	8 months	August (2015) – March (2016)	1
	PRL	1 month	August	14
	PRL	1 month	September	38
	PRL	2 months	August & September	60
	PRL	6 months	October (2015) – March (2016)	0
	PRL	8 months	August (2015) – March (2016)	27
2016	PRL	1 week	27 July – 3 August	0
	PRL	1 week	3 August – 10 August	0
	PRL	2 weeks	27 July – 10 August	35
	PRL	2 weeks	3 August – 24 August	29
	PRL	2 weeks	24 August – 7 September	0
	PRL	6 weeks	27 July – 5 October	68

Table 3.4 Seasonality correlations of *Chrysaora chesapeakei* life-stages. Strobilae and Polyp data from Calder (1974) as well as medusae abundance from the 2016 sonar survey and planula recruitment from the 2016 settlement tower study were centered and normalized. Also included are Pearson's correlations between life stages, including strobilae, polyps and planula recruitment with a 1-month lag

	Medusae		**Polyps**	
	Corr	**p-value**	**Corr**	**p-value**
Strobilae	0.31	0.55	0.84*	0.04
Planula Recruitment	0.66	0.66	-0.99*	0.02
Polyps	-0.61	0.84		
Strobilae w/1-month lag	0.99*	0.02		
Polyps w/1-month lag	0.99*	0.04		
Planula Recruitment w/1-month lag	0.99*	0.02		

*Significance level, $\alpha <= 0.05$

Table 3.5 Generalized Linear Model (GLM) selection and validation for polyp presence/absence using a negative binomial distribution and explanatory variables including Residence Time (RT) in July and January as well as their interactions. Akaike Information Criterion (AIC) was used to differentiate between models with 'Probit,' 'Logit' or 'cloglog' link functions. K=10 cross-validation error (CVE) was used to validate models and aid in model selection. Cells shaded in gray highlight the best performing model in predicting the probability of polyp presence in Chesapeake Bay.

Model	**Link**	**p – Value** *Significance level, α <= 0.05			**AIC**	**CVE**
I **RT July**	Probit	0.06			77.92	0.40
	Logit	0.06			77.49	0.40
	cloglog	0.10			78.32	0.39
II **RT Jan**	Probit	0.04*			77.30	0.43
	Logit	0.08			78.09	0.43
	cloglog	0.07			77.79	0.43
III **RT Jan + July**	Probit	RT Jan: 0.40	RT Jul: 0.75		79.20	0.45
	Logit	RT Jan: 0.41	RT: 0.74		79.39	0.45
	cloglog	RT Jan: 0.42	RT: 0.75		79.70	0.44
IV **RT Jan * July**	Probit	RT Jan: 0.05*	RT Jul: 0.01*	RT Jan * RT Jul: 0.02*	71.17	0.33
	Logit	RT Jan: 0.02*	RT Jul: 0.06	RT Jan * RT Jul: 0.02*	71.35	0.33
	cloglog	RT Jan: 0.01*	RT Jul: 0.06	RT Jan * RT Jul: 0.02*	71.28	0.33

Chapter 4: Spatial structure of *Chrysaora chesapeakei* medusae within a shallow coastal waterscape

Abstract

The goal of spatial ecology is to detect spatial patterns and related ecological events. The Chesapeake Bay sea nettle (*Chrysaora chesapeakei*) was surveyed using an adaptive resolution imaging sonar (ARIS) in a Chesapeake Bay subestuary to collect high-resolution data in May – September 2016 – 2017. The survey was conducted within a shallow coastal waterscape in the tidal Patuxent River that recognized a source-sink spatial dichotomy in which *Chrysaora* requires hard substrate in shallow creeks for its benthic polyp stage to complete its life history. The mesoscale spatial distributions of *Chrysaora* differed annually, with relatively lower abundance and less dispersal in 2016, and higher abundance and more dispersal in 2017. Results also highlight the importance of sampling jellyfish source habitat, where medusae could be 10 times more abundant in the tidal creek (source) than in adjacent river channel (dispersal habitat). It was concluded that it is essential to sample jellyfish populations within the proper spatial context to understand their population dynamics and long-term trends.

Introduction

Within a local Chesapeake Bay waterscape, a source population of benthic polyps was identified in St. Leonard's Creek of the Patuxent River (Chapter 3), upestuary from CBL where visual counts of *Chrysaora* medusae had been observed for more than 50 years (Chapter 1). Using high-resolution sonar data (Chapter 2) to overcome sampling limitations, this chapter explores the localized patterns of *Chrysaora* distribution, defined by a source-sink framework, highlighting the role of a small tidal creek within a sub-estuary study area or waterscape (Patuxent River, Chesapeake Bay).

The multi-scale approach of my research was conducted to recognize and define the central role that scale plays in determining the outcome of observations (Levin 1992, Schneider 1994, Peterson and Parker 1998). It is well accepted among scientists that there are no natural definitions of scale, and species patterns are reflected at all ranges of scales with contrasting variability (Levin 1992). For example, scale-variant spatial patterns are often detectable for some species, such as regularity at small scales and clustering at larger scales (Jordano et al. 2003, Dale & Fortin 2014), although this phenomenon is difficult to detect with marine organisms, particularly in shallow water habitat where sampling gear and data resolution are limiting factors.

I deployed an Adaptive Resolution Imaging Sonar (ARIS) system to collect sonar data on *Chrysaora* in a Chesapeake Bay tributary and analyzed medusa density and distribution through space and time at a fine grain size i.e. high sampling resolution. Robust data collection and processing procedures allowed me to

investigate spatial patterns at multiple scales with an unprecedented evaluation of fine-scale *Chrysaora* spatial dynamics. Quantifying and comparing variability in abundance and spatial patterns of medusae is important for understanding dispersal and subsequent life-history success of *Chrysaora* (and other jellyfish spp.) in a dynamic, shallow habitat where environmental conditions can vary greatly from year to year (Cargo & King 1990a, Purcell et al. 2000, Breitburg & Fulford 2006). I hypothesized that patterns in medusae dispersion were a multi-scale response to interannual variation in abundance noted in 2016 and 2017. My hypotheses stated that spatial dependency would be observed in both the fine scale (<5m) and mesoscale (<10 km) observations of *Chrysaora* dispersion, with contrasting patterns between years. Specifically, I aimed to investigate the role of abundance at the fine and coarse scale, with respect to clustering and dispersal of *Chrysaora* medusae and also aggregations of medusae that formed patches, where I hypothesized increased clustering in high-density years.

Materials and Methods

Study Sites

The Chesapeake Bay is the nation's largest estuary with environmental conditions that vary spatially, seasonally, and interannually. The hydrodynamics of estuaries (physical processes) are tightly coupled with biogeochemical properties like salinity, nutrient transport, hypoxia etc. (Hagy et al. 2000, Hong & Shen 2012). The research of this dissertation focused on the lower portion of the tidal Patuxent River, a mid-Bay tributary. Discharge rates from the USGS Station 01594440

(https://waterdata.usgs.gov/usa/nwis/uv?01594440) served as a proxy to describe differences in winter and summer flow conditions of the Patuxent River waterscape (Fig. 4.1) in 2016 and 2017 (Hagy et al. 2000). Wind direction and wind speed (mph) across the summers of 2016 and 2017, were sourced from the Patterson Park Station in St. Leonard MD (www.wunderground.com).

Three habitats were selected to investigate *Chrysaora* source-sink dynamics in a Chesapeake Bay waterscape from source to dispersal habitat (Fig. 4.1). The study included a transect in each habitat; the north to south St. Leonard's Creek (SLC) transect was approximately 3 km long and began mid-way up the creek, ending in the mouth of SLC where it met the Patuxent River channel. The transect continued across the upper Patuxent River channel with a horizontal trajectory (from east to west) approximately 2.5 km in length (UPX). A third transect was a horizontal cross-section of the lower portion of the Patuxent River (LPX) channel, covering an average distance of 2 km. Within the sub-estuary and across the different habitats, it was assumed that jellyfish in the Patuxent River channel were mainly sourced from St. Leonard's Creek (SLC) while the Patuxent River channel (UPX, LPX) was considered dispersal habitat. *Chrysaora* in the lower Patuxent (LPX) also could have been sourced from adjacent creeks, including Cuckold Creek and Hellen's Creek (Fig. 4.1). Additional research is needed to assess differences in creek production and transport of medusae into the Patuxent River channel.

Field Sampling

The three habitats SLC, UPX and LPX were sampled (approximately bi-weekly) from 26 May - 28 August in 2016 (8 sample events), and from 08 June - 31 August in 2017 (9 sample events) for a total of 17 surveys. The majority of sampling events began in LPX during high-tide and proceeded upriver to UPX and then into SLC.

The ARIS3000 (Soundmetrics) was deployed, a sonar camera capable of recording high-definition data in highly turbid waters that are characteristic of the study sites. The ARIS3000 was attached to a polearm that pivoted on the gunwale of the 21-ft research vessel (Fig. 4.2). A live feed was recorded using a laptop computer and ARISScope software (Soundmetrics) with an applied 'Tow' filter. A portable 125V generator powered both the sonar camera and the laptop computer.

When submerged approximately 1 m below the surface, the camera was towed at the slowest possible speed of 1 knot, and data were recorded at a rate of 15 frames s^{-1} for the highest possible resolution. In 2016 the ARIS was deployed with a downward trajectory, i.e. an average pitch angle approximately 50° from the water's surface and the camera pointed towards the stern. In 2017 the pitch angle was changed to improve resolution (75°) and the face of the camera was reversed to point ahead to the bow. For most of the deployments, the depth-of-view of the camera was limited to 7 m. The deep area of the river channel (UPX and LPX) habitat was sampled by maximizing the camera depth-of-view from 7 m to 15 m, thus sampling >150,000 m^3, in hopes of detecting jellyfish at deeper ranges, although few medusae were found (<5 medusae overall). Maximizing the depth-of-view limited resolution of

the camera and made processing more challenging. Consequently, the sample range was limited to 7 m considering the low counts of medusae observed beyond this depth. These changes in deployment did not affect the quality of the data but instead improved efficiency of data collection and processing by optimizing the sampling procedures. For example, higher resolution images allowed for easier and faster identification of *Chrysaora*, though they were still detectable in lower-resolution data. Temperature and salinity were recorded every second along the tow path using an RBR Concerto CTD, which was deployed 1 m below the water surface. A handheld Garmin GPS unit was used to map the trajectory of transects during each sampling event (~ 5 hours per survey).

Sonar Data Processing

In 2016 there were more than 11.5 hours of data (627,518 frames) and in 2017 12.5 hours of data were recorded (676,113frames) for a total of 1,303,631 frames. Each frame was manually inspected using ARISfish software, and positively identified jellyfish were counted and marked in the water column with recorded depths of an individual accurate to 0.1 m. Using interpolated transect tracks (s^{-1}) as well as the latitude and longitude of all counted *Chrysaora*, sample volume and sample depth were calculated for each recorded frame using image analysis methods adapted from (Shahrestani et al. 2017). Frames were aggregated to standardize jellyfish counts; *Chrysaora* medusa occurrence was summed within cubic meter bins (Fig. 4.3).

Multi-Scale Spatial Analysis

Fine-scale patterns (<5 m) were explored by observing the 2D point patterns of *Chrysaora* observations in a 5 m (water column depth) by 5 m (distance along transect) window within high-density bins from 2016 and 2017 (Fig. 4.4). Completely Spatially Random (CSR) points were generated using the 'spatstat' package in R to create a theoretical envelope and compared the empirical values using the G-function which estimates the nearest-neighbor distance distributions (Bivand et al. 2008). The G-function was used as a test for the spatial homogeneity of the data at the smallest relevant scale (5 m) whereby deviations between the theoretical Poisson process (CSR), and empirical results are suggestive of spatial aggregations or dispersal. The 5 m x 5 m window size was selected due to the estimations of the G-function that considers a radius have the size of the largest possible disc created in the space. The vertical space was limited by the water-column i.e. depth, so I opted for a square window with a 5 m vertical length by a 5 m horizontal width.

At the mesoscale, spatial patterns of *Chrysaora* were investigated along the distance of sampled transects (1-3 km). It was necessary to account for the small-scale variability in the start and stop locations between surveys and among habitat, as well as the meandering tracks in SLC due to the geomorphology of the study site (Fig. 4.1). To do so, a variable 'river distance' was designated which represents the closest distance (m) an individual *Chrysaora* medusa is to a source point within a transect. The source point of each transect was defined as the northern (SLC) or eastern (UPX, LPX) most sample location on any given survey within each of the three study sites. Mesoscale patterns of spatial autocorrelation were analyzed in the

count data by binning the jellyfish observations into 5-m segments, using the river distance variable, and plotting Autocorrelation Functions (ACF) for data collected in all three habitats in the peak week of each year.

Spatially Explicit GAM

Fine-scale predictions of local abundance were estimated using a Generalized Additive Model (GAM), which is a nonparametric extension of the generalized linear model. A GAM was selected as the most appropriate model because it can incorporate spatial and temporal autocorrelation, which was inherent in the dataset. Model selection for the most parsimonious model included screening for low values of Akaike Information Criterion (AIC) as well as high values of global deviance (%) explained by the model. The final GAM was used to generate spatially explicit estimates of *Chrysaora* abundance within the study habitat across years. The GAM was fit for both the creek (SLC) and channel (UPX, LPX) sites of the Patuxent River waterscape using non-parametric smoother functions with R statistical software ('mgcv' package). The following model format was selected:

Chrysaora count ~ negative binomial = year + s(week of year, by=creek/channel) + s(river distance, by=creek/channel) + log(volume).

For spatially explicit estimates the 'raster' package in R was used to grid and project the waterscape into 8 m x 6.25 m grid cells, assigning values of *river distance* and *volume* to each cell. The volume of each cell (400 m^3) within the waterscape was

calculated by multiplying the surface area of each cell (50 m^2) by 8-m depth. The abundance estimates were limited to the upper 8 m of the water column because of low numbers of medusae counted below that depth.

Results

High-Resolution Sonar Data

A total of 57,846 *Chrysaora* were counted and geolocated over the course of the study and their positions mapped in the water column to visualize their spatial distribution in the vertical and horizontal directions (depth vs distance-along-transect), accurate to 0.1 m (Fig. 4.4, Fig. 4.6). Overall, across sites, cruises and years, medusae maintained themselves at depths between 2 and 4 m, although the mean depth of *Chrysaora* was nearer the surface in 2017 (μ = 2.3 m, SD = 0.8 m), compared to 2016 (μ = 3.1 m, SD = 1.1 m). Continuous counts of *Chrysaora* along transects revealed variable density distributions and dispersal patterns between sites and survey events (Fig. 4.4).

Across all habitats, highest counts of medusae were found in the creek (SLC). In this source creek, 75% of the population was contained in less than <1.0% percent of the total volume sampled within each survey, with an exception on 28 June 2016, when the jellyfish were more dispersed across the sampled transect in SLC (Fig. 4.4). During the peak density weeks in 2016 and 2017, the densest aggregations occurred in SLC where 75% of *Chrysaora* were contained in 0.6% of the sampled volume in 2016 and in 0.2% of the sampled volume in 2017. In the 2016 surveys conducted after 28 June, 75% of the population was concentrated at the initial point of the SLC

transect, towards the creek's headwaters (Fig. 4.1). This observation contrasted with 2017 when the densest aggregations of *Chrysaora* were located ~1.5 km downstream from the headwater site in four of the seven surveys, including the peak density week of 18 July 2017 (Fig. 4.4).

Multiscale Spatial Analyses

The relative density within 5-m bins was highest during the peak week in St. Leonard's Creek (2017) and had the greatest number of medusae per 5-m bin (Fig. 4.7). The highest density of *Chrysaora* was observed in the creek during the peak week in 2016. No other habitat or surveys in 2016 had high or medium density aggregations outside of SLC and the peak week. The result differed in 2017 when high-density patches were found in all three site locations during the peak week. The ratio of high to low-density bin frequency in the SLC (2:25) was similar between years.

By investigating the spatial point patterns of *Chrysaora* within a 5 m (depth) by 5 m (distance-along-transect) window, I documented the densest aggregations of jellyfish in 2016 and 2017. Results of the CSR simulation and G-tests indicated spatial randomness of jellyfish distribution in the water column in 2016 (Fig. 4.8). In 2017, water-column medusae spatial aggregation was detected although deviations of the empirical data from the theoretical CSR simulation were minimal and mostly non-significant, suggesting spatial randomness of medusae in the water column in both years at the 5-m scale.

Spatial patterns at a larger scale were examined through generated ACF plots (Fig. 4.9) and revealed contrasting spatial dynamics of *Chrysaora* during the peak weeks of each year in 2016 and 2017. In both years, the strongest patterns of sinusoidal decay, i.e. density gradient of *Chrysaora* over space occurred within the creek (Fig. 4.9, SLC). In 2016, the range of spatial autocorrelation was limited to 50-100 m for the three peaks that may represent individual patches in SLC. The distance between apparent patches in the same week and transect may be an artifact of the time-lag between strobilating polyps that generally show patterns of bi-weekly periodicity. Increased density of *Chrysaora* in 2017 was reflected in the spatial autocorrelation observed across all habitats, although the rates of decay were less robust, with much wider ranges of *Chrysaora* dispersal (~500 m).

Spatially Explicit Predictions

Using a spatially explicit GAM, the spatial-temporal nature of the data was addressed by incorporating a river distance variable which accounted for the spatial autocorrelation inherent in the data as well as 'week of the year,' which modeled seasonality. Water-column depth, temperature, and salinity did not significantly explain the patterns observed in the data and were excluded from the model. The final model performed well and explained 84.8% ($R^2 = 0.76$) of the global deviance observed in the dataset. The final GAM had the lowest AIC value well below (-1000) relative to other models in which salinity, temperature, and depth had been included as possible explanatory values. A Negative Binomial distribution was selected as the best family describing the data, and greatly outperformed both Gaussian and Zero-Inflated Poisson distributions in the GAM.

The spatially-explicit model allowed estimation of total abundance and evaluation of patterns of dispersion in the study habitat in 2016 and 2017 (Table 4.1). Estimated abundance of *Chrysaora* in the entire waterscape was approximately 3 times higher in 2017 than in 2016 (Fig. 4.5). Higher density in 2017 was also apparent in the SLC during the peak week when 38 medusae/100 m^3 were counted compared to 20 medusae/100 m^3 in 2016. The highest abundances estimated throughout the entire waterscape, including SLC, UPX and LPX (Fig. 4.1), occurred during the weeks of 21 July 2016 and 18 July 2017; 495,179 and 1,609,360, respectively (Table 4.1). Investigating weeks with similar abundance between years i.e. 495,179 on 21 July 2016 and 436,362 on 24 July 2017, there was a strong contrast in the dispersion of jellyfish between the study sites. For example, during these weeks 83% of the jellyfish were found in the creek (SLC) in 2016, while in 2017, 88% were found in the channel (UPX and LPX).

Discussion

The major hypothesis of this chapter stated that differences in abundance between 2016 and 2017 would lead to variable spatial patterns among the creek/channel sites and between years. Although there was an estimated three times more medusae in 2017 than in 2016, it should be noted that results from this study revealed similar overall patterns of *Chrysaora* dispersion and seasonality not only across 2016 and 2017, but also when compared to previous studies conducted in Chesapeake Bay tributaries (Cargo & Schultz 1966, Cones & Haven 1969, Loeb 1972, Calder 1974, Baird & Ulanowicz 1989, Purcell 1992a, Suchman & Sullivan

1998, Brown et al. 2002, Breitburg & Fulford 2006, Decker et al. 2007a, Breitburg & Burrell 2014, Tay & Hood 2017). Whereby, spatial patterns of *Chrysaora* across sites, revealed the greatest concentration of medusae in the sluggish headwaters of an adjacent creek, i.e. St. Leonard's Creek (SLC) as opposed to channel sites i.e. the upper (UPX) and lower (LPX) Patuxent river channel (Fig. 4.1). This indicates that although *Chrysaora* medusae are weak swimmers, observed higher densities of *Chrysaora* in the source creek throughout the season suggest that medusae were able to remain in source habitat with only a portion of their population transported to the river channel.

Increased transport of *Chrysaora* medusae to the Patuxent River channel i.e. UPX and LPX, was clearly observed in 2017, and may begin to describe the difference in spatial patterns hypothesized at the coarse scale between years. It is unclear if the higher densities in 2017 led to increased transport perhaps related to space and resource limitation. Other potential advective factors i.e. wind, river discharge, geomorphology of sites (Purcell et al. 2000, Graham et al. 2001, Suchman & Brodeur 2005, Decker et al. 2007a, Hamner & Dawson 2009, Kaneshiro-Pineiro & Kimmel 2015, Tay & Hood 2017) may have contributed to dispersal although the mechanisms that control the rate of transport of *Chrysaora* from source to dispersal habitat are unclear. Previous studies conducted in the Chesapeake Bay mainstem found *Chrysaora* abundance to be correlated with patterns of temperature and salinity (Brown et al. 2002, Decker et al. 2007a, Brown et al. 2013) which suggests a coupling between biogeochemical and biophysical processes in the Bay (Hagy et al. 2000, Hong & Shen 2012). However, temperature and salinity were not significant

variables explaining the spatial patterns noted between creek and channel sites in this study. Additional production in other nearby adjacent creeks (Hellen's creek & Cuckold Creek), and subsequent dispersal to the lower channel (LPX) likely contributed to the abundance in the lower channel site, though to what extent is difficult interpret. More research should be done to understand the production of different creeks, and whether *Chrysaora* production scales with the presence of oyster reefs, water depth, or shoreline type.

Application of advanced technology has allowed for an unprecedented look at the spatial patterns of a jellyfish species in the vertical and horizontal distribution of a waterscape. In sampling thousands of jellyfish, I was able to identify the mean depth of occurrence of jellyfish and observed the vertical and position of *Chrysaora* in 2016 and 2017 within the water column (Fig. 4.6). However, on 18 July 2018 and 22 Aug 2018 (Fig. 4.6) dense aggregations occurred along a possible pycnocline, which is common with many scyphozoans species, where they are exposed to less turbulence, slower mass transfer, as well as high prey concentrations (Keister et al. 2000, Graham et al. 2001, Purcell et al. 2014). While vertical distributions of jellyfish did not differ much between years, *Chrysaora* spatial patterns and abundance within and among the three study sites were highly variable in 2016 and 2017 and are poorly understood.

A multi-scale approach to ecological studies is often necessary to explain the combination of effects that are reflected in spatial patterns of organisms, e.g., homogeneity or regularity at smaller scales and aggregation at larger scales. In the case of fine-scale *Chrysaora* patterns, I had hypothesized that spatial dependency and clustering would be observed in 5-m segments, with higher levels of aggregation in

2017, the higher abundance year. However, I rejected this hypothesis. The fine-scale locations of *Chrysaora* in the water column were spatially random in both years, despite the fact that abundance was three times higher in 2017. The observed pattern of random dispersion in the water column may reflect a lack of social behaviors or interactions among species in which point patterns are responsive to a multitude of uncontrollable factors (i.e. potentially wind, tidal forcing, discharge in the case of *Chrysaora*). The random patterns in fine-scale distributions of *Chrysaora* are likely shaped by advective forces acting on the patch as a whole, rather than behavior of individual medusae.

Spatial autocorrelation and patchiness at the coarse scale have been observed for *Chrysaora chesapeakei.* For example, Tay & Hood 2017) reported medusae patches to be spatially dependent and aggregated at the kilometer scale. Using the high-resolution count data, I hypothesized my results would reveal similar levels of spatial autocorrelation detected with jellyfish patches at the coarse scale, particularly with high densities in 2017, which I suggested would lead to an increased level of clustering due to space limitation. However, I rejected this hypothesis and found the opposite to be true, i.e., *Chrysaora* were more clustered and less dispersed in the low-density year, 2016.

I hypothesized that differences in mesoscale spatial autocorrelation between years, i.e. the increased dispersion and spatial dependence in 2017, could have been caused by high-magnitude advective forces. However, there were no significant differences in Patuxent River discharge in June-August 2016 and 2017. Furthermore, summertime wind did not differ significantly between 2016 and 2017. In each year,

~37% of summer winds blew from the southwest, with an average speed of 7.8 m s^{-1}. The results suggest that mesoscale spatial patterns of jellyfish were controlled by differences in medusae transport from the source to the sink that were responsive to space/resource limitation in the high abundance year although the mechanisms are unclear. Specifically, I observed relatively lower abundance and less dispersal in 2016, and higher abundance with more dispersal in 2017. I suggest that by remaining in creeks during low-density years, *Chrysaora* lessens the risk of being transported to new, but potentially unfavorable habitat. In a high-density year like 2017, transport to new habitat would be less risky and a favored strategy for population success, i.e. expanding their distribution to potentially mitigate competition for resources.

A closer look at the growth and transport of *Chrysaora* patches revealed the appearance of high density aggregations of *Chrysaora* in the source creeks (Fig. 4.7), which more than likely coincided with strobilation events (mass asexual reproduction), occurring 40-60 days prior, a time duration that allows for strobilation and growth of juveniles (1-2 mm) to a size detectable by the sonar camera (bell diameter approximately 7-10 cm). In the creek in 2016, assuming the appearance of medusae reflected the first strobilation event, followed by the appearance of high-density aggregations (second strobilation event), there were only two possible strobilation events. However, in 2017, there appeared to be three strobilation events. The first with the appearance of *Chrysaora* for the season, and the second and third events attributed to high-density aggregations three weeks apart. The difference in the potential number of successful strobilation events from year to year may begin to explain the high variability in medusa magnitude noted from 2016 to 2017.

Strobilation events are the primary method of asexual reproduction and numerical growth for non-holoplankton scyphozoans worldwide (Arai 2009, Lucas et al. 2012b), and the success of early life stages is said to affect the magnitude of a jellyfish bloom from year to year (Cargo and King 1990). Though it is difficult to provide evidence for the exact mechanisms that lead to a third strobilation event as I observed in 2017 or its lack in 2016, the strong contrast in estimated abundance between years (495,179 medusae in 2016, and 1,609,360 in 2017, Table 4.1) allowed for a unique opportunity to explore the multi-scale spatial patterns of *Chrysaora* medusae that reflect stark differences in dispersion patterns.

Conclusion

The multi-scale dispersion patterns analyzed and reported in this study were only feasible due to the collection of high-resolution spatial data that would have been unattainable with common sampling methods (nets, seines) in marine environments, in which multiple observations are spatially compressed into a single point. Innovative methods such as sonar sampling proved successful in this research, mitigating the difficulties of sampling in shallow habitats by providing continuous count data along a transect, with enough resolution to quantify spatial patterns of medusa distributions at multiple scales. At the fine-scale (5m) physical forcing may have led to the random dispersion patterns observed for jellyfish in the water column. However, at the coarse scale (between study sites) *Chrysaora* dispersion may have been due to biological factors i.e. strobilation and subsequent density, and different rates of transport observed in contrasting years of abundance. Exhaustion of resources as well as space limitation may have led to increased transport from source to

dispersal habitat in the high-abundance year 2017. Decreased transport in 2016 suggests that, even though jellyfish density was low, the population managed to mitigate for decreased abundance by its substantial retention near source habitat. Considering the large population increase observed in 2017, the 2016 population was quite successful in ensuring the longevity of future generations of *Chrysaora* in the Patuxent River.

References

Arai MN (2009) The potential importance of podocysts to the formation of scyphozoan blooms: a review. Hydrobiologia 616:241-246

Baird D, Ulanowicz RE (1989) The seasonal dynamics of the chesapeake bay ecosystem. Ecol Monogr 59:329-364

Bivand RS, Pebesma EJ, Gómez-Rubio V, Pebesma EJ (2008) Applied spatial data analysis with R, Vol 747248717. Springer

Breitburg D, Burrell R (2014) Predator-mediated landscape structure: seasonal patterns of spatial expansion and prey control by *Chrysaora* quinquecirrha and Mnemiopsis leidyi. Marine Ecology Progress Series 510:183-200

Breitburg DL, Fulford RS (2006) Oyster-sea nettle interdependence and altered control within the Chesapeake Bay ecosystem. Estuaries and Coasts 29:776-784

Brown CW, Hood RR, Li Z, Decker MB, Gross TF, Purcell JE, Wang HV (2002) Forecasting system predicts presence of sea nettles in Chesapeake Bay. Eos, Transactions American Geophysical Union 83:321-326

Brown CW, Hood RR, Long W, Jacobs J and others (2013) Ecological forecasting in Chesapeake Bay: Using a mechanistic–empirical modeling approach. Journal of Marine Systems 125:113-125

Calder DR (1974) Strobilation of the Sea Nettle, *Chrysaora quinquecirrha*, under Field Conditions. Biol Bull 146:326-334

Cargo DG, Schultz LP (1966) Notes on the biology of the sea nettle, *Chrysaora quinquecirrha*, in Chesapeake Bay. Chesapeake Science 7:95-100

Cargo DG, King DR (1990) Forecasting the abundance of the sea nettle,*Chrysaora quinquecirrha*, in the Chesapeake Bay. Estuaries 13:486-491

Cones HN, Haven DS (1969) Distribution of *Chrysaora quinquecirrha* in the York River. Chesapeake Science 10:75-84

Dale MRT, Fortin MJ (2014) Spatial Analysis: A Guide For Ecologists, Vol. Cambridge University Press

Decker MB, Brown CW, Hood RR, Purcell JE and others (2007) Predicting the distribution of the scyphomedusa *Chrysaora* quinquecirrha in Chesapeake Bay. Marine Ecology Progress Series 329:99-113

Graham WM, Pages F, Hamner WM (2001) A physical context for gelatinous zooplankton aggregations: a review. Hydrobiologia 451:199-212

Hagy JD, Boynton WR, Sanford LP (2000) Estimation of net physical transport and hydraulic residence times for a coastal plain estuary using box models. Estuaries 23:328-340

Hamner WM, Dawson MN (2009) A review and synthesis on the systematics and evolution of jellyfish blooms: advantageous aggregations and adaptive assemblages. Hydrobiologia 616:161-191

Hong B, Shen J (2012) Responses of estuarine salinity and transport processes to potential future sea-level rise in the Chesapeake Bay. Estuarine, Coastal and Shelf Science 104-105:33-45

Jordano P, Bascompte J, Olesen JM (2003) Invariant properties in coevolutionary networks of plant–animal interactions. Ecology letters 6:69-81

Kaneshiro-Pineiro MY, Kimmel DG (2015) Local Wind Dynamics Influence the Distribution and Abundance of *Chrysaora* quinquecirrha in North Carolina, USA. Estuaries and Coasts 38:1965-1975

Keister JE, Houde ED, Breitburg DL (2000) Effects of bottom-layer hypoxia on abundances and depth distributions of organisms in Patuxent River, Chesapeake Bay. Marine Ecology Progress Series 205:43-59

Loeb MJ (1972) Strobilation in the Chesapeake Bay sea nettle *Chrysaora quinquecirrha.* I. The effects of environmental temperature changes on strobilation and growth. Journal of Experimental Zoology 180:279-291

Lucas CH, Graham WM, Widmer C (2012) Jellyfish life histories: Role of polyps in forming and maintaining scyphomedusa populations. In: Lesser M (ed) Advances in Marine Biology, Vol 63, Vol 63. Elsevier Academic Press Inc, San Diego, p 133-196

Purcell JE (1992) Effects of predation by the scyphomedusan *Chrysaora quinquecirrha* on zooplankton populations in Chesapeake Bay, USA. Marine Ecology Progress Series 87:65-76

Purcell JE, Brown ED, Stokesbury KDE, Haldorson LH, Shirley TC (2000) Aggregations of the jellyfish Aurelia labiata: abundance, distribution, association with age-0 walleye pollock, and behaviors promoting aggregation in Prince William Sound, Alaska, USA. Marine Ecology Progress Series 195:145-158

Purcell JE, Decker MB, Breitburg DL, Broughton KJ (2014) Fine-scale vertical distributions of Mnemiopsis leidyi ctenophores: predation on copepods relative to stratification and hypoxia. Marine Ecology Progress Series 500:103-120

Shahrestani S, Bi H, Lyubchich V, Boswell KM (2017) Detecting a nearshore fish parade using the adaptive resolution imaging sonar (ARIS): An automated procedure for data analysis. Fisheries Research 191:190-199

Stoyan D, Penttinen A (2000) Recent Applications of Point Process Methods in Forestry Statistics. Statistical Science 15:61-78

Suchman CL, Sullivan BK (1998) Vulnerability of the copepod Acartia tonsa to predation by the scyphomedusa *Chrysaora* quinquecirrha: effect of prey size and behavior. Mar Biol 132:237-245

Suchman CL, Brodeur RD (2005) Abundance and distribution of large medusae in surface waters of the northern California Current. Deep-Sea Res Part II-Top Stud Oceanogr 52:51-72

Tay J, Hood RR (2017) Abundance and patchiness of *Chrysaora quinquecirrha* medusae from a high-frequency time series in the Choptank River, Chesapeake Bay, USA. Hydrobiologia 792:227-242

Figures and Tables

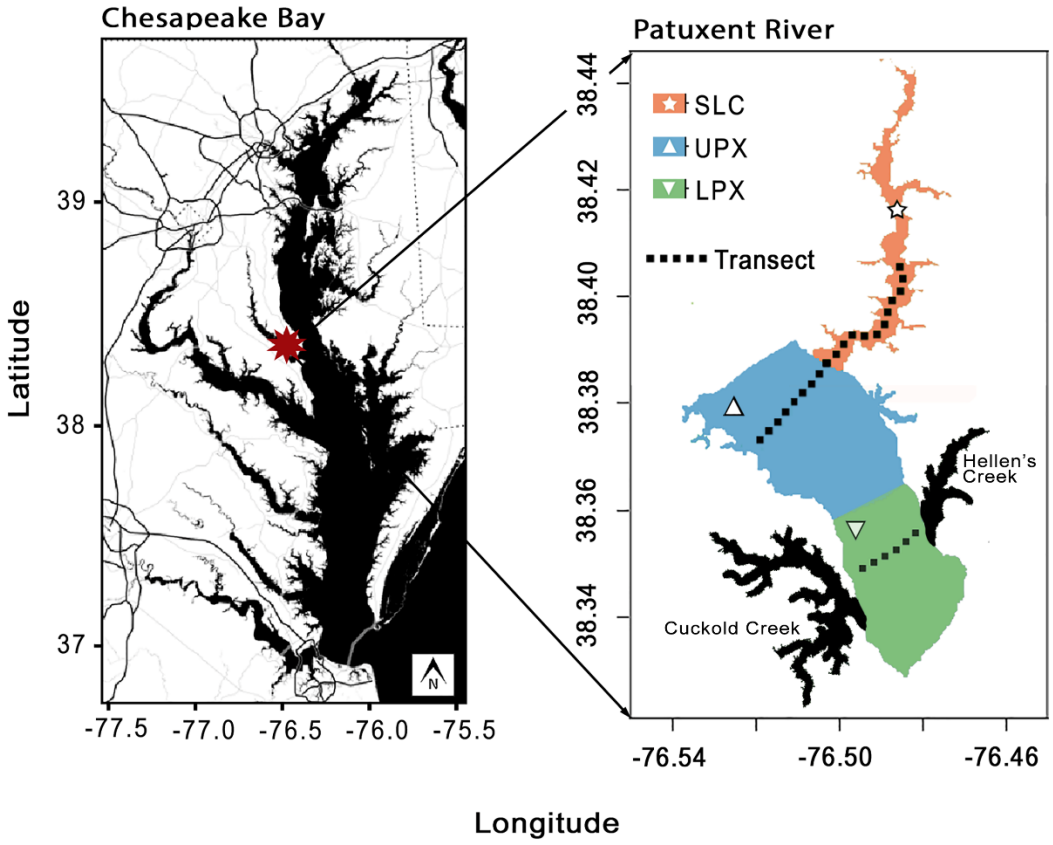

Figure 4.1 Patuxent River, Chesapeake Bay, USA waterscape, showing three habitat sites: 1) St. Leonard's Creek (SLC, star), a creek adjacent to the mid-portion of the Patuxent River Channel. The upper portion of the channel sites in the waterscape (UPX, triangle), and the lower portion of the study site waterscape (LPX, upside down triangle). The dotted black lines represent approximate trajectories of survey transects in the 2016 and 2017 summer season

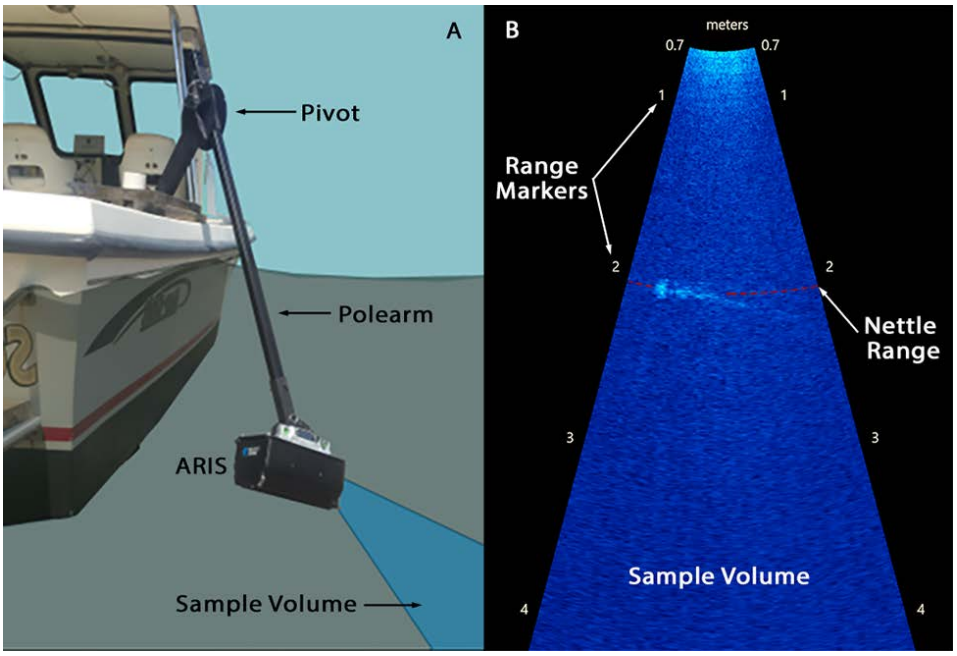

Figure 4.2 The ARIS sonar camera (SoundMetrics, Inc) was towed along transect lines while attached to a small research vessel (A). The mounting gear included a pivot that attached to the gunwale of the research vessel and was fitted with a polearm that extends approximately 1/3 of a meter into the water column. The ARIS camera was affixed to the end of the polearm with a mounting plate and the pitch of the camera had an average deployment angle of 55 ° below the water's surface. SoundMetrics software (ARISFish) records footage as seen in panel B, whereby *Chrysaora chesapeakei* >7-10 cm in bell diameter were detectable and marked in the water column. The range markers denote the range of the field-of-view of the camera and the dashed red line (B) is the range of an individual nettle as detected by Aris Fish software. The surface area of the blue triangle (B) created by the compression of 3D data (ARISScope) was estimated as sample volume

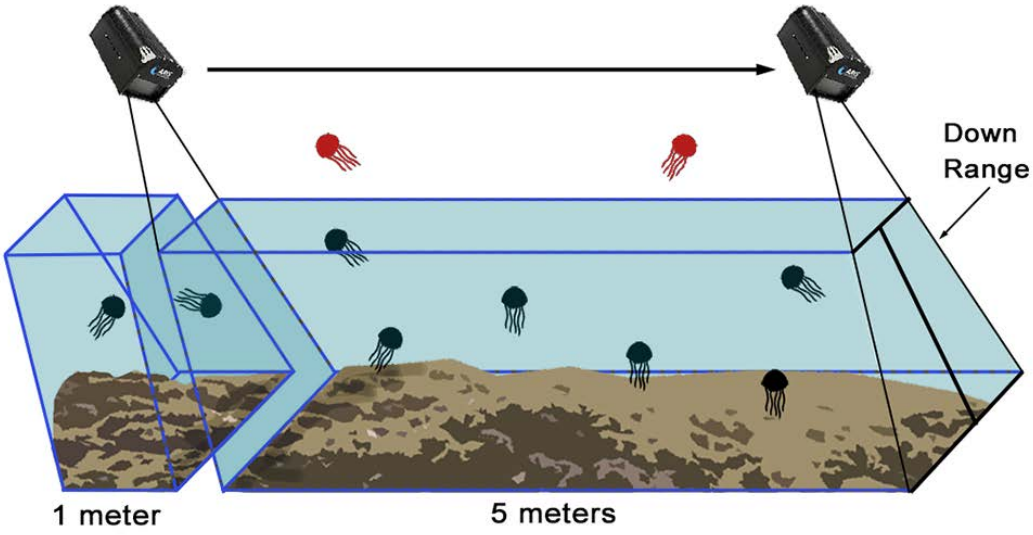

Figure 4.3 Conceptual diagram of transect binning, whereby data recorded along the transects were divided into 5-m segments. Within-bin density was estimated by counting medusae within a 5-m bin and estimating the volume of each 5-m bin. The first meter or so of the sample volume is cut off, whereby only black jellyfish in the image above are counted and red jellyfish are undetectable.

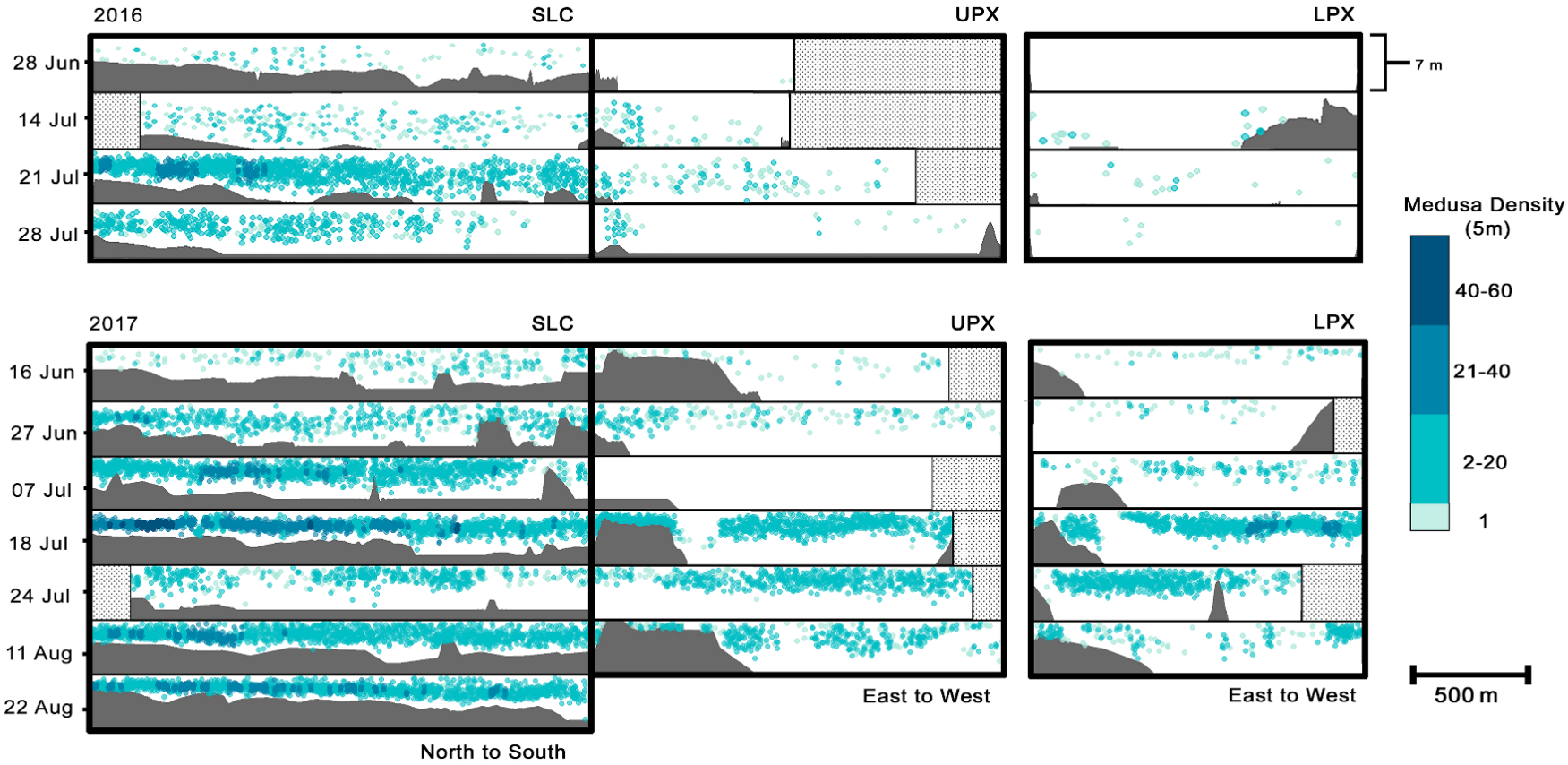

Figure 4.4 Seafloor depth profiles (0-7 m) and depth of *Chrysaora chesapeakei* in the water column for each transect from June through July 2016 and June through August 2017. The gray polygons along the x-axis represent the sea-floor as detected along the

transect tracks from north to south (SLC) or east to west (UPX, LPX). Dark blue dots are an overlap of 40-60 or more medusae within the same sample volume at that transect position, and the lightest shade of blue dots represent individual jellyfish

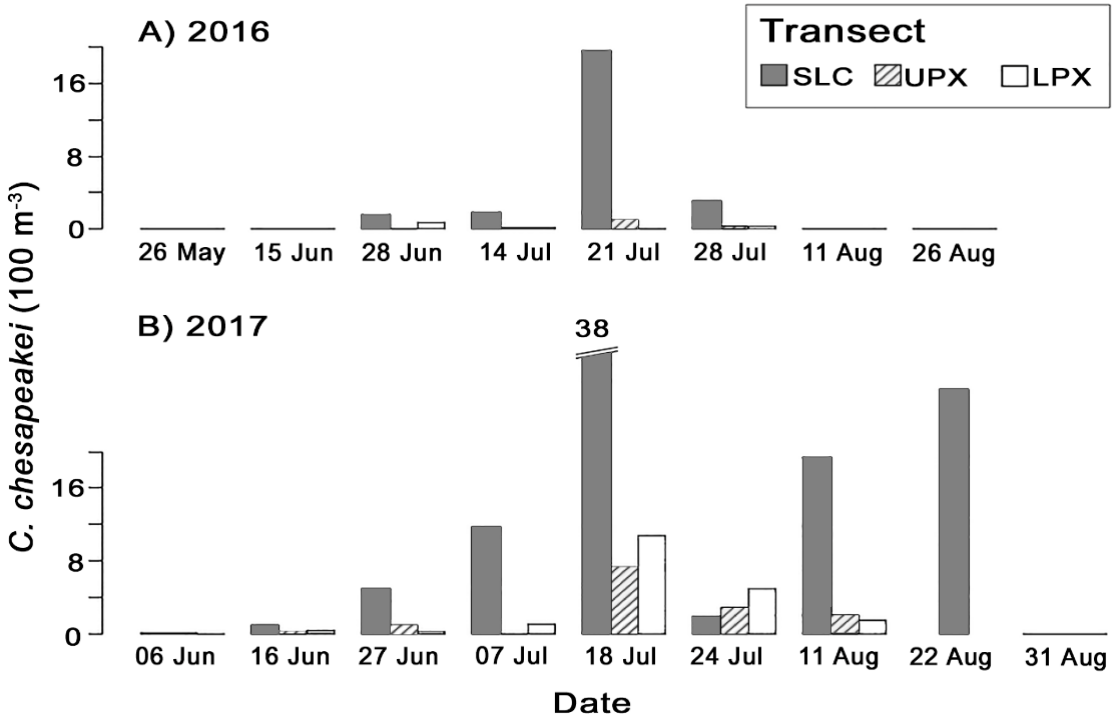

Figure 4.5 Density of *Chrysaora chesapeakei* (individuals per 100 m^3) computed for each transect in A) 2016 and B) 2017. The black bars represent St. Leonard's Creek (SLC), while gray bars represent densities in the Upper Patuxent River Channel (UPX), and white bars represent medusae density in the lower Patuxent River Channel. Surveys were approximately bi-weekly in 2016 and 2017. No data were collected at transect sites UPX and LPX on 22 August 2017.

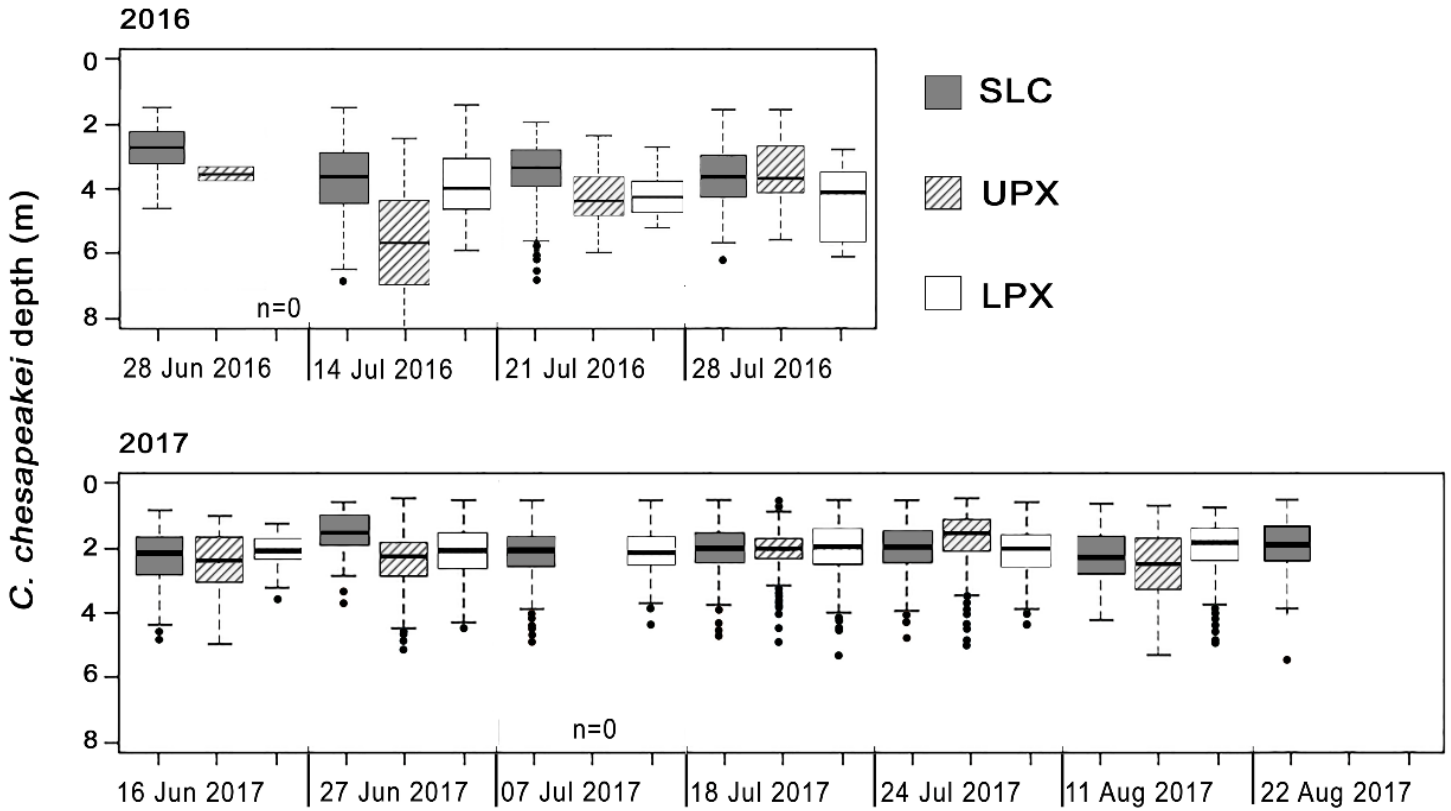

Figure 4.6 Estimated depth (meters) of *Chrysaora chesapeakei* vertical distribution in A) 2016 and B) 2017 summer season. Boxes are median and interquartile range, whiskers are minimum and maximum. The gray boxes represent St. Leonard's Creek (SLC), while

white boxes represent the Upper Patuxent River Channel (UPX), and hatched boxes represent the lower Patuxent River Channel (LPX). Surveys were approximately bi-weekly in 2016 and 2017. No data were collected in transect sites UPX and LPX on 22 August 2017

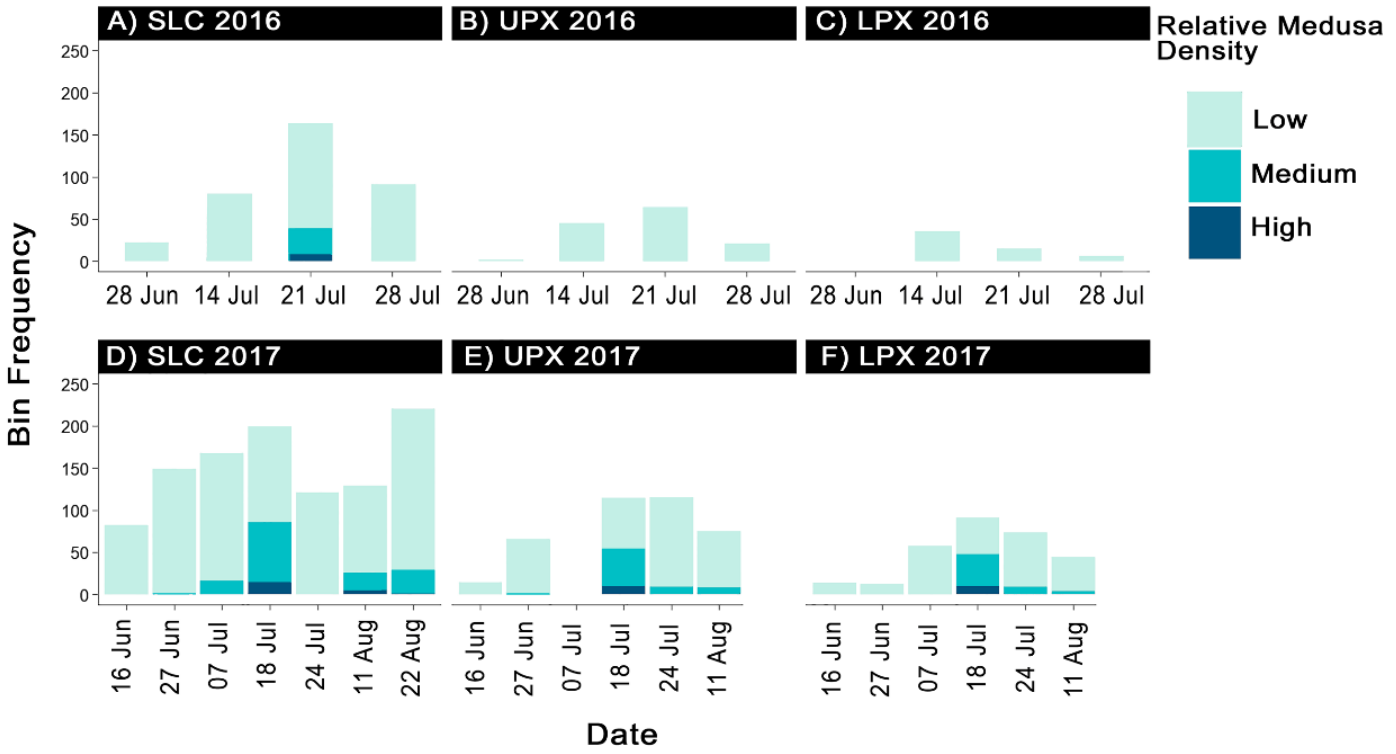

Figure 4.7 Relative *Chrysaora chesapeakei* density noted between years and across habitats. Transects were binned into 5 m and the relative density within each bin was categorized as low, medium or high within years and each transect study-site; St. Leonard's Creek (SLC), the Upper Patuxent River channel (UPX) and the Lower Patuxent River channel (LPX). In 2016 (A-C) low counts represent

bins with 1 – 40, medium density bins have 40 - 80 medusae and high-density bins contain 81 - 120 medusae. In 2017, the ranges are higher due to higher overall density. Low counts in 2017 represent bins that contain 1 - 60 medusae, medium bins have 60 - 120 medusae and high counts contain 120 - 180 medusae. Overall, the highest frequency of high-density medusae clusters occurred on 18 July 2017 in St. Leonard's Creek (SLC)

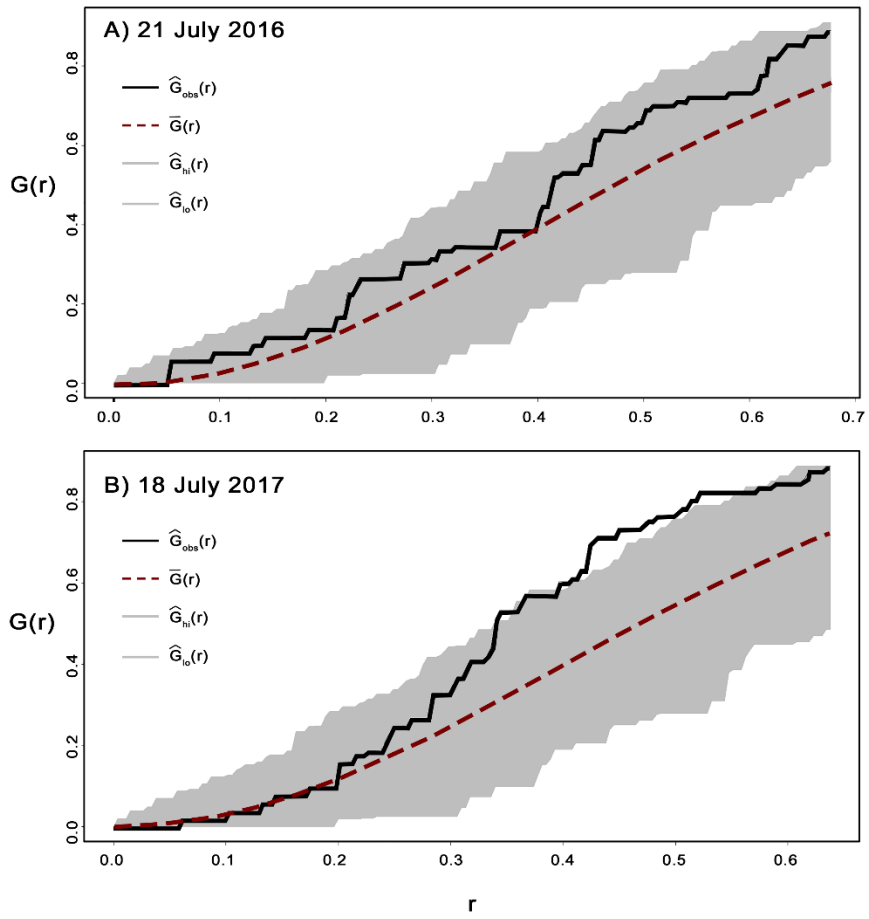

Figure 4.8 Complete Spatial Randomness (CSR) plot test of *Chrysaora chesapeakei* during the peak density week of 2016 (21 July) and 2017 (18 July). G(r) estimates of point patterns within a 5-m depth vs 5-m distance-along-transect window reflect the nearest neighbor distance distribution function, and r is the distance between medusae or points. The solid black line was computed from medusae observations; the dashed red line represents the CSR or random Poisson point pattern; the shaded area reflects the confidence range for a 95% significance level of the generated CSR patterns.

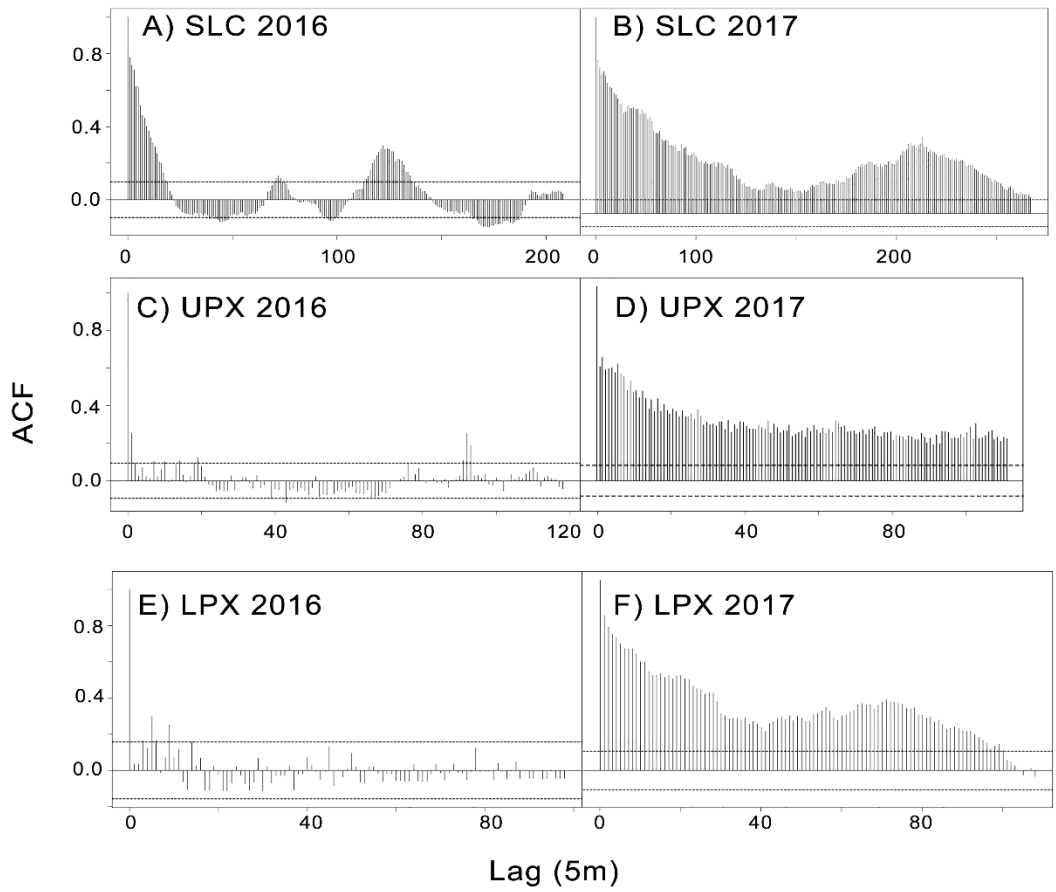

Figure 4.9 Sample AutoCorrelation Function (ACF) plots of *Chrysaora chesapeakei*, binned into 5-m distances along the transect lines in St. Leonard's Creek (SLC), the upper Patuxent River channel (UPX) and the lower Patuxent River Channel (LPX) observed during the peak weeks of medusae abundance on 21 July 2016 (A, C, E), and 18 July 2017 (B, D, F)

Table 4.1 Generalized Additive Model (GAM) predictions of *Chrysaora chesapeakei* medusae in 2016 and 2017 upper and lower Patuxent River *channel* (UPX and LPX) and an adjacent *creek*, St. Leonard's Creek (SLC) with 95% high and low confidence intervals. The GAM considered spatial and temporal variables (i.e. week and river distance) that accounted for the seasonal and spatial dependency in the distribution of *C. chesapeakei*

	Creek			Channel			Total		
	Medusa	**CI High**	**CI Low**	**Medusa**	**CI High**	**CI Low**	**Medusa**	**CI High**	**CI Low**
2016									
28 Jun	15,093	18,019	12,166	32	6,071	0	15,125	24,090	12,166
14 Jul	56,430	59339	53520	19,524	24,998	14,049	75,954	84,337	67,569
21 Jul	413,474	416,383	410,564	81,705	87,144	76,265	495,179	503,527	486,829
28 Jul	68,355	71,265	65,444	6,989	12,462	1,515	75,344	83,727	66,959
2017									
16 Jun	25,346	25,994	24,697	2,423	5,568	0	27,769	31,562	24,697
27 Jun	114,530	115,176	113,883	53,987	56,218	51,755	168,517	171,394	165,638
07 Jul	256,441	257,067	255,814	65,982	68,560	63,403	322,423	325,627	319,217
18 Jul	824,373	825,018	823,727	784,987	786,648	783,325	1,609,360	1,611,666	1,607,052
24 Jul	52,142	52,788	51,495	384,220	385,930	382,509	436,362	438,718	434,004
11 Aug	590,971	591,616	590,325	132,106	133,920	130,291	723,077	725,536	720,616

Conclusions

The successful use of sonar technology to detect and observe *Chrysaora* was a major milestone in this research, proving itself useful in capturing and processing images of *Chrysaora* medusae in the water column. In addressing my research goals, I was able to successfully calibrate the deployment of the ARIS sonar camera for towed deployment along transects that captured the spatial dynamics of *Chrysaora.* To address the massive amounts of data produced, I developed image analysis procedures to extract necessary information from the sample space that was then used to calculate jellyfish density. Although machine learning techniques were used to identify fish (Chapter 2), identifying jellyfish species presented a different challenge, and remains a work in progress. However, *Chrysaora* medusae were easily identified in the water column through manual observations of recorded data, and the coupling of manual counts and automated sample space processing allowed for a robust sampling procedure to assess medusae populations in turbid environments.

Regarding the four distinct life stages of *Chrysaora* (planula larvae, polyps, ephyrae, and medusae), recognition of spatial trends has the potential to shed light on the complex population dynamics that support its persistence in the Chesapeake Bay ecosystem. With accurate information on *Chrysaora* dispersal and on variables that control observable spatial patterns at multiple scales, it is possible to begin to draw links between life stages and to characterize crucial components of *Chrysaora*'s ecology. Results of my investigations of the spatial patterns of *Chrysaora* polyps and medusae agree with previous reported findings that both life stages are more concentrated in tidal creeks than in the mainstem of Chesapeake Bay and subestuary

channels. However, the characteristics that define creeks as source habitat for polyps is less clear.

My research (Chapter 3) demonstrated that polyps were a critical, if not the most critical stage, controlling the spatial range of *Chrysaora* Bay-wide. Medusae are the main dispersal vector to new habitat, because they transport "potential" planula larvae, affecting the subsequent settlement of polyp colonies into a habitat and thus promoting medusae presence in the following year. However, it is not only polyp settlement that determines if *Chrysaora* persists in a habitat. I hypothesized that newly settled polyps also must survive the winter if they were to successfully introduce medusae to the waterscape in the following year via strobilation. This appears to have been the case due to the over-wintering survival of polyps at the Patuxent River site (PRL, Chapter 3) compared to low survivability at the Horn Point site on the Choptank mainstem (HPL, Chapter 3). In this case, both sites were conducive to settlement of polyps but not overwintering survival. This begs the question, where do polyps survive the winter and why? Many studies have pinpointed the sluggish headwaters of a creek, as opposed to an open river channel, as prime source habitat for polyps. Results of my research corroborate these findings but suggest that settlement of polyps may occur within creek or channel sites, while overwintering survival is more likely to occur in enclosed and protected creeks (Chapter 3).

Unfavorable salinity regimes have been previously suggested as a mechanism that causes polyp mortality (Cargo & King 1990a, Purcell et al. 1999, Holst & Jarms 2010); however, the mesoscale similarity of salinity from the the PRL (Mackall

Cove) site, and the HPL Choptank River channel site from Chapter 3, observed does not explain the differences in winter mortality between sites. Residence time (correlates with salinity) was explored because it characterized the advective forces of the sites and was considered a proxy to describe the hydrodynamic field of the waterscape. Residence time proved useful in explaining polyp distribution for large-scale spatial analyses but data were insufficient to describe factors operating at the mesoscale and fine scale (Chapter 3). Focus on these smaller spatial extents might reveal differences in the polyp microenvironment, including chemistry, physics and possible biological interactions that relate to competition for space with other epiphytic organisms.

The variability in the overwintering success of newly settled polyps also led to two other notable findings (Chapter 3). First, sampling polyps in the Fall, as a potential marker for medusae presence and abundance the following season, could lead to major predictive errors. Second, strobilation of newly settled polyps did not occur until the colonies had successfully survived the winter and experienced the warming Spring temperatures that cue the strobilation process.

The St. Leonard's creek (SLC) site and the PRL site within St. Leonard's creek (Mackall Cove, Chapter 3) were both identified as source habitat for *Chrysaora* polyps. To address hypotheses (Chapter 4), I described the spatial structure of the medusae population over the course of two years with contrasting levels of abundance. I correctly hypothesized that the spatial range and transport of medusae patches, as they were dispersed from their source, would vary significantly between years. However, I unexpectedly discovered increased clustering at the coarse

scale (between sites) in a low-density year, likely due to lower rates of transport from the source (creek) to sink (channel) when compared to the high abundance year of 2017. These contrasts in dispersal patterns have implications for the Patuxent River trophic system, particularly in high abundance years when spatial interference might operate. The variability in the spatial range of medusae patches advected from source creeks could potentially affect habitat utilization by juvenile forage fish and mysid shrimp that are utilizing the productive shallow habitat concurrently. Spatial interference by swarms of stinging medusae is also apparent in the California upwelling system where large swarms of *Chrysaora fuscescens* keep fish away from potential resources (Brodeur et al. 2008).

Although I hypothesized clustering of *Chrysaora* at the fine scale in the water column my research showed (Chapter 4) that the fine-scale spatial patterns of *Chrysaora* medusae were random, across two years, although there was a significant difference in density between years. This indicates that even in a low-density year, individual medusae were likely in close proximity to insure successful spawning. Nevertheless, it is highly possible that the observed fine-scale and random spatial patterns may not persist as *Chrysaora* are dispersed further downstream from source sites. Tthe likelihood of successful spawning may rely largely on the ability of medusae to remain in close proximity. The random spatial patterns also suggested that individual medusae are not strong enough swimmers to surpass current-driven controls, like tidal forces and wind. The ecological or behavioral processes that explain the ability of individual medusae to maintain themselves within the creek habitat is still largely unclear.

Much of jellyfish monitoring has been disparate, coarse, and conducted out of temporal and spatial context. There remain multiple challenges that can compromise sampling fragile, transparent, patchy and ephemeral gelatinous species. The introduction of the ARIS technology in my research (Chapter 2) greatly alleviated these challenges. ARIS technology allowed for insight not only into the ecology of the *Chrysaora* but also exemplified the critical roles scale, extent and spatial structure play to accurately understand jellyfish ecology.

Future Research

There is still much to be learned about the life-history of *Chrysaora*, especially with regard to other stages, for example ephyrae and planula larvae. My research on jellyfish in the Chesapeake Bay initiated using cutting-edge technology and innovative sampling approaches to understand jellyfish communities, spatial ecology, production, and dispersal. Future research should address the following:

1. While sonar sampling techniques prove incredibly useful, manual processing of jellyfish images and data was quite tedious. The processing efforts have the potential to be greatly reduced through the incorporation of machine learning techniques. Essentially, this requires teaching a computer to identify and count jellyfish automatically (Chapter 2). The technology and tools needed for such an undertaking are well studied and would include such methodology as Deep Neural Networking, which takes a systematic approach to classify obscure objects by networking common features. The application of image analysis and machine learning to identify jellyfish (and other organisms) in real time is foreseeable in the near future and would greatly reduce the effort and resources that currently constrain data acquisition and resolution.
2. With regard to the seasonal and spatial dynamics of polyps (Chapter 3), increasing spatial resolution (i.e., settlement plates in more sites) may be less important than long-term monitoring of polyp colonies within established source sites. While my research was able to follow polyp settlement, growth and overwinter survival from July – March, no information was collected on the polyps that survived the winter and would strobilate in the Spring. The

sampling scheme for my settlement study was destructive because settlement plates removed from the water were not returned. However, it is feasible to remove settlement plates and then return them to their previous location, maintaining the polyp populations and tracking growth and production through Spring and early summer, to enumerate rates of production and describe the population dynamics of *Chrysaora* polyps. This would provide valuable insight into the production rates (asexual and strobilation) that lead to a strobilation event and subsequent controls on the interannual variation of medusae abundance in Chesapeake Bay.

3. Size structure information on *Chrysaora* (bell size) can be generated from data collected with the sonar camera. By incorporating size and identifying size-structure of patches, we can track growth of a population and potentially track individual patches. The jellyfish that make up a patch likely share strobilation times and collectively experience the same advective forces that may maintain the patch, making this future research highly feasible.
4. Preliminary analyses suggested that the orientation of medusae in the water-column may differ between years, although more research is needed to validate the findings. Nevertheless, contrasting (between years) orientation behavior may help to explain the mechanistic controls on medusae dispersal from source habitat and should be an important consideration for future research.
5. The sonar data could be used to explore spatial and temporal interactions with species-level inferences, because our data was not limited to observing

Chrysaora. In fact, the sonar data include similar high-resolution spatially-explicit images of ctenophores, mysid shrimp, juvenile forage fish, juvenile pelagic fish, and the occasional blue crab and cow-nose ray. Spatial overlap and research on the biological interactions between these species i.e. forage fish displacement and ctenophore predation by *Chrysaora,* would help quantify the potential impact of *Chrysaora* on the trophic ecology of the ecosystem.

6. Finally, with the availability of high-resolution spatial data and recognition of the important role dispersal plays in the population dynamics of *Chrysaora* in Chesapeake Bay, a particle tracking model would be valuable to simulate the potential transport of medusae, ephyrae and planula larvae, taking into consideration the swim speeds and the advective forces of a Chesapeake Bay waterscape. This model would contribute to understanding of factors that support polyp settlement and the spatial growth of a *Chrysaora* population, i.e. potential to settle into and colonize a new habitat.

References

Able KW (2005) A re-examination of fish estuarine dependence: evidence for connectivity between estuarine and ocean habitats. Estuarine, Coastal and Shelf Science 64:5-17

Able KW, Grothues TM, Rackovan JL, Buderman FE (2014) Application of Mobile Dual-frequency Identification Sonar (DIDSON) to Fish in Estuarine Habitats. Northeastern Naturalist 21:192-209

Aglieri G, Papetti C, Zane L, Milisenda G, Boero F, Piraino S (2014) First Evidence of Inbreeding, Relatedness and Chaotic Genetic Patchiness in the Holoplanktonic Jellyfish Pelagia noctiluca (Scyphozoa, Cnidaria). PLOS ONE 9:e99647

Arai MN (2009) The potential importance of podocysts to the formation of scyphozoan blooms: a review. Hydrobiologia 616:241-246

Arai MN (2012) A functional biology of Scyphozoa, Vol. Springer Science & Business Media

Baird D, Ulanowicz RE (1989) The Seasonal Dynamics of The Chesapeake Bay Ecosystem. Ecological Monographs 59:329-364

Barbier EB, Hacker SD, Kennedy C, Koch EW, Stier AC, Silliman BR (2011) The value of estuarine and coastal ecosystem services. Ecological monographs 81:169-193

Bayha KM, Collins AG, Gaffney PM (2017) Multigene phylogeny of the scyphozoan jellyfish family Pelagiidae reveals that the common U.S. Atlantic sea nettle comprises two distinct species (*Chrysaora quinquecirrha and C. chesapeakei*). PeerJ 5:e3863

Bayley PB, Herendeen RA (2000) The efficiency of a seine net. Trans Am Fish Soc 129:901-923

Becker A, Cowley PD, Whitfield AK, Järnegren J, Næsje TF (2011a) Diel fish movements in the littoral zone of a temporarily closed South African estuary. Journal of Experimental Marine Biology and Ecology 406:63-70

Becker A, Whitfield AK, Cowley PD, Järnegren J, Næsje TF (2011b) An assessment of the size structure, distribution and behaviour of fish populations within a temporarily closed estuary using dual frequency identification sonar (DIDSON). Journal of Fish Biology 79:761-775

Becker A, Holland M, Smith JA, Suthers IM (2016) Fish Movement Through an Estuary Mouth Is Related to Tidal Flow. Estuaries and Coasts 39:1199-1207

Benjamin MA, Rigby RA, Stasinopoulos DM (2003) Generalized Autoregressive Moving Average Models. Journal of the American Statistical Association 98:214-223

Bi H, Guo Z, Benfield MC, Fan C, Ford M, Shahrestani S, Sieracki JM (2015) A semi-automated image analysis procedure for in situ plankton imaging systems. PLoS One 10:e0127121

Bivand RS, Pebesma EJ, Gómez-Rubio V, Pebesma EJ (2008) Applied spatial data analysis with R, Vol 747248717. Springer

Boero F, Bouillon J, Gravili C, Miglietta MP, Parsons T, Piraino S (2008) Gelatinous plankton: irregularities rule the world (sometimes). Marine Ecology Progress Series 356:299-310
Bollinger M, Kline R (2015) Validating side scan sonar as a fish survey tool over artificial reefs in the Gulf of Mexico. The Journal of the Acoustical Society of America 137:2334-2334
Boswell KM, Wilson MP, Wilson CA (2007) Hydroacoustics as a tool for assessing fish biomass and size distribution associated with discrete shallow water estuarine habitats in Louisiana. Estuaries and Coasts 30:607-617
Boswell KM, Wilson MP (2008) A semiautomated approach to estimating fish size, abundance, and behavior from dual-frequency identification sonar (DIDSON) data. North American Journal of …
Boswell KM, Wilson MP, Cowan JH (2008) A Semiautomated Approach to Estimating Fish Size, Abundance, and Behavior from Dual-Frequency Identification Sonar (DIDSON) Data. North American Journal of Fisheries Management 28:799-807
Bozdogan H (1987) Model selection and Akaike's information criterion (AIC): The general theory and its analytical extensions. Psychometrika 52:345-370
Breitburg D, Burrell R (2014) Predator-mediated landscape structure: seasonal patterns of spatial expansion and prey control by Chrysaora quinquecirrha and Mnemiopsis leidyi. Marine Ecology Progress Series 510:183-200
Breitburg DL, Adamack A, Rose KA, Kolesar SE and others (2003) The pattern and influence of low dissolved oxygen in the Patuxent River, a seasonally hypoxic estuary. Estuaries 26:280-297
Breitburg DL, Fulford RS (2006) Oyster-sea nettle interdependence and altered control within the Chesapeake Bay ecosystem. Estuaries and Coasts 29:776-784
Breitburg DL, Crump BC, Dabiri JO, Gallegos CL (2010) Ecosystem engineers in the pelagic realm: alteration of habitat by species ranging from microbes to jellyfish. Integrative and Comparative Biology 50:188-200
Brewer RH (1984) the influence of the orientation, roughness, and wettability of solid-surfaces on the behavior and attachment of planulae of cyanea (cnidaria, scyphozoa). Biological bulletin 166:11-21
Brewer rh (1991) morphological differences between, and reproductive isolation of, 2 populations of the jellyfish cyanea in long-island-sound, usa. Hydrobiologia 216:471-477
Brewer RH, Feingold JS (1991) The effect of temperature on the benthic stages of Cyanea (Cnidaria: Scyphozoa), and their seasonal distribution in the Niantic River estuary, Connecticut. Journal of Experimental Marine Biology and Ecology 152:49-60
Brodeur RD, Suchman CL, Reese DC, Miller TW, Daly EA (2008) Spatial overlap and trophic interactions between pelagic fish and large jellyfish in the northern California Current. Marine Biology 154:649-659
Brodeur RD, Link JS, Smith BE, Ford M, Kobayashi D, Jones TT (2016) Ecological and economic consequences of ignoring jellyfish: a plea for increased monitoring of ecosystems. Fisheries 41:630-637

Brotz L, Cheung WWL, Kleisner K, Pakhomov E, Pauly D (2012) Increasing jellyfish populations: trends in Large Marine Ecosystems. Hydrobiologia 690:3-20
Brown CW, Hood RR, Li Z, Decker MB, Gross TF, Purcell JE, Wang HV (2002) Forecasting system predicts presence of sea nettles in Chesapeake Bay. Eos, Transactions American Geophysical Union 83:321-326
Bum BK, Pick FR (1996) Factors regulating phytoplankton and zooplankton biomass in temperate rivers. Limnology and Oceanography 41:1572-1577
Calder DR (1974) Strobilation of the Sea Nettle, *Chrysaora quinquecirrha*, under Field Conditions. Biological Bulletin 146:326-334
Cargo DG, Schultz LP (1966) Notes on the biology of the sea nettle, *Chrysaora quinquecirrha*, in Chesapeake Bay. Chesapeake Science 7:95-100
Cargo DG, Schultz LP (1967) Further observations on the biology of the sea nettle and jellyfishes in Chesapeake Bay. Chesapeake Science 8:209-220
Cargo DG (1975) Comments on the Laboratory Culture of Scyphozoa. In: Smith WL, Chanley MH (eds) Culture of Marine Invertebrate Animals: Proceedings — 1st Conference on Culture of Marine Invertebrate Animals Greenport. Springer US, Boston, MA, p 145-154
Cargo DG (1979) Observations on the settling behavior of planular larvae of Chrysaora quinquecirrha. International Journal of Invertebrate Reproduction 1:279-287
Cargo DG, King DR (1990) Forecasting the abundance of the sea nettle,*Chrysaora quinquecirrha*, in the Chesapeake Bay. Estuaries 13:486-491
Chatfield C (2000) Time-series forecasting, Vol. Chapman and Hall/CRC
Clifford HC, Cargo DG (1978) Feeding rates of the sea nettle, Chrysaora quinquecirrha, under laboratory conditions. Estuaries 1:58-61
Condon RH, Steinberg DK, Del Giorgio PA, Bouvier TC, Bronk DA, Graham WM, Ducklow HW (2011) Jellyfish blooms result in a major microbial respiratory sink of carbon in marine systems. Proceedings of the National Academy of Sciences:201015782
Condon RH, Graham WM, Duarte CM, Pitt KA and others (2012) Questioning the Rise of Gelatinous Zooplankton in the World's Oceans. BioScience 62:160-169
Condon RH, Duarte CM, Pitt KA, Robinson KL and others (2013) Recurrent jellyfish blooms are a consequence of global oscillations. Proceedings of the National Academy of Sciences 110:1000-1005
Cones HN, Haven DS (1969) Distribution of *Chrysaora quinquecirrha* in the York River. Chesapeake Science 10:75-84
Cowan JH, birdsong rs, houde ed, priest js, sharp wc, mateja gb (1992) enclosure experiments on survival and growth of black drum eggs and larvae in lower chesapeake bay. Estuaries 15:392-402
Crossman JA, Martel G, Johnson PN, Bray K (2011) The use of Dual-frequency IDentification SONar (DIDSON) to document white sturgeon activity in the Columbia River, Canada. Journal of Applied Ichthyology 27:53-57
Dale MRT, Fortin MJ (2014) Spatial Analysis: A Guide For Ecologists, Vol. Cambridge University Press

Dawson MN, Martin LE (2001) Geographic variation and ecological adaptation in *Aurelia* (Scyphozoa, Semaeostomeae): some implications from molecular phylogenetics. Hydrobiologia 451:259-273
Dawson MN, Martin LE, Penland LK (2001) Jellyfish swarms, tourists, and the Christ-child. In: Jellyfish Blooms: Ecological and Societal Importance. Springer, p 131-144
Decker MB, Brown CW, Hood RR, Purcell JE and others (2007) Predicting the distribution of the scyphomedusa *Chrysaora quinquecirrha* in Chesapeake Bay. Marine Ecology Progress Series 329:99-113
Dong J, Sun M, Purcell JE, Chai Y, Zhao Y, Wang A (2015) Effect of salinity and light intensity on somatic growth and podocyst production in polyps of the giant jellyfish Nemopilema nomurai (Scyphozoa: Rhizostomeae). Hydrobiologia 754:75-83
Duarte CM, Pitt KA, Lucas CH, Purcell JE and others (2012) Is global ocean sprawl a cause of jellyfish blooms? Frontiers in Ecology and the Environment 11:91-97
Duke NC, Ball MC, Ellison JC (1998) Factors influencing biodiversity and distributional gradients in mangroves. Glob Ecol Biogeogr Lett 7:27-47
Efron B (1992) Bootstrap Methods: Another Look at the Jackknife. In: Kotz S, Johnson NL (eds) Breakthroughs in Statistics: Methodology and Distribution. Springer New York, New York, NY, p 569-593
Feigenbaum D, Kelly M (1984) Changes in the lower Chesapeake Bay food chain in presence of the sea nettle Chrysaora quinquecirrha (Scyphomedusa). Marine Ecology Progress Series 19:39-47
Gibbons MJ, Richardson AJ (2013) Beyond the jellyfish joyride and global oscillations: advancing jellyfish research. Journal of Plankton Research 35:929-938
Gili J-M, Coma R (1998) Benthic suspension feeders: their paramount role in littoral marine food webs. Trends in Ecology & Evolution 13:316-321
Graham WM, Pages F, Hamner WM (2001) A physical context for gelatinous zooplankton aggregations: a review. Hydrobiologia 451:199-212
Graham WM, Gelcich S, Robinson KL, Duarte CM and others (2014) Linking human well-being and jellyfish: ecosystem services, impacts, and societal responses. Frontiers in Ecology and the Environment 12:515-523
Gröndahl F (1988) A comparative ecological study on the scyphozoans *Aurelia aurita*, *Cyanea capillata* and *C. lamarckii* in the Gullmar Fjord, western Sweden, 1982 to 1986. Marine Biology 97:541-550
Grosjean P, Picheral M, Warembourg C, Gorsky G (2004) Enumeration, measurement, and identification of net zooplankton samples using the ZOOSCAN digital imaging system. ICES Journal of Marine Science 61:17
Haddock SHD (2004) A golden age of gelata: past and future research on planktonic ctenophores and cnidarians. In: Fautin DG, Westfall JA, Cartwrigh P, Daly M, Wyttenbach CR (eds) Coelenterate Biology 2003: Trends in Research on Cnidaria and Ctenophora. Springer Netherlands, Dordrecht, p 549-556
Hagy JD, Boynton WR, Sanford LP (2000) Estimation of net physical transport and hydraulic residence times for a coastal plain estuary using box models. Estuaries 23:328-340

Hamner WM, Dawson MN (2009) A review and synthesis on the systematics and evolution of jellyfish blooms: advantageous aggregations and adaptive assemblages. Hydrobiologia 616:161-191
Han CH, Uye SI (2009) Quantification of the abundance and distribution of the common jellyfish Aurelia aurita sl with a Dual-frequency IDentification SONar (DIDSON). Journal of Plankton Research
Holst S, Jarms G (2007) Substrate choice and settlement preferences of planula larvae of five Scyphozoa (Cnidaria) from German Bight, North Sea. Mar Biol 151:863-871
Holst S, Jarms G (2010) Effects of low salinity on settlement and strobilation of scyphozoa (Cnidaria): Is the lion's mane Cyanea capillata (L.) able to reproduce in the brackish Baltic Sea? Hydrobiologia 645:53-68
Hong B, Shen J (2012) Responses of estuarine salinity and transport processes to potential future sea-level rise in the Chesapeake Bay. Estuarine, Coastal and Shelf Science 104-105:33-45
Hoover RA, Purcell JE (2009) Substrate preferences of scyphozoan Aurelia labiata polyps among common dock-building materials. Hydrobiologia 616:259-267
Hubot N, Lucas CH, Piraino S (2017) Environmental control of asexual reproduction and somatic growth of Aurelia spp. (Cnidaria, Scyphozoa) polyps from the Adriatic Sea. PLoS One 12:16
Hughes JB, Hightower JE (2015) Combining Split-Beam and Dual-Frequency Identification Sonars to Estimate Abundance of Anadromous Fishes in the Roanoke River, North Carolina. North American Journal of Fisheries Management 35:229-240
Jordano P, Bascompte J, Olesen JM (2003) Invariant properties in coevolutionary networks of plant–animal interactions. Ecology letters 6:69-81
Jung S, Houde ED (2003) Spatial and temporal variabilities of pelagic fish community structure and distribution in Chesapeake Bay, USA. Estuarine, Coastal and Shelf Science 58:335-351
Kaneshiro-Pineiro MY, Kimmel DG (2015) Local Wind Dynamics Influence the Distribution and Abundance of Chrysaora quinquecirrha in North Carolina, USA. Estuaries and Coasts 38:1965-1975
Keister JE, Houde ED, Breitburg DL (2000) Effects of bottom-layer hypoxia on abundances and depth distributions of organisms in Patuxent River, Chesapeake Bay. Marine Ecology Progress Series 205:43-59
Kennedy TL, Turner TF (2011) River channelization reduces nutrient flow and macroinvertebrate diversity at the aquatic terrestrial transition zone. Ecosphere 2:1-13
Kikinger R (1992) *Cotylorhiza tuberculata* (Cnidaria: Scyphozoa)-Life history of a stationary population. Marine Ecology 13:333-362
Kimball ME, Rozas LP, Boswell KM, Cowan Jr JH (2010) Evaluating the effect of slot size and environmental variables on the passage of estuarine nekton through a water control structure. Journal of Experimental Marine Biology and Ecology 395:181-190
Kolesar SE, Rose KA, Breitburg DL (2017) Hypoxia Effects Within an Intra-guild Predation Food Web of *Mnemiopsis leidyi* Ctenophores, Larval Fish, and

Copepods. In: Justic D, Rose KA, Hetland RD, Fennel K (eds) Modeling Coastal Hypoxia: Numerical Simulations of Patterns, Controls and Effects of Dissolved Oxygen Dynamics. Springer International Publishing, Cham, p 279-317
Levin SA (1992) The problem of pattern and scale in ecology: the Robert H. MacArthur award lecture. Ecology 73:1943-1967
Li J (2003) A wavelet approach to edge detection. Sam Houston State University
Liu W-C, Lo W-T, Purcell JE, Chang H-H (2009) Effects of temperature and light intensity on asexual reproduction of the scyphozoan, *Aurelia aurita* (L.) in Taiwan. Hydrobiologia 616:247-258
Loeb MJ (1972) Strobilation in the Chesapeake Bay sea nettle *Chrysaora quinquecirrha.* I. The effects of environmental temperature changes on strobilation and growth. Journal of Experimental Zoology 180:279-291
Lucas CH (1996) Population dynamics of Aurelia aurita (Scyphozoa) from an isolated brackish lake, with particular reference to sexual reproduction. Journal of Plankton Research 18:987-1007
Lucas CH (2001) Reproduction and life history strategies of the common jellyfish, Aurelia aurita, in relation to its ambient environment. Hydrobiologia 451:229-246
Lucas CH, Graham WM, Widmer C (2012) Jellyfish Life Histories: Role of Polyps in Forming and Maintaining Scyphomedusa Populations. Advances in marine biology 63:133
Makabe R, Kurihara T, Uye S-I (2012) Spatio-temporal distribution and seasonal population dynamics of the jellyfish Aurelia aurita s.l. studied with Dual-frequency IDentification SONar (DIDSON). Journal of Plankton Research 34:936-950
Mills CE (2001) Jellyfish blooms: are populations increasing globally in response to changing ocean conditions? Hydrobiologia 451:55-68
Olesen NJ, Frandsen K, Riisgard HU (1994) Population-dynamics, growth and energetics of jellyfish aurelia-aurita in a shallow fjord. Marine Ecology Progress Series 105:9-18
Omori M, Ishii H, Fujinaga A (1995) Life history strategy of *Aurelia aurita* (Cnidaria, Scyphomedusae) and its impact on the zooplankton community of Tokyo Bay. ICES Journal of Marine Science 52:597-603
Pitt KA (2000) Life history and settlement preferences of the edible jellyfish Catostylus mosaicus (Scyphozoa : Rhizostomeae). Marine Biology 136:269-279
Pitt KA, Budarf AC, Browne JG, Condon RH (2014) Bloom and Bust: Why Do Blooms of Jellyfish Collapse? In: Pitt KA, Lucas CH (eds) Jellyfish Blooms. Springer Netherlands, Dordrecht, p 79-103
Purcell JE, Grover JJ (1990) Predation and food limitation as causes of mortality in larval herring at a spawning ground in british-columbia. Marine Ecology Progress Series 59:55-61
Purcell JE (1992) Effects of predation by the scyphomedusan *Chrysaora quinquecirrha* on zooplankton populations in Chesapeake Bay, USA. Marine Ecology Progress Series 87:65-76

Purcell JE, Nemazie DA, Dorsey SE, Houde ED, Gamble JC (1994a) Predation mortality of bay anchovy *Anchoa mitchilli* eggs and larvae due to scyphomedusae and ctenophores in Chesapeake Bay. Marine Ecology Progress Series 114:47-58

Purcell JE, White JR, Roman MR (1994) Predation by gelatinous zooplankton and resource limitation as potential controls of Acartia tonsa copepod populations in Chesapeake Bay. Limnology and Oceanography 39:263-278

Purcell JE, White JR, Nemazie DA, Wright DA (1999) Temperature, salinity and food effects on asexual reproduction and abundance of the scyphozoan *Chrysaora quinquecirrha*. Marine Ecology Progress Series 180:187-196

Purcell JE, Brown ED, Stokesbury KDE, Haldorson LH, Shirley TC (2000) Aggregations of the jellyfish Aurelia labiata: abundance, distribution, association with age-0 walleye pollock, and behaviors promoting aggregation in Prince William Sound, Alaska, USA. Marine Ecology Progress Series 195:145-158

Purcell JE, Arai MN (2001) Interactions of pelagic cnidarians and ctenophores with fish: a review. Hydrobiologia 451:27-44

Purcell JE (2005) Climate effects on formation of jellyfish and ctenophore blooms: a review. J Mar Biol Assoc UK 85:461-476

Purcell JE, Uye S-i, Lo W-T (2007) Anthropogenic causes of jellyfish blooms and their direct consequences for humans : a review. Marine Ecology Progress Series 350:153-174

Purcell JE, Hoover RA, Schwarck NT (2009) Interannual variation of strobilation by the scyphozoan *Aurelia labiata* in relation to polyp density, temperature, salinity, and light conditions *in situ*. Marine Ecology Progress Series 375:139-149

Purcell JE (2012) Jellyfish and Ctenophore Blooms Coincide with Human Proliferations and Environmental Perturbations. In: Carlson CA, Giovannoni SJ (eds) Annual Review of Marine Science, Vol 4, Vol 4. Annual Reviews, Palo Alto, p 209-235

Purcell JE, Breitburg DL, Decker MB, Graham WM, Youngbluth MJ, Raskoff KA (2013) Pelagic Cnidarians and Ctenophores in Low Dissolved Oxygen Environments: A Review. In: Coastal Hypoxia: Consequences for Living Resources and Ecosystems. American Geophysical Union, p 77-100

Rahbek C (2005) The role of spatial scale and the perception of large-scale species-richness patterns. Ecology letters 8:224-239

Richardson AJ, Bakun A, Hays GC, Gibbons MJ (2009) The jellyfish joyride: causes, consequences and management responses to a more gelatinous future. Trends in Ecology & Evolution 24:312-322

Rigby RA, Stasinopoulos DM (2005) Generalized additive models for location, scale and shape (with discussion). Journal of the Royal Statistical Society: Series C (Applied Statistics) 54:507-554

Rozas LP, Minello TJ (1997) Estimating densities of small fishes and decapod crustaceans in shallow estuarine habitats: a review of sampling design with focus on gear selection. Estuaries 20:199-213

Said SE, Dickey DA (1984) Testing for unit roots in autoregressive-moving average models of unknown order. Biometrika 71:599-607
Sanz-Martín M, Pitt KA, Condon RH, Lucas CH, Novaes de Santana C, Duarte CM (2016) Flawed citation practices facilitate the unsubstantiated perception of a global trend toward increased jellyfish blooms. Global Ecology and Biogeography 25:1039-1049
Shahrestani S, Bi H, Lyubchich V, Boswell KM (2017) Detecting a nearshore fish parade using the adaptive resolution imaging sonar (ARIS): An automated procedure for data analysis. Fisheries Research 191:190-199
Shahrestani S, Bi H (2018) Settlement and survival of Chrysaora chesapeakei polyps: implications for adult abundance. Marine Ecological Progress *Accepted*
Shahrestani S, Bi H, Lankowicz K, Fan C, McLean N, Zhang L (*Submitted*) Spatial structure of *Chrysaora chesapeakei* medusae within a shallow coastal waterscape. Limnology and Oceanography
Shilane D, Evans SN, Hubbard AE (2010) Confidence intervals for negative binomial random variables of high dispersion. Int J Biostat 6:Article 10
Sommer U, Stibor H, Katechakis A, Sommer F, Hansen T (2002) Pelagic food web configurations at different levels of nutrient richness and their implications for the ratio fish production: primary production. Hydrobiologia 484:11-20
Sponaugle S, Cowen RK, Shanks A, Morgan SG and others (2002) Predicting self-recruitment in marine populations: Biophysical correlates and mechanisms. Bull Mar Sci 70:341-375
Stasinopoulos DM, Rigby RA (2007) Generalized additive models for location scale and shape (GAMLSS) in R. Journal of Statistical Software VV
Suchman CL, Sullivan BK (2000) Effect of prey size on vulnerability of copepods to predation by the scyphomedusae Aurelia aurita and Cyanea sp. Journal of Plankton Research 22:2289-2306
Sullivan LJ, Kremer P (2011) Gelatinous Zooplankton and Their Trophic Roles, Vol. Elsevier Academic Press Inc, San Diego
Turner MG, Dale VH, Gardner RH (1989) Predicting across scales: theory development and testing. Landscape ecology 3:245-252
Wiegner TN, Seitzinger SP, Breitburg DL, Sanders JG (2003) The effects of multiple stressors on the balance between autotrophic and heterotrophic processes in an estuarine system. Estuaries 26:352-364
Wiens JA (1989) Spatial scaling in ecology. Functional ecology 3:385-397
Zhang F, Sun S, Jin X, Li C (2012) Associations of large jellyfish distributions with temperature and salinity in the Yellow Sea and East China Sea. Hydrobiologia 690:81-96